CHALMERS
UNIVERSITY OF TECHNOLOGY

Experimental investigation on electrical resistivity of SFRC

Master's Thesis in the Master's Programme Structural Engineering and Building Technology

LUCÍA ABAD ZAPICO

MASTER'S THESIS 2015:84

Experimental investigation on electrical resistivity of SFRC

Master's Thesis in the Master's Programme Structural Engineering and Building Technology

LUCÍA ABAD ZAPICO

Department of Civil and Environmental Engineering
Division of Structural Engineering
Concrete Structures

CHALMERS UNIVERSITY OF TECHNOLOGY
Göteborg, Sweden 2015

Experimental investigation on electrical resistivity of SFRC
Master's Thesis in the Master's Programme Structural Engineering and Building Technology

LUCÍA ABAD ZAPICO

Examensarbete 2015:84 / Institutionen för bygg- och miljöteknik,
Chalmers tekniska högskola 2015

Department of Civil and Environmental Engineering
Division of Structural Engineering
Concrete Structure
Chalmers University of Technology
SE-412 96 Göteborg
Sweden
Telephone: + 46 (0)31-772 1000

Cover:
Reinforcement bars with and without rust spots
Chalmers Reproservice. Göteborg, Sweden, 2015

Experimental investigation on electrical resistivity of SFRC

Master's thesis in the Master's Programme Structural Engineering and Building Technology

LUCÍA ABAD ZAPICO
Department of Civil and Environmental Engineering
Division of Structural Engineering
Concrete Structures
Chalmers University of Technology

ABSTRACT

Reinforced concrete is widely used within the construction industry, being considered as the most important construction material as it combines the best properties of its components: tensile strength of steel and compressive strength of concrete at a relatively low cost compared with other materials. It is used in the construction of civil structures such as bridges or harbour piers, which need large amount of reinforcement making corrosion of steel one of the most critical parameters in assessing their service life. Lately, steel fibres have been used together with traditional reinforcement bars to limit the crack widths and minimize the chloride ingress to reduce the risk of pitting corrosion. To this extent, it seems that the use of steel fibres would be beneficial in larger constructions; however, there is also a concern that the decrease in resistivity caused by the conductivity of the fibres may increase the corrosion rate of the steel bars.

This master thesis is divided in two different parts: resistivity studies and corrosion rate experiments. The first one aims to identify how steel fibres influence the resistivity of concrete and the second one to determine whether a measured low resistivity of steel fibre reinforced concrete could lead to increased corrosion rate of steel reinforcement bars.

For the resistivity studies, the results show that resistivity was affected by numerous parameters among which moisture content should be highlighted, as it is the one with larger influence. It was determined that electrical resistivity of concrete decreases with increasing fibre contents and also that the orientation of fibres, something that is achieved by the pouring process, has an effect on the measured values.

During the corrosion rate experiments, the galvanic current flowing through reinforcement bars was measured and with the help of Faraday's law, the theoretical weight loss of those bars associated to the reduction of their cross-section was calculated. After comparing the different values in specimens with different fibre contents from three month's chloride exposure, no significant evidence was found indicating that steel fibres may influence the corrosion rate of traditional reinforcement bars.

Keywords: Steel fibre reinforced concrete, electrical resistivity, corrosion rate, galvanic current, steel fibre reinforced concrete durability.

Contents

ABSTRACT II
CONTENTS III

TABLE OF FIGURES V
PREFACE VIII

1 INTRODUCTION 1
1.1 Background 1
1.2 Purpose and objectives 1
1.3 Methodology 2
1.4 Limitations 2

2 LITERATURE REVIEW 4
2.1 Resistivity 4
2.1.1 Theoretical background 4
2.1.2 Existing studies 4
2.1.3 Effects of DC stray current on the steel fibres 14
2.2 Corrosion rate 15
2.2.1 Theoretical background 15
2.2.2 Existing studies 17

3 EXPERIMENTAL PROGRAMME FOR RESISTIVITY TESTS 22
3.1 Test specimens 22
3.2 Methodology 24
3.2.1 Saturated specimens and resistivity measurements 25
3.2.2 Determination of the desorption curve 26
3.2.3 Forced dried specimens 27
3.2.4 Natural dried specimens 28
3.2.5 Effects of steel fibres on the resistivity of concrete under DC 28

4 EXPERIMENTAL PROGRAMME TO STUDY CORROSION RATE 30
4.1 Test specimens 30
4.2 Methodology 31

5 RESISTIVITY TEST RESULTS 34
5.1 Saturated specimens in tap water 34
5.1.1 Effects of degree of hydration and frequency 34
5.1.2 Effects of fibre orientation and frequency 36

5.1.3 Position in the slab 39
5.2 Saturated specimens in chlorides 41
5.2.1 Effects of degree of hydration and frequency 41
5.2.2 Effects of fibre orientation and frequency 42
5.2.3 Position in the slab 45
5.3 Effect if moisture content 47
5.4 DC Measurements 49

6 CORROSION RATE RESULTS 52

7 DISCUSSION OF THE ELECTRICAL RESISTIVITY RESULTS 55
7.1 Saturated specimens in tap water 55
7.1.1 Effects of degree of hydration and frequency 55
7.1.2 Effects of fibre orientation and frequency 56
7.1.3 Position in the slab 57
7.2 Saturated specimens in chloride solution 58
7.2.1 Effects of degree of hydration and frequency 58
7.2.2 Effects of fibre orientation and frequency 59
7.2.3 Position in the slab 59
7.2.4 Chlorides compared with tap water 60
7.3 Effect of moisture content 61
7.4 DC Measurements 62

8 DISCUSSION OF THE CORROSION RATE EXPERIMENT 64

9 CONCLUSIONS 65
9.1 Conclusions of the resistivity part 65
9.2 Conclusions of the corrosion rate part 66

10 REFERENCES 67

APPENDIX A: CONCRETE PROPERTIES 72
Porosity 72
Compressive strength test 75

APPENDIX B: SORPTION CURVES 76

APPENDIX C: WATER LOSS MODELLING 78

APPENDIX D: MOISTURE CONTENT 79

Table of figures

Figure 1 Resistivity against w/c (Gjørv et al. 1977) 5
Figure 2 Resistivity against aggregate content (Büyüköztürk & Taşdemir 2013) . 6
Figure 3 Resistivity against fibre volume (Solgaard et al. 2013) 7
Figure 4 Resistivity against water saturation (Gjørv et al. 1977) 8
Figure 5 Resistivity against moisture condition (Büyüköztürk & Taşdemir 2013) 9
Figure 6 Resistivity against Temperature (Hope et al. 1985) 10
Figure 7 Resistivity against age. (Hope et al. 1985) 11
Figure 8 Resistivity affected by chloride content (Henry, 1964) 12
Figure 9 Deviation from theoretical resistivity in dry concrete (Larsen et al. 2007) 13
Figure 10 Deviation from theoretical resistivity in wet concrete (Larsen et al. 2007) 13
Figure 11 Electric analogy for the two-slope behaviour of SFRC 14
Figure 12 Current transferred by the fibres as a function of the potential gradient (Solgaard et al. 2013) 15
Figure 13 Structural consequences of corrosion in reinforced concrete structures 17
Figure 14 Carbonation- and chloride-induced corrosion 18
Figure 15 Percentage of reinforcement showing corrosion in relation with chloride content (Vassie 1984) 20
Figure 16 Cutting of specimens from cast concrete slabs 23
Figure 17 Pouring from the centre 24
Figure 18 Schematic of the uniaxial resistivity test 26
Figure 19 Test arrangement to study the effects of steel fibres on the resistivity of concrete under DC 29
Figure 20 Test specimen for corrosion rate experiments 31
Figure 21 Reinforcement bars before and after being manually brushed 31
Figure 22 Beam partially subjected in a 10%NaCl solution 32
Figure 23 Resistivity test arrangement 34
Figure 24 Grade of hydration, tap water, 100 Hz. Average values of position and direction of measurement 35
Figure 25 Grade of hydration, tap water, 120 Hz. Average values of position and direction of measurement 35
Figure 26 Grade of hydration, tap water, 1000 Hz. Average values of position and direction of measurement 36
Figure 27 Fibre orientation, tap water, 1% fibre volume – 100 Hz. Average value of position in the slab 36
Figure 28 Fibre orientation, tap water, 0.75% fibre volume – 100 Hz. Average value of position in the slab 37
Figure 29 Fibre orientation, tap water, 0.5% fibre volume – 100 Hz. Average value of position in the slab 37
Figure 30 Fibre orientation, tap water, 0% fibre volume – 100 Hz. Average value of position in the slab 37

Figure 31 Fibre orientation, tap water, 1% fibre volume – 1000 Hz. Average value of position in the slab 38
Figure 32 Fibre orientation, tap water, 0.75% fibre volume – 1000 Hz. Average value of position in the slab 38
Figure 33 Fibre orientation, tap water, 0.5% fibre volume – 1000 Hz. Average value of position in the slab 38
Figure 34 Fibre orientation, tap water, 0% fibre volume – 1000 Hz. Average value of position in the slab 39
Figure 35 Position in the slab and fibre orientation, tap water, 1% fibre content, 1000 Hz 39
Figure 36 Position in the slab and fibre orientation, tap water, 0.75% fibre content, 1000 Hz 40
Figure 37 Position in the slab and fibre orientation, tap water, 0.5% fibre content, 1000 Hz 40
Figure 38 Position in the slab and fibre orientation, tap water, 0% fibre content, 1000 Hz 40
Figure 39 Grade of hydration, chloride solution, 100 Hz. Average values of position and direction of measurement 41
Figure 40 Grade of hydration, chloride solution, 120 Hz. Average values of position and direction of measurement 42
Figure 41 Grade of hydration, chloride solution, 1000 Hz Average values of position and direction of measurement 42
Figure 42 Fibre orientation, chloride solution, 1% fibre volume – 100 Hz. Average value of position in the slab 43
Figure 43 Fibre orientation, chloride solution, 0.75% fibre volume – 100 Hz. Average value of position in the slab 43
Figure 44 Fibre orientation, chloride solution, 0.5% fibre volume – 100 Hz. Average value of position in the slab 43
Figure 45 Fibre orientation, chloride solution, 0% fibre volume – 100 Hz. Average value of position in the slab 44
Figure 46 Fibre orientation, chloride solution, 1% fibre volume – 1000 Hz. Average value of position in the slab 44
Figure 47 Fibre orientation, chloride solution, 0.75%fibre volume – 1000 Hz. Average value of position in the slab 44
Figure 48 Fibre orientation, chloride solution, 0.5% fibre volume – 1000 Hz. Average value of position in the slab 45
Figure 49 Fibre orientation, chloride solution, 0% fibre volume – 1000 Hz. Average value of position in the slab 45
Figure 50 Disposition in the slab and fibre orientation, chloride solution, 1% fibre content, 1000 Hz 46
Figure 51 Disposition in the slab and fibre orientation, chloride solution, 0.75% fibre content, 1000 Hz 46
Figure 52 Disposition in the slab and fibre orientation, chloride solution, 0.5% fibre content, 1000 Hz 46
Figure 53 Disposition in the slab and fibre orientation, chloride solution, 0% fibre content, 1000 Hz 47
Figure 54 Comparison of rows with 1% fibre content. Average value of all the specimens in the three directions 47

Figure 55 Comparison of rows with 0.75% fibre content Average value of all the specimens in the three directions 48
Figure 56 Comparison of rows with 0.5% fibre content. Average value of all the specimens in the three directions 48
Figure 57 Comparison of rows with 0% fibre content. Average value of all the specimens in the three directions 49
Figure 58 Current vs. voltage in cubes A 49
Figure 59 Current vs. voltage in cubes B 50
Figure 60 Current vs. voltage in cubes C 50
Figure 61 Resistivity values calculated with an increasing voltage at low and high voltages 51
Figure 62 Resistivity values calculated with a decreasing voltage at low and high voltages 51
Figure 63 Estimated reinforcement bar weight loss in position a 52
Figure 64 Estimated reinforcement bar weight loss in position b 52
Figure 65 Estimated reinforcement bar weight loss in position c 53
Figure 66 Estimated penetration rate in position a 53
Figure 67 Estimated penetration rate in position b 54
Figure 68 Estimated penetration rate in position c 54
Figure 69 Corrected curves from (Hedenblad 1967) 77
Figure 70 Calculated desorption curve, w/c=0.47 and C=385 77

Tables

Table 1 Relationship between resistivity and corrosion rate (Langford & Broomfield 1987) 16
Table 2 Criteria for the assessment of corrosion in terms of resistivity 18
Table 3 Mixture proportions, kg/m3 22
Table 4 Slump flow in mm 22
Table 5 Experimental plan 25
Table 6 Mixture proportions, kg/m3 30
Table 7 Resistivity [Ωm] of samples submerged in a chloride solution compared to resistivity [Ωm] of samples submerged in tap water 60
Table 8 Compressive strength test for the concrete used in the resistivity tests 75
Table 9 Compressive strength test for the concrete used in the corrosion rate tests 75
Table 10 Calculated absorption and desorption values 76
Table 11 Initial and final state of Row 4 78
Table 12 Initial and final state of Row 1 79
Table 13 Initial and final state of Row 2 80
Table 14 Initial and final state of Row 6 81
Table 15 Initial and final state of Row 7 82

Preface

This Master's Thesis was carried out at the division of Structural Engineering within the Department of Civil and Environmental Engineering at Chalmers University of Technology in collaboration with Thomas Concrete Group.

First, I would like to thank my supervisors, Carlos Gil and Ingemar Löfgren for their continuous advice during the whole project, their availability to discuss any problem that came up to me and also for their help in the laboratory while preparing the specimens, something I could not have done by myself. I would like to express my gratitude to Prof. Tang Luping, examiner of the project, for helping clearing up the doubts related to unexpected results in the laboratory with his extensive knowledge in the field.

Moreover I would like to thank Sebastian Almfeldt for his help in the design and the execution of the experimental work and I would also like to thank my Spanish supervisor, Prof. María Jesús Lamela, for her help, availability and advice in choosing Chalmers to continue my studies.

I cannot forget all the people I met during these two amazing years in Göteborg, friends that made this experience unforgettable and without whom I would not have enjoyed so much this city. Thank you. And also, I would like to name my friends in Spain for their support whenever I needed it during this period far from them.

Por último, gracias a mis padres. Sin su apoyo, todo esto no habría pasado.

1 Introduction

1.1 Background

Reinforced concrete is widely used within the field of Civil Engineering and could be considered, nowadays, as the most important material in the construction industry as it combines the best from both materials: the tensile strength of steel and the compressive strength of concrete. Furthermore, it is relatively inexpensive compared with other construction materials. Structures like bridges, harbour piers, tunnels or hydraulic projects like dams or quays require the use of dense concrete, thick concrete covers and strict crack width limitations due to the risk of chloride induced corrosion. These structures then, require large reinforcement amounts, making corrosion one of the most critical parameters in the determination of their durability and service life.

The service life of reinforcements t_l, is usually modelled by assuming two time periods: the time to initiation of corrosion t_i and its propagation t_p. Thus, $t_l = t_i + t_p$ (Tuutti 1982). The electrical resistivity has correlations with both periods as it works as an indicator of where the chloride penetration will occur quickest in the initiation phase and as it affects to the corrosion rate in the propagation period (Polder 2001) making this property being one of the most important parameters that influence the service life of structures of this type.

Steel fibres are commonly used in buildings and industrial floors as their effectiveness in providing crack control have already been proved and in addition, if alkali silica reaction occurs, fibres contribute to controlling the expansion.

To this extent, it seems that using fibres in larger constructions will be beneficial, but there is also a concern that a decrease in the electrical resistivity caused by the conductivity of the fibres may increase the corrosion rate.

1.2 Purpose and objectives

This master thesis aims to identify how steel fibres influence the resistivity of concrete and whether a measured low resistivity of steel fibre reinforced concrete (SFRC) could lead to increased corrosion rate of steel reinforcing bars.

It is assumed that the steel fibres may decrease the electrical resistivity of concrete as they are a conductive material, but the main aim addressed during the first part of this project is to investigate to which extent their content and orientation will affect this property and its change with time, under different moisture conditions that will be simulated in the laboratory and also measured under different frequencies and with different techniques, e.g. AC and DC.

The second part of the project will aim to identify the relationship between the addition of fibres with its consequent change in the electrical resistivity of concrete, and the corrosion rate of conventional reinforcement bars.

1.3 Methodology

In order to achieve the aims of this project, two different types of experiments were carried out in the laboratory. First, a study on how steel fibres affect the electrical resistivity of concrete was carried out. This included not only the influence of the fibre volume but also the influence of the moisture content. Then, the intention was to quantify the impact of steel fibres on the corrosion rate of conventional reinforcement bars embedded in concrete.

For the resistivity test, the specimens were cast using four different fibre dosages: 1%, 0.75%, 0.5% and 0%. After curing, some of the specimens were kept saturated both, in tap water and in chloride solution, some of them were placed inside an oven to let them dry to different moisture conditions and others were left drying under natural conditions. For the saturated specimens, measurements on the resistivity were taken each week to observe not only the differences in between the degree of saturation but also the effect of time on it. Then, when each specimen reached the previously determined moisture content, the resistivity was measured to compare how the exposure conditions affect it.

To study the influence of fibres on the corrosion rate, specimens with an embedded reinforcement bar as a working electrode and connected to a counter electrode in the form of a stainless steel bar were cast. Just as in the resistivity test, samples with four different fibre dosages were studied. In this case, at the time of mixing, chloride was included to accelerate the corrosion process and all the specimens were kept in a salt solution over the experiment duration.

1.4 Limitations

The electrical resistivity of concrete is a property that is influenced by many parameters, including those related to its composition (especially porosity and pore structure), the moisture content and the measuring methods.

With regard to the exposure conditions, although the moisture content is the main factor affecting it, concrete resistivity is also strongly influenced by the temperature. There are numerous studies related to the influence of this parameter and even a correction curve was developed in (Spencer 1937) to adjust the results to a reference temperature. Consequently, it was decided that all the measurements were going to be made at laboratory conditions disregarding temperature effects.

In relation to the composition of concrete, many factors affect its resistivity such as the water-cement ratio, the quantity of cement added, the type and volume of aggregates or whether additions such as fly ash or silica fume are used. All the specimens were made with the same composition to reduce the influence of these factors, the only differences were with relation to the fibre content which, as said before, range from 0% to 1% in four different mixes. Also although there are many types of fibres in the market, made with different materials, properties and aspect ratio, only one type was tested.

Another factor that affects the resistivity is the chloride content in concrete. In the first part of the project, no chlorides were added as part of the composition of the samples but some of them were submerged in a 3.5% NaCl solution to study the effects on resistivity. During the second part, the chlorides were included in two ways, directly adding to the mix 2% NaCl by weight of cement and then, by placing the specimens in a 10% NaCl solution.

2 Literature review

2.1 Resistivity

2.1.1 Theoretical background

The electrical resistivity ρ (Ω·m) of a material describes its electrical resistance, which is the ratio between applied voltage and resulting current multiplied by a cell constant, is thus a geometry independent property (Hornbostel et al. 2013) and it is quantified through Ohm's law:

$$R = \frac{V}{I} = \rho \frac{l}{A}$$

where R is the electrical resistance (Ω) which can be measured applying a voltage and measuring the current I circulating (A) and $\frac{l}{A}$ is the cell constant where l is the distance between electrodes (m) and A is the cross section area (m^2) (Andrade & Andrea 2010). The inverse of resistivity is conductivity σ (S/m).

Electrical resistivity in concrete is ascribed to micro-structural properties such as porosity and pore solution characteristics. The degree of saturation of the pore structure (relative humidity) has been identified as the most important factor influencing concrete resistivity (Hornbostel et al. 2013) but not only the environment is a determinant factor, the composition of the material also affects the electrical resistivity: the type of cement used (Portland or blended cements), the *w/c*, the presence of chloride ions or whether the concrete is carbonated or not (Bertolini et al. 2004).

There are many factors influencing the resistivity, and it varies between 10^6 Ω·m for oven dried samples to 10 Ω·m for saturated concrete (Whiting & Nagi 2003), making its range to be one of the greatest of any material property.

2.1.2 Existing studies

As resistivity of concrete depends on many parameters, there have been a lot of studies related to it. The parameters that influence the resistivity of concrete are related to the materials involved in the mix, to the environment and also to the measurement methods. The list of authors that investigated this property of plain concrete is widely extensive although this number decreases substantially when it comes to fibre reinforced concrete. The main conclusions out of their discussions will be described in this part of the project together with graphs to help getting a better understanding on electrical resistivity behaviour and also to motivate the election of parameters that were going to be studied and also how the study was going to be performed.

Effects of composition

The electrical resistivity of concrete is a property related to the microstructure of the cement paste, and then, all the factors influencing the cement matrix will also influence the resistivity.

It was determined by (Hughes et al. 1985) that the resistivity of the cement paste is lower compared with the other materials forming concrete, which means that the higher the cement paste content in a concrete mix, the lower the resistivity.

The water cement ratio is a factor that also affects the resistivity but it must be noted that its effects differ significantly in mortar and in concrete when studied under the same conditions, something that is explained as an effect of the difference in aggregate size (Gjørv et al. 1977). Also, the resistivity of mortar is about 1/5 the resistivity of concrete made out of the same paste. When it comes strictly to concrete, (Monfore 1968) found out that the resistivity of the cement paste increases as water-cement ratio decreases determining that the resistivity of a paste with a water-cement ratio of 0.6 was half the resistivity of a paste with a water-cement ratio of 0.4.

Both, cement content and water-cement ratio have also a combined effect on the resistivity. (Hughes et al. 1985) found a decrease of 50% in the resistivity of concrete when increasing the water-cement ratio by 0.15 for a cement content of 400 kg/m^3 while the same change in a concrete mix with 350 kg/m^3, lead to a decrease the resistivity by less than a 40 %.

Finally, the effect of the water-cement ratio is affected by the degree of saturation of concrete. Greater effects in resistivity due to changes of water-cement ratios can be found when the degree of saturation is lower as it can be seen in Figure 1, that shows the results of the studies of (Gjørv et al. 1977), which measured how resistivity was affected by an increase of water cement ratio exposed to different conditions:

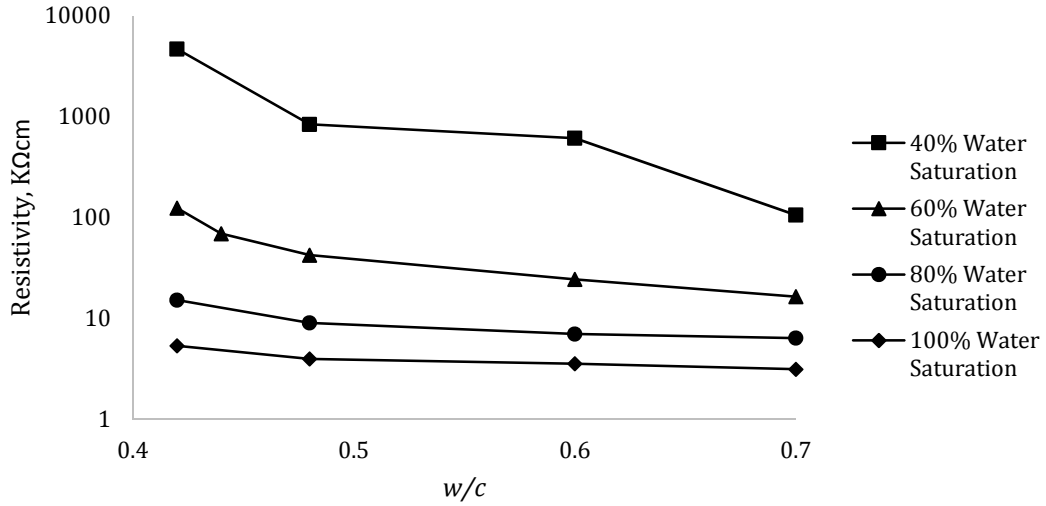

Figure 1 Resistivity against w/c (Gjørv et al. 1977)

Other parameters related to the composition of concrete that also affect the electrical resistivity is the volume and type of aggregate. (Monfore 1968) made studies on different types of aggregates to find its resistivity value. Depending on

the type of aggregate, the resistivity could range from 180 Ω·m in the case of sandstone to values of 8800 Ω·m in the case of granite, which are enormous comparing them to the ones in the cement paste. Due to the quantities used in the mix of concrete, the influence of these aggregates in not decisive although increasing the aggregate content will also increase the resistivity (Hughes et al. 1985). According to (Büyüköztürk & Taşdemir 2013), not only the volume of aggregates makes an effect on the resistivity of concrete but also the type and the size affect it. Using samples with crushed stones (16-32 mm) and others with crushed stone sand (0-4 mm) it was corroborated that a higher content increases the resistivity but also it was found that the bigger the aggregate, the higher the resistivity as it can be observed in Figure 2. This was explained due to the higher porosity present in the interfacial zone between aggregates and cement paste. The interfacial zone increases its total volume with smaller aggregates due to a larger aggregate surface area.

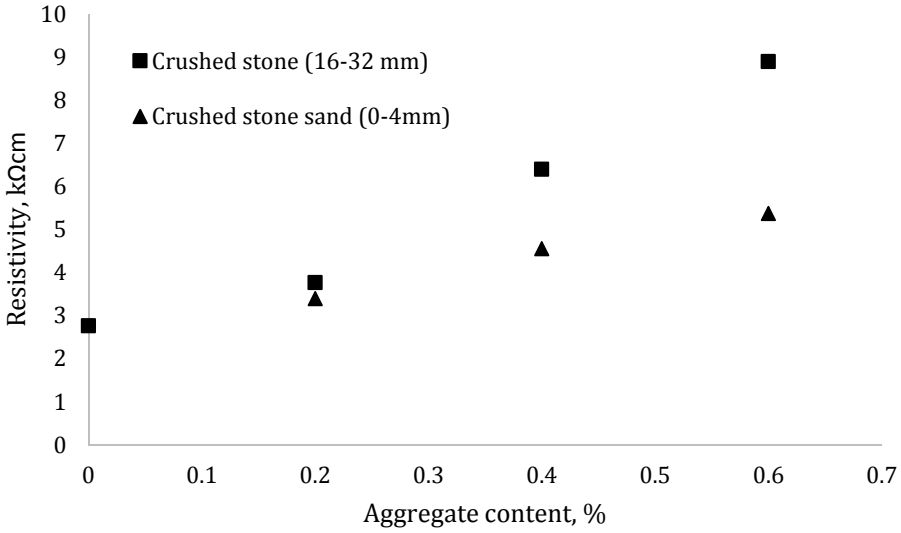

Figure 2 Resistivity against aggregate content (Büyüköztürk & Taşdemir 2013)

Effects of fibre content

The main purpose of adding fibres to a concrete mix is to improve the mechanical properties of the composite, but there are some cases in which these fibres can potentially affect the electrical behaviour of the concrete. This effect becomes manifest when the fibres are conductive with respect to the concrete matrix, something that may occur when using steel or carbon fibres.

When enough conductive inclusions exist in the mix, the composite acts as an electrical conductor (Solgaard et al. 2010) and being resistivity the inverse of conductivity, its value decreases. The resistivity of samples containing fibres can differ in large proportions depending on the location of the measurements and this is because the heterogeneity and the anisotropy of the concrete are directly dependent on the presence of steel inclusions within the matrix (Lataste et al. 2008).

So it is safe to say that the resistivity is always lower for mixes containing fibres than when compared with plain concrete when measuring with AC although this fact is not so clear with DC.

As previously discussed, the influence of the volume fraction of steel fibres does not generate such a big impact in the electrical resistivity of concrete as the variation of the moisture content but it has been shown that the relative impact of adding steel fibres gets higher when the moisture content of the concrete decreased (Solgaard et al. 2013) as it can be seen in Figure 3.

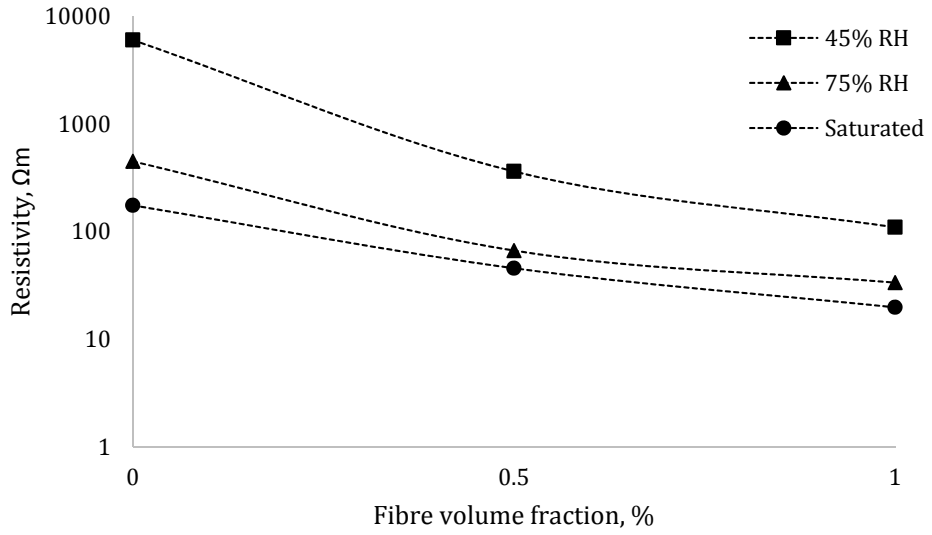

Figure 3 Resistivity against fibre volume (Solgaard et al. 2013)

Effects of fibre orientation

Even less studies have been carried out to study this parameter, but according to (Lataste et al. 2008), the electrical behaviour of concrete and specially, its resistivity is affected not only by the presence of fibres but also by their orientation. It was demonstrated that the higher resistivity value is found when the fibres are oriented perpendicularly to the direction of measurement. This can be simply explained when imaging the fibres as a net on a transversal plane: when the electrical current is injected parallel to it, the net supports electrical current conduction and thus, decreases the electrical resistivity but, when the current is applied perpendicularly to it, its influence on conduction is minor and so is the decrease of resistivity.

Effects of moisture content

The parameter that affects the electrical resistivity of concrete most is the moisture content. To help understanding why this happens, there is a need of explaining how this is also related to the pore structure of the cement paste, as the current is carried by pore water. It was (Powers 1958) who defined a difference in between pores, classifying them into three types: the air voids which are the

ones that enter in the paste during the mixing of fresh concrete, the capillary pores and the gel pores in which the total evaporable water is held.

In general terms, it can be said that when the moisture content decreases, the electrical resistivity of concrete increases as there is less pore water and thus, less current can be transported. In these terms, (Hunkeler 1996) determined that the conductivity of concrete is essentially zero at a relative humidity of 40% and although at this condition there is still water in the gel pores, it is not conductive as it is bonded to the surface of the cement paste. The effects of the drying of concrete on its resistivity were studied in (Gjørv et al. 1977) by drying specimens with different water-cement ratios from 100% to 20% saturation. The resistivity was measured in four different saturation levels as it can be seen in Figure 4, and the results verified that there is an increase in resistivity when moisture content decreases but also shows that the water-cement ratio also has an effect on resistivity.

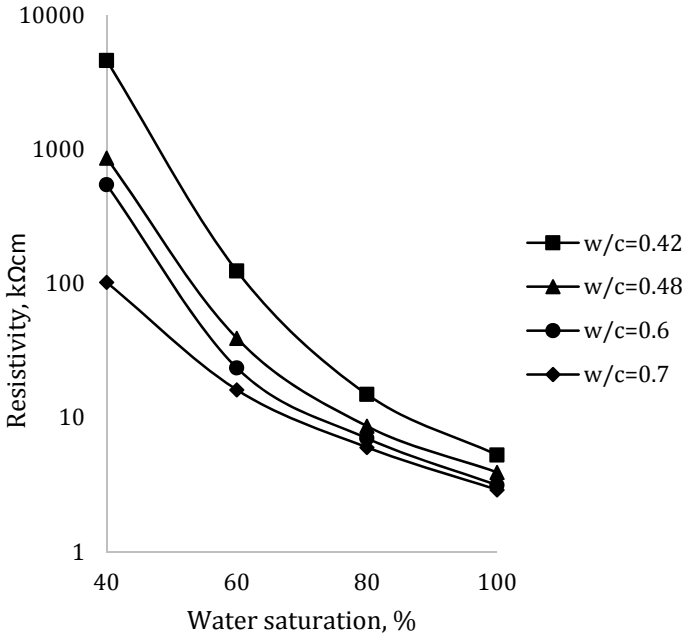

Figure 4 Resistivity against water saturation (Gjørv et al. 1977)

Also in (Büyüköztürk & Taşdemir 2013), specimens were subjected to three different environments: saturated condition with dry surface, air-dry and oven dry. As it can be seen in Figure 5, the air dry condition increased the resistivity in almost 2 kΩ·cm with respect to the saturated one and the oven dry showed values that doubled the ones for air-dry condition. All results supported that more pore water implies a better current conduction and thus, lower resistivity.

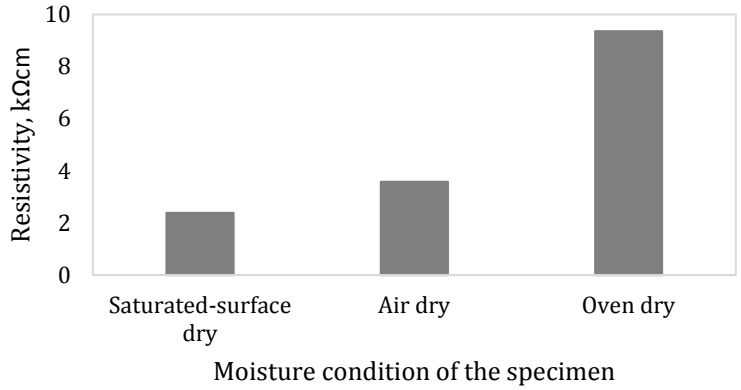

Figure 5 Resistivity against moisture condition (Büyüköztürk & Taşdemir 2013)

The extreme case is found when the samples are oven dried and (Hammond & Robson 1955) determined a value for the resistivity of $4x10^4$ MΩ·cm.

Effects of temperature

Temperature is a parameter that also affects resistivity and its effects depend directly on the behaviour of the electrolyte: as the temperature raises, the viscosity of the fluids (in this case the pore water) decreases facilitating the ion mobility. The current is carried by these ions and thus, the resistivity decreases (McNeill 1980).

This relationship is given directly by the law of (Rasch & Hinrichsen 1908), as expressed in Arrhenius equation:

$$R_2 = R_1 e^{A\left(1/T_2 - 1/T_1\right)}$$

where R_1 and R_2 are resistances (Ω) at temperatures T_1 and T_2 (K) and A is the activation energy (K).

Due to the numerous changes that can be produced in temperature in a short period of time, (Spencer 1937) developed a curve to correct resistivity measurements to a basis of 21 °C, curve that was later completed by (Woelfl & Lauer 1979) by adding data from (Monfore 1968). The three studies found a sensitivity of about 3% per degree Celsius (with reference to 21°C) decreasing the resistance with increasing temperature and also suggesting that the temperature effect is independent from other previously commented aspects of the composition of concrete.

Curing the specimens at 21 °C for 54 days over water in a container first and then over a salt solution (75% RH) for 14 days, (Hope et al. 1985) measured the resistivity in different water-cement ratio mixes under different temperatures finding the results represented in Figure 6:

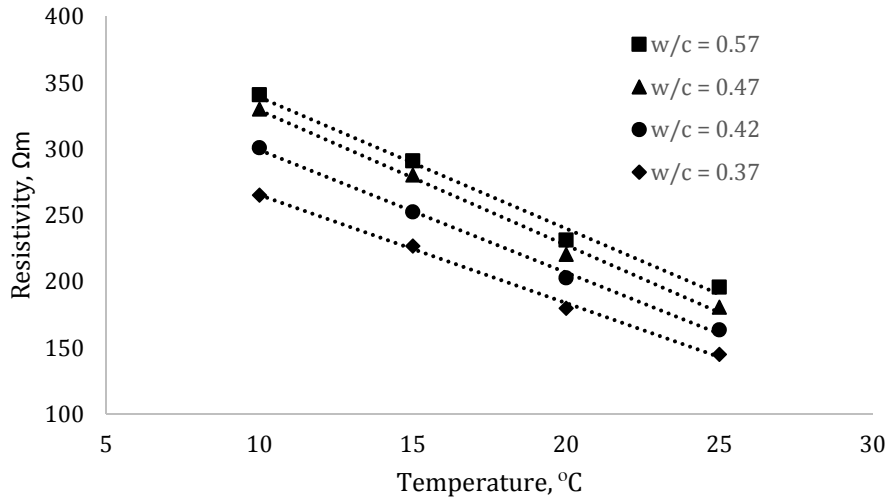

Figure 6 Resistivity against Temperature (Hope et al. 1985)

The results showed in Figure 6 corroborate the assumption that resistivity increases with decreasing temperature and also verify the data from (Woelfl & Lauer 1979) being the tendencies all parallel.

The value for the constant *A*, in the above equation, known as activation energy, varied within different studies. (Monfore 1968), with the studies about cement paste set it to 2200 K while in (Hope et al. 1985), the experiments in concrete defined its value to 2900 K. Finally, the studies in (Elkey & Sellevold 1995) determined *A* in a range that could go from 2000 K to 5000 K being the most common values around 3000 K. They also suggested that the temperature effect is dependent on the grade of saturation on the concrete as it was found that with conditions below 30% RH, the sensibility was around 5% per degree Celsius while in environments over 70% RH this sensibility decrease to 3% per degree Celsius.

Effects of time

As a general rule, it can be said that resistivity tends to increase with time, although once again, this rise depends on the curing environment. The increase for air-cured specimens is due to a loss of moisture while the one for moist curing is based on the hydration of the cement and thus, the first one is bigger.

When speaking about the moist curing, first it was (Monfore 1968) who found out that resistivity doubled its value between 7 and 90 days when studying moist cured concrete with a water-cement ration of 0.40. This was later corroborated with similar results by (Mc Carter et al. 1981): from 1 to 30 days, the resistivity increased by a factor of 1.5 and then, up to the 120 days their study last, the resistivity just varied slightly, concluding that the 90% of the rise happens during the first month of curing. This last fact, was also supported by the studies in (Hope et al. 1985) which also showed that the greatest growth in the resistivity values occurs during the first 30 days of curing. The results from these experiments are shown in Figure 7.

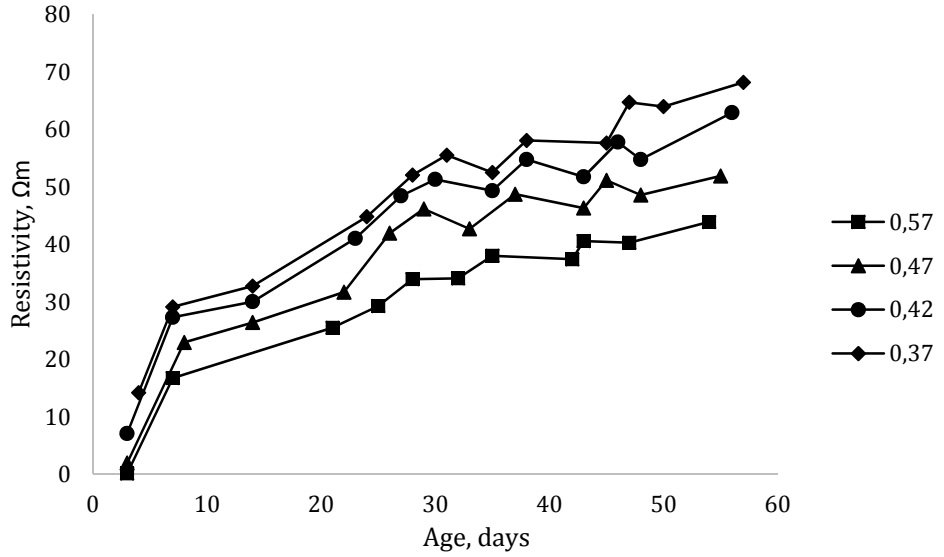

Figure 7 Resistivity against age. (Hope et al. 1985)

These greater raises in the air-cured concrete, were later corroborated in other studies. (Monfore 1968) found a 20-fold increase in specimens that were first cured in water for seven days and then exposed to a 50% relative humidity conditions over a year. Also (Woelfl & Lauer 1979) found in their studies that the resistivity increased by a factor of 30 from 3 to 23 days.

Effects of chlorides

As it was previously mentioned, the resistivity is affected by the characteristics of the electrolyte. It is known that the conductivity of an electrolyte is proportional to the number of ions that can be found in it and to the velocity of these. Water by itself has a small amount of ions and thus, its conductivity is low but when adding sodium chloride (NaCl) to it, the molecules of the dissolved salt dissociate to form both negative chloride ions and positive sodium ions that increase the conductivity of the fluid considerably (McNeill 1980). Being the conductivity the inverse of the resistivity, this last decreases.

Chloride ingress is one of the most important parameters that influence the corrosion of reinforcements and because of this, several studies have been performed with interest in including chlorides in the mixing water. It is assumed that it would reduce the electrical resistance of concrete in accelerated corrosion tests with impressed current but it will also reduce the initiation period in reinforced concrete corroding naturally.

Adding sodium chloride into the mix of concrete will decrease the resistance and this effect is more severe as the saturation increases. (Elkey & Sellevold 1995) found in their studies that saturated concrete with 6% NaCl per cement weight in its mix had a resistivity that was less than 40% of the one in concrete without added chlorides. They also found that a difference in chloride content would not make a big difference as similar values were measured for 3% and 6%, meaning

that there must be a value in which the addition of more chlorides does not affect the conductivity of the electrolyte.

Along the same lines, (Henry 1964) studied four different types of concrete with sodium chloride contents that went from 0 to 31.3 g of salt per kg of water and as it can be seen in Figure 8 determined that the highest resistivity value was found in the concrete without added chlorides and that once there are chlorides in the mix, the content just influences the resistivity slightly. Also in this direction, (Hunkeler 1996) found a decrease in resistivity of 27% when adding 0.45% of chlorides per cement weight to the mix.

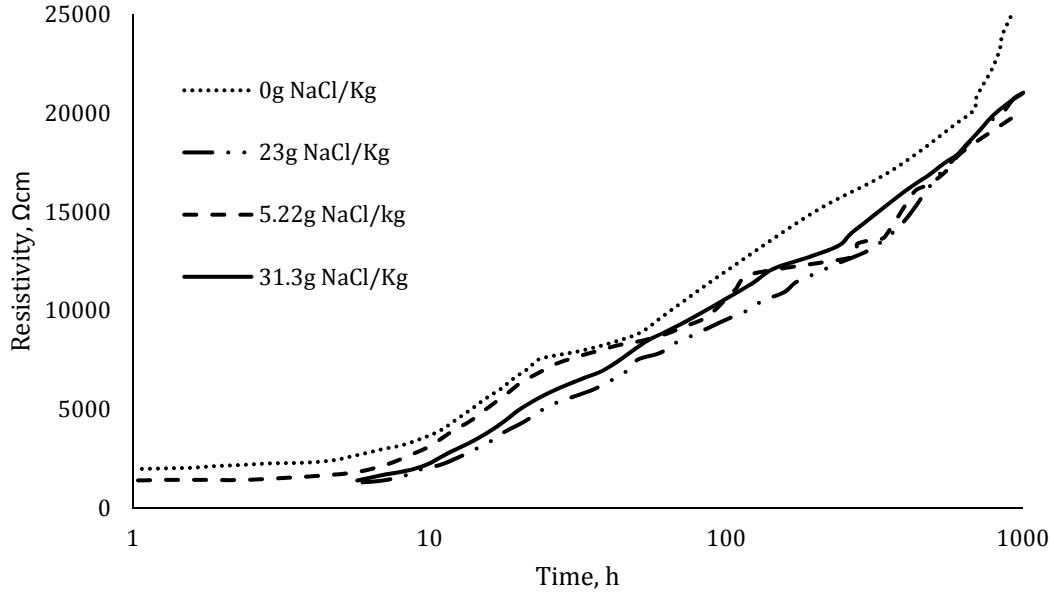

Figure 8 Resistivity affected by chloride content (Henry, 1964)

Frequency

As the resistivity of concrete is one of the main parameters to assess the corrosion tendency of structures, different types of measurements have been made on it with interesting results. Some of the authors such as (Torrents et al. 2000), (Peled & Shah 2001) or (Mason et al. 2002) studied the resistivity by measuring it with electrochemical impedance spectroscopy at high frequencies and confirmed that indeed, the frequency affects the resistivity and also that this dependence is affected by moisture content and temperature of the concrete.

The resistivity is measured indirectly by a system with two electrodes placed on each side of the concrete specimen to measure its resistance. Usually the equipment used can work with frequencies that go from 100 Hz to 100 kHz. It was demonstrated in (Larsen et al. 2007) that the effect of frequency in ranges from 100 Hz to 1000 Hz can be neglected in wet concrete (around 90% in their experiments) but are not as small with drier concrete (below 60%) when it comes to temperatures above zero. In both cases, when temperatures drop below zero, the effects of frequency are higher. The deviations in resistivity with respect to the modelled resistivity values at different temperatures (20, 2, -14 and -28°C) found

in (Larsen et al. 2007) are plotted for dry and wet concrete in Figure 9 and Figure 10 respectively.

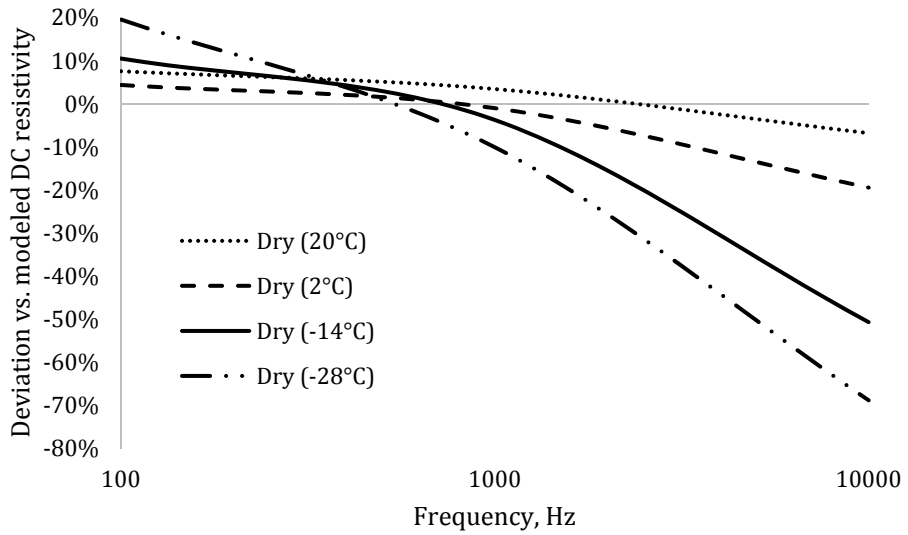

Figure 9 Deviation from theoretical resistivity in dry concrete (Larsen et al. 2007)

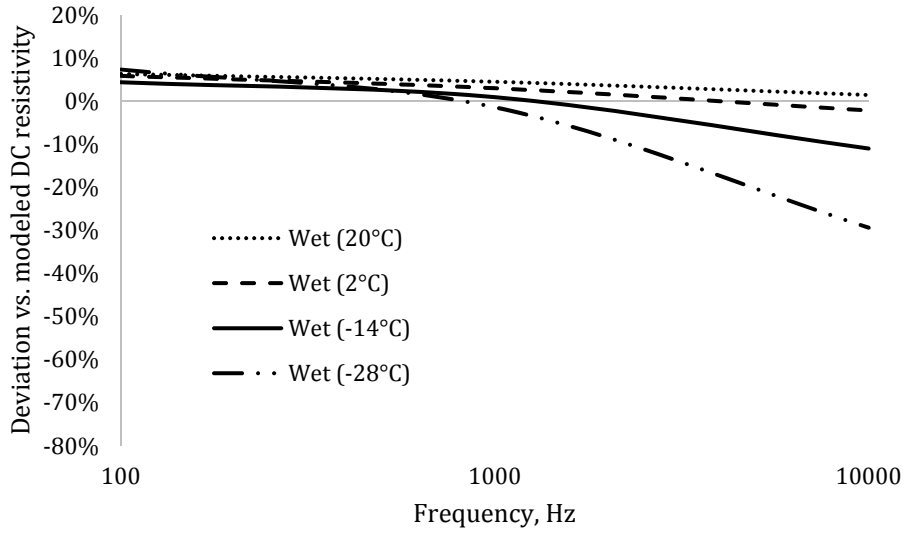

Figure 10 Deviation from theoretical resistivity in wet concrete (Larsen et al. 2007)

In conclusion, and as it can be seen in the graphs, it can be said that the measurements in the range from 100 Hz to 1000 Hz will be accurate enough to determine the electrical resistivity of concrete at temperatures above zero.

2.1.3 Effects of DC stray current on the steel fibres

There are plenty of studies on the damages that stray current can cause to reinforced concrete but there are not so many on how the stray current affect fibre reinforced concrete.

The stray current is originated in DC distribution lines, railway systems or alternating current among other sources, and flows through structures either outside the concrete, e.g. pipeline, or inside the concrete through the reinforcement bars or the steel fibres, being the last case the one studied in this project.

Stray current corrosion in fibre reinforced concrete is less aggressive than the same type of corrosion in concrete with reinforcement bars. The main reason for this is the short length of the fibres which causes that, in the volumes that fibres are added to the concrete mix (0.25-1%), fibres are not usually in contact and thus, there is no continuous metallic path for the stray current to go through (ACI Committee 544.5R-10 2010).

When it comes to composites in which one of the components is conductive, as it is the case of fibre reinforced concrete, it is common that the intensity-voltage plots are nonlinear. The slope of the intensity-voltage plots corresponds to the inverse of the DC resistance of the sample. According to the results showed in (Wen & Chung 1999) and (Hixson et al. 2003), plain concrete shows a single slope (linear) behaviour while fibre reinforced concrete shows a two-slope behaviour: at low voltages, the slope is flatter and when it reaches a certain voltage, the slope becomes higher showing a lower resistance.

The reason for this two-slope behaviour to happen is that the conductive fibres have thin, resistive and high capacity layers on their surface that insulate the fibres at low fields in DC making them behave as insulating fibres but, when the field is raised, the layers short out and the fibres start to act as conductive elements inside the concrete. (Torrents et al. 2000) explains this two-slope behaviour with an electric analogy based on the simplified equivalent circuit represented in Figure 11, where the fibre coating is represented as a frequency-activated switch. With low fields it would act as an open circuit due to the coating resistance that make the fibres behave as insulating elements but when the field is raised the switch is thrown. In both cases, the resistance of fibres is neglected.

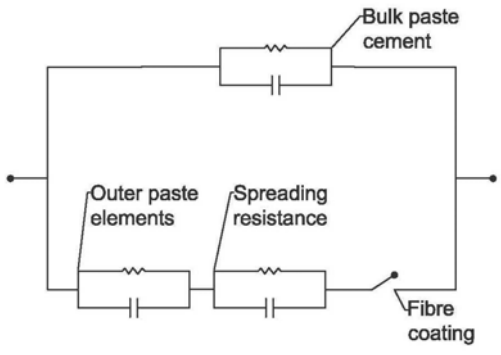

Figure 11 Electric analogy for the two-slope behaviour of SFRC

This phenomena was also studied in (Solgaard et al. 2013) concluding that when there is no chloride contamination, the stray current only circulates through the steel fibres above a voltage of 1.2 V (a potential gradient of around 15 V/m as shown in Figure 12) and that there is an important length effect as due to the disposition of the fibres in the concrete, this is randomly distributed and without forming continuous paths, the stray current would be forced to enter and exit fibres dissipating the driving voltage so the risk of stray current corrosion on fibre reinforced concrete is low.

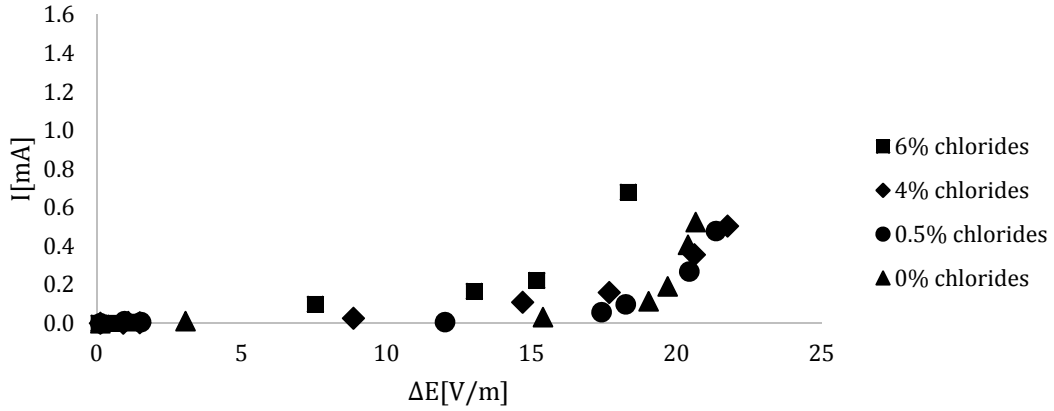

Figure 12 Current transferred by the fibres as a function of the potential gradient (Solgaard et al. 2013)

2.2 Corrosion rate

2.2.1 Theoretical background

There are four elements that have to be present for corrosion to occur, these are: (1) an anode where the metal oxidizes; (2) a cathode where a reduction process occurs; (3) an electrical connection between both; and (3) an electrolyte surrounding them. In the case of steel reinforced concrete, it is the concrete itself which works as an electrolyte. The potential measured gives an indication of the thermodynamic state of steel and with it, the probability of corrosion can be estimated. In aerated concrete, resistivity can also limit the rate at which corrosion proceeds.

The corrosion rate could be defined as the amount of corrosion produced by a unit of surface area when referred to a specific period of time. An indication of the average corrosion rate of a concrete sample over a certain period of time can be found by weighting differences before and after submitting the sample to the corrosive environment (Andrade & Alonso 1996) while corrosion rate measurements are usually performed by means of polarization resistance techniques.

There are some authors that determined that the increase of resistivity could limit the corrosion as there is less current passing through the electrolyte. In Table 1, suggested values by (Langford & Broomfield 1987) can be found although later on, (Broomfield et al. 1993) determined that to consider a low corrosion rate,

resistivity must exceed 500 Ω·m and that corrosion can be stop entirely with a resistivity value over 1000 Ω·m.

Table 1 Relationship between resistivity and corrosion rate (Langford & Broomfield 1987)

Resistivity, Ω·m	Corrosion rate
< 50	Very high
50 – 100	High
100 – 200	Moderate to low
> 200	Low

Corrosion rate can be expressed as penetration rate measured in μm/year although in laboratory test, it is usually measured in electrochemical unit i.e. in mA/cm^2. The conversion of electrochemical parameters into gravimetric ones is made by Faraday´s law:

$$\frac{I \cdot t}{F} = \frac{\Delta W}{W_m / Z}$$

Being I the electrical current (A), t time (s), F Faraday´s constant (9.65×10^4 C mol^{-1}), ΔW weight loss due to corrosion (g), W_m molecular weight of metal and Z its valence (Andrade & Alonso 1996).

The corrosion rate can be negligible if it is below 2 μm/year, low between 2 and 5 μm/year, moderate between 5 and 10 μm/year, intermediate between 10 and 50 μm/year, high between 50 and 100 μm/year and very high for values above 100 μm/year (Bertolini et al. 2004).

Corrosion directly affects the service life of reinforced concrete structures and the effect on its safety could be fatal if it is not taken into account during the design phase. Corrosion of reinforcement is usually indicated either by rust spots on the surface of the concrete or by damages to its cover. These damages are caused by the tensile stresses created by the increment of volume the corrosion products cause, which may, in turn, generate cracks or spalling. Also when the corrosion is localized, the cross section of the reinforcing bars is reduced decreasing the loading capacity and the fatigue strength of the structure (Bertolini et al. 2004). A summary of the consequences of corrosion in concrete structures is shown in Figure 13.

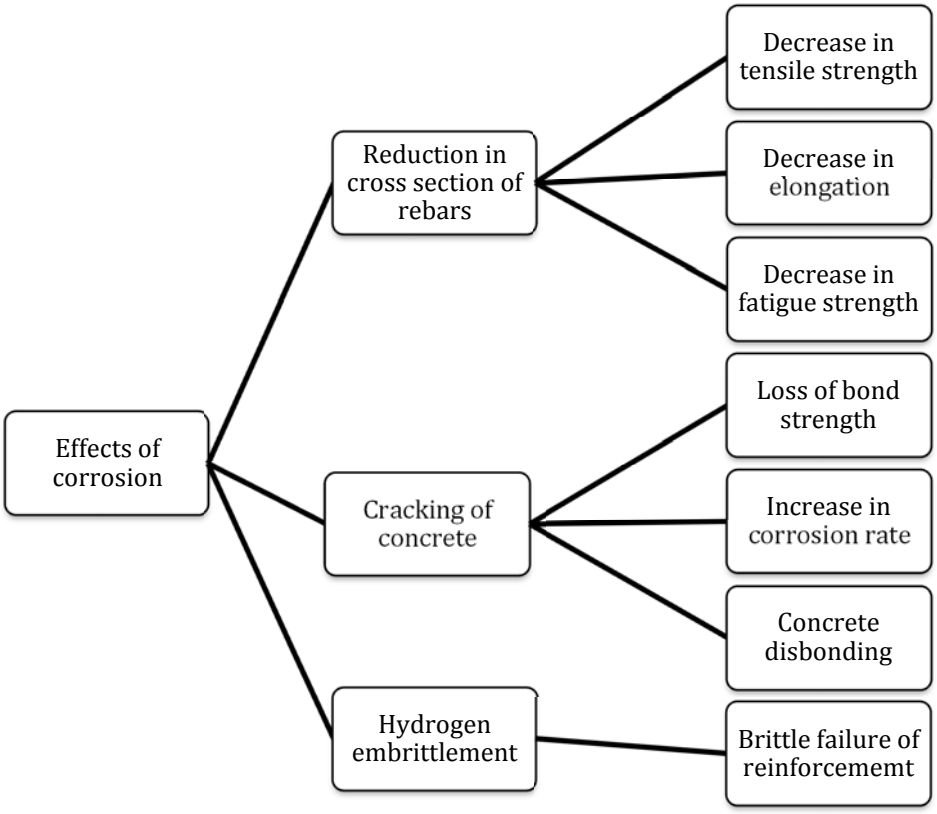

Figure 13 Structural consequences of corrosion in reinforced concrete structures.

2.2.2 Existing studies

The transport of ions through the concrete matrix is one of the parameters that control the corrosion process of the embedded reinforcement steel bars. The electrical resistivity of a material determines the capacity it has to transfer charged particles, e.g. ions and thus corrosion rate and electrical resistivity are related to each other.

Once the relationship between resistivity of concrete and corrosion rate is accepted, the assumption would be that an increasing concrete resistivity will decrease the corrosion rate under common environmental exposure conditions (Hornbostel et al. 2013). However, some differences are found in the studies published, making it impossible to state a single rule in between the parameters as this relationship also depends on other parameters e.g. type of corrosion or measurement method. The criteria to quantify the corrosion rate with the electrical resistivity is wide and differs within studies, e.g. see Table 2. The importance of finding this relationship lays on the difficulties of measuring the corrosion rate in the field compared with measuring the electric resistivity, and with it, the assessment of the corrosion stage of a structure would be more efficient: cheaper and faster, and this is the main reason why so many studies aimed at it.

Table 2 Criteria for the assessment of corrosion in terms of resistivity

References	Corrosion rate in terms of resistivity [Ωm]		
	High	**Moderate**	**Low**
(Cavalier & Vassie 1981)	<50	50-120	>120
(Hope et al. 1985)	<65	65-85	>85
(López & González 1993)	<70	70-300	>300-400
(Morris et al. 2002)	<100	100-300	>300
(González et al. 2004)	<200	200-1000	>1000
(Elkey & Sellevold 1995)	<50	Under discussion	>100-730
(Andrade & Alonso 1996)	<100	100-1000	>1000-2000
(Polder et al. 2001)	<100	100-1000	>1000
(Broomfield & Millard 2002)	<50	50-200	>200
(Smith et al. 2004)	<80	80-120	>120

The objective of this section is to try to help understanding the relationship in between corrosion rate and electrical resistivity by identifying the parameters that affect it. To achieve this, an extensive literature review on previous studies was made and similarities and differences in between the studies are commented.

Type of corrosion

The alkaline nature of concrete naturally provides a protective coating to the embedded reinforcing bars, but this passivation layer can break down due to two different mechanisms: the reduction of the alkalinity caused by carbonation or the presence of chloride ions. While carbonation induced corrosion affects to a larger area of reinforcement surface and to a wider range of structures, chloride induced corrosion is more dangerous to the structure as it develops localized pits but in a more aggressive way (Figure 14).

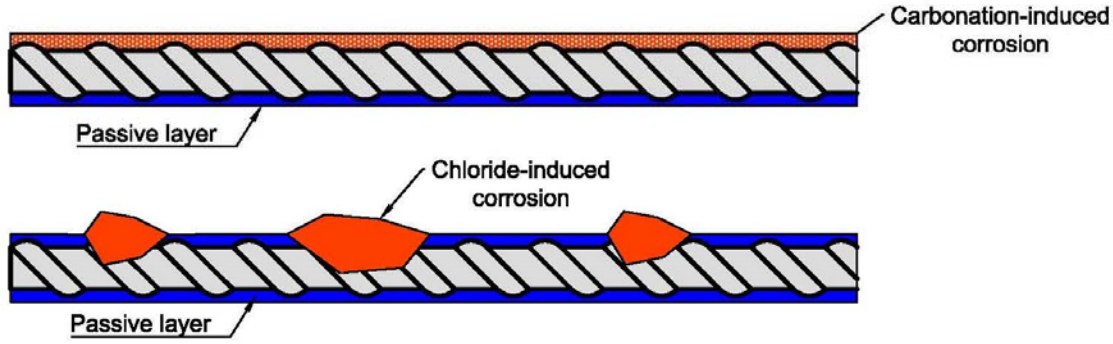

Figure 14 Carbonation- and chloride-induced corrosion

Carbonation is the process that neutralizes the alkalinity of concrete when the calcium hydroxide, $Ca(OH)_2$, found in the cement matrix reacts with carbon dioxide, CO_2, forming calcite, $CaCO_3$. The usual concrete pore solution pH of about

12-13 drops to values below 9, turning the passivation layer unstable and allowing corrosion in the rebar if the adequate conditions are present (Heiyantuduwa et al. 2006).

Carbonation in chloride contaminated concrete causes the bound chlorides, as calcium chloroaluminate hydrates, to be released making the pore solution even more aggressive (Tuutti 1982). The only damages that carbonation cause in concrete is that it may shrink. Indeed, in case of OPC, the concrete may increase its strength leaded by a reduction in its porosity (Bertolini et al. 2004).

Both exposure factors and concrete properties affect the rate of carbonation. When speaking about the first group, humidity has an important role as the diffusion of CO_2 within concrete is slowed down through water filled pores, reaching a zero CO_2 diffusion rate in water-saturated samples. But also, water is needed for the carbonation reaction to occur so in completely dry samples, carbonation can be neglected (Tuutti 1982). The other two factors included in this group are the CO_2 concentration in the atmosphere and the temperature, both being directly proportional to the carbonation rate. Being affected by this parameters, carbonation of concrete is nowadays gaining importance because of the climate change (Yoon et al. 2007).

The concrete properties that mainly affect its carbonation rate are its permeability and its alkalinity. The permeability affects the diffusion of CO_2: a decrease in the capillary porosity slows down the penetration of carbonation and this is reached by decreasing the water-cement ratio (Sergi 1986). Alkalinity has lower effects in the carbonation rate. It is directly proportional to concrete capacity to fix CO_2 but its effects can be compensated with a lower permeability of the cement paste (Bertolini et al. 2004).

On the other side, chloride-induced corrosion results in localized pits. In this case, the cathodic area is much bigger than the cathodic area creating a macrocell in between both and it usually occurs when the active corroding bar is coupled to other one with lower corrosion rate (Hansson et al. 2006) although it is also possible to find macrocells on single bars exposed to different environments.

Historically, chlorides have been added to the concrete mix unknowingly through contaminated additions or deliberately to accelerate the hydration. Nowadays, the European standard EN 206 allows maximum chloride content additions from 0.2 to 0.4% chloride ions by mass of binder in reinforced concrete or 0.1 to 0.2% for prestressing reinforcement in order to limit the chloride induced corrosion. Chlorides also penetrate in concrete from the environment, mainly in marine environments and roads that use de-icing agents. It can be seen in Figure 15 that the probability of having reinforcement bars corroding strongly depends on the chloride content of the concrete they are embedded in.

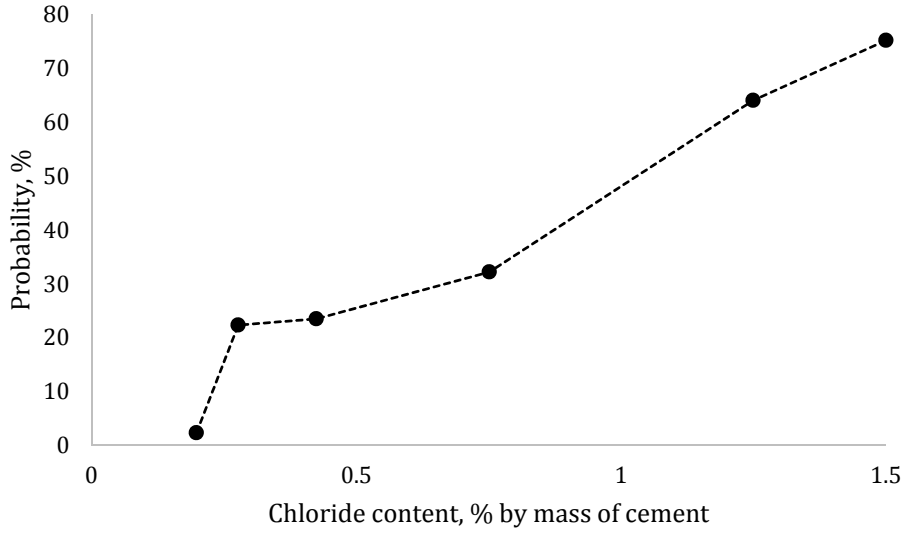

Figure 15 Percentage of reinforcement showing corrosion in relation with chloride content (Vassie 1984)

Chloride induced corrosion starts once the chloride values in the concrete reach a critical value that is known as threshold value. This value is different depending on numerous factors e.g. the pH of concrete, the electrochemical potential of steel or the environmental conditions the concrete is subjected to. Submerged structures need higher levels of chlorides to initiate the corrosion than structures exposed to the atmosphere as the oxygen supply is hampered (Alonso et al. 2002). The chloride content required by a structure to reach average corrosion rates higher than 2 mA/m^2 is defined as its chloride threshold (Andrade 2003).

The threshold level covers a wide range of values, but usually a higher content of chlorides turns into a higher frequency of finding corrosion, i.e. (Vassie 1984) found out in a survey of UK concrete highway bridges that 76% of the bridges showed corrosion at chloride levels above 1.5% by weight of cement but that the percentage drops to 2% when the chloride content was less than 0.2%. With results like this, there is a dispute whether if chloride content should be considered a threshold level or if it should considered as a parameter for assessing the risk of corrosion.

The damages caused by this type of corrosion are more critical as once the corrosion is initiated, the environment inside pits is very aggressive, increasing the chloride content and lowering the alkalinity which leads to an acceleration of the corrosion rate (Bertolini et al. 2004).

Steel fibres combined with traditional steel reinforcement bars

Steel fibres are more and more frequent used together with reinforcement bars in structural concrete. The main reason for this combination is that, while traditional reinforcement bars act with structural purposes, steel fibres minimize the crack widths implementing the permeability and thus, improving the protection of the steel rebars.

As explained before, in the presence of enough chlorides, the passivation layer naturally formed to protect the steel embedded in concrete breaks down allowing

pitting corrosion, which causes, among other, a reduction in the cross section of the bars which could compromise the security of the structure. If the cracks in concrete are minimized, the chloride ingress will be reduced and thus the risk of pitting corrosion will decrease. In this direction, it seems that the addition of fibres would be beneficial although there is also a concern about how this would affect the corrosion rate.

In order to determine if the addition of steel fibres would be beneficial, several studies were made on that topic. Some of them, i.e. (Mangat & Gurusamy 1987) (Raupach & Dauberschmidt 2002) or (Dauberschmidt & Raupach 2005) determined a better behaviour of steel fibre with respect to corrosion compared with traditional reinforcement when the structures are exposed to a chloride environment. The chloride threshold in which corrosion initiates is higher when it comes to steel fibres, something that could be explained either by the short length of the fibres or by the interfacial layer formed in between fibre and concrete. But also the quality of the steel and how much surface defects exists have an influence.

Other studies instead, determined that the since the cover depth of fibre reinforced concrete is almost inexistent and thus fibres close to the surface exposed to the chlorides would corrode and degrading the surface (Granju & Balouch 2005). Also (Solgaard et al. 2013) observed that under extreme conditions, that is when fibres are depassivated and exposed to a corroding environment, the reduction of electrical resistivity may lead to a noticeable increase in the corrosion rate.

So as it can be seen, it seems to be no agreement in between the studies and so, further studies on the topic should be made to be able to safely determine if the addition of steel fibres is beneficial for the service life or reinforced concrete structures.

3 Experimental programme for resistivity tests

Four different mixes were used to investigate the influence of the fibre content under different moisture conditions on the electrical resistivity of concrete. One of the mixes had no fibres at all in order to be able to compare it with the others and to isolate the effect of the addition of steel fibres.

3.1 Test specimens

For casting the samples, every mix used the same types of materials: the steel fibres were cold drawn steel wire fibres with hooked ends, d=0.55 mm and l=35 mm. The aggregates had a maximum size of 8 mm and tap water was used for the mixing. The mix designs, which had a 0.47 *w/c* ratio, are further explained in Table 3.

Table 3 Mixture proportions, kg/m3

Component	Mix 1	Mix 2	Mix 3	Mix 4
Cement (CEM I 42.5 N SR3 MH/LA)	385	385	385	385
Limestone filler (Limus 40)	180	180	180	180
Fine aggregate (Sand 0/4)	478	474	472	470
Fine aggregate (Sand 0/4)	482	477	476	474
Coarse aggregate (5/8)	635	630	627	625
Effective water	181	181	181	181
Superplasticizer-Glenium 51/58	7.7	7.7	7.7	7.7
Fibre-Steel Dramix® 65-735-BN(Volume, %)	0	0.5	0.75	1

First, the sand, the cement and the filler were dry-mixed, then the coarse aggregates and the fibres (if the mix required so) were added together with tap water. When all these elements were completely mixed, superplasticizer was progressively added to achieve the proper consistency. Following the Standard Test Method for Slump Flow of Self-Consolidating Concrete EN 12350-8 the slump-flow was determined by measuring the flow diameters in two orthogonal directions. These values are given in Table 4.

Table 4 Slump flow in mm

Mix	Slump flow [mm]
1	650
2	700
3	690
4	660

From each mix, a slab specimen 560x360x125 mm (*l* x *w* x *h*) was cast together with two cubes with side length 150 mm to test compressive strength of concrete,

(the test results can be found in Appendix A). After curing for 24 hours, they were de-moulded and prepared for cutting. The specimens used were the same for the different mixes within this part of the investigation: cubes with side length 70 mm cut from the cast slabs. These cubes A1-C7, were extracted at a depth of 30 mm from the top layer and, as seen in Figure 16, the end-pieces were discarded. This was done because the mould could affect the homogeneous dispersion of the fibres.

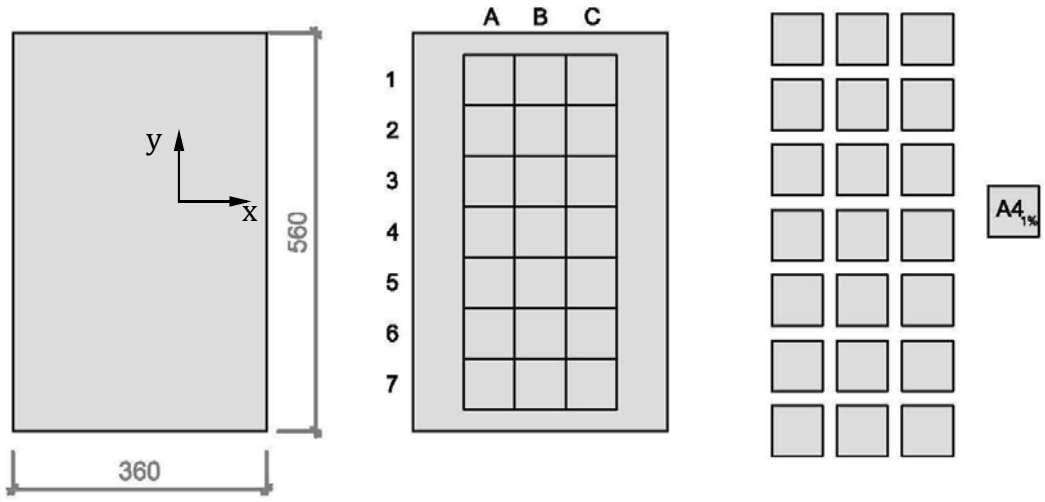

Figure 16 Cutting of specimens from cast concrete slabs

The homogeneity of the mix and the orientation of the fibres have a direct relation with the pouring process. As the study concerns the effects of the orientation of the fibres, it was important to try to ensure a two dimensional orientation so that the majority of the fibres were placed parallel to a plane. Based on previous laboratory studies (Lataste et al. 2008) and (Barnett et al. 2010), it was decided that the mix should be poured in the mould from the centre as they tend to align perpendicular to the direction of flow and through a V-funnel with a rectangular section so that the pouring is continuous (EN 12350-9). Once the funnel was filled with the mix, the gate was opened to let the concrete fall into the mould. The funnel was continuously filled until the mould was completely filled. The process can be seen in Figure 17.

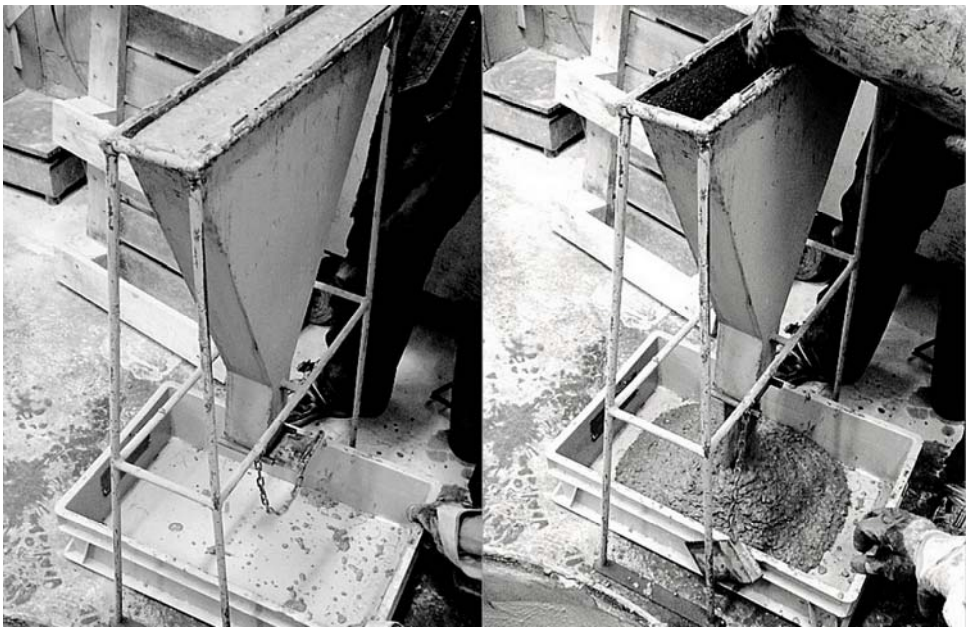

Figure 17 Pouring from the centre

3.2 Methodology

As was found in the literature review, among all the variables affecting the resistivity of concrete, moisture content is, by far, the most important one. This is because of the electrical current passing through concrete is mainly travelling in the form of dissolved ions in the pore fluid ("pore water"). As the moisture content of concrete decreases there is less pore water to carry the current, and the resistivity increases (Nesic et al. 2004).

From each slab, 21 cubes were cut and from now on, they will be classified by rows, from 1 to 7. Each row represents a case of study, so there would be, at least, three specimens of each mix studied under the same conditions.

According to the experimental plan, one row was submerged in tap water to keep the specimens saturated, another was submerged in a chloride solution and the others were dried to a specific moisture content. From the latter, some rows were natural dried at controlled laboratory conditions and the remaining specimens were placed in an oven at 50°C to force them to dry faster. The central row of each slab (4) was kept in the oven until it was completely dry to help estimating the water loss curve of the mix. This plan is summarized in Table 5. It should be noted that when designing this plan, it was considered that in the slabs with higher fibre contents (mixes 3 and 4), due to symmetry reasons, rows 1-7 and 2-6 should have similar behaviours and thus, they were matched to reach to the same relative humidity. In the table, the "N" stands for natural drying and the "F" for forced drying.

Table 5 Experimental plan

Row	Chlorides (%)	RH (%)
1	0	50N
2	0	75N
3	3.5	100
4	0	0F
5	0	100
6	0	75F
7	0	50F

3.2.1 Saturated specimens and resistivity measurements

As soon as they were cut into cubes, rows 3 and 5 of each mix were submerged into a chloride solution and tap water respectively, and the resistivity of each mix was measured every week, starting on day 7 with a constant alternating current with three different frequencies: 100 Hz, 120 Hz and 1000 Hz. The specimens in row 3 were submerged in a 3.5% NaCl solution in order to quantify the effects of increasing the conductivity of the electrolyte.

The uniaxial resistivity test used is quite simple and fast, facilitating the monitoring of the different values through all the weeks the experiment took place. The resistivity of a concrete sample with known dimensions and saturated with water or a chloride solution is calculated using the following equation:

$$\rho = \frac{A}{L} \cdot \frac{U_{s+sp} - U_{sp}}{I}$$

being ρ the resistivity (Ωm), A the cross-sectional area (m^2) of the specimen, L its thickness (m), I the applied current (A) and U_{sp+s} and U_{sp} the potentials (V) measured with the concrete specimen (sponge + sample) and without the concrete specimen (sponge only).

The test arrangement used in the laboratory, which can be seen in Figure 18, uses two conductive plates acting as electrodes in between of which the concrete sample is placed. Wet sponges are used as a contact media to create a good electrical contact between the specimen and the electrodes as this is one of the important assumptions of this test (Spragg et al. 2013). It is assumed that the sponges have an associated resistance and thus, two measures should be made in each case with correction purposes: one with the sponges and the concrete sample and one only with the sponges that will act as a reference (Newlands et al. 2007). In order not to change the concentration of the chloride solution, aluminium foil was used to wrap the sponges and avoid them from absorption of the chlorides when the test was applied in row 3.

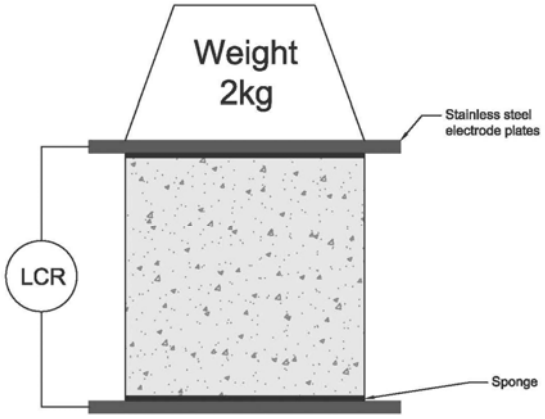

Figure 18 Schematic of the uniaxial resistivity test

Neither voltage nor current were parameters changed during the studies and thus, instead of measuring the potentials and with the aid of a multimeter, the resistances of both, the sample and the reference were directly measured, being the equation now transformed into:

$$\rho = \frac{A}{L} \cdot (R_{s+sp} - R_{sp})$$

In order to study the influence of the fibre orientation, the resistivity was measured in three different directions. According to (Lataste et al. 2008), it is expected that the results show noticeable differences in between the parallel and the perpendicular directions of measuring.

3.2.2 Determination of the desorption curve

Although most of the specimens were placed in the oven to dry at an age of 28 days according to the recommendations, some of them were placed in the oven 5 days before, at an age of 23 days in order to monitor the drying process and to help estimating the time the other samples needed to be in the oven. The samples selected for this purpose were the ones in row 4 as they were the ones to be kept in the oven until they were completely dry, and thus, their behaviour at a certain relative humidity was not compromised by this early entrance in the oven.

The mixes used had a *w/c* ratio of 0.47 with a cement content of 385 kg/m^3. The desorption curves determined by (Hedenblad 1996) do not include this *w/c* but assuming a linear behaviour, the value was interpolated from the ones with 0.4 and 0.5 after the correction factor of the cement content was applied. Further information about this procedure is given in Appendix B.

Once a desorption curve for the mix was defined, the required mass losses to achieved the desired relative humidities i.e. RH = 75% and RH = 50%, were calculated based on it. Before placing the specimens in the oven at 50°C, the excess

water was removed with dry paper and all the specimens were weighed. Initially, measurements were performed each hour to plot the weight loss.

It should be noticed that the required weight loss calculated with the sorption isotherm was expressed in kg/m^3 of concrete and thus, the weight loss required by each cube slightly differs from the others as it is directly dependent on its volume. Taking this into account, the mass loss for each cube was calculated and then, the cubes were divided into groups based on their fibre content as a relation in between this and the drying time was found.

Once the samples got to a 50% RH state, the water loss progression was no longer significant for the experiment and thus, specimens were no longer weighed every hour. As mentioned before, these samples were intended to get completely dry so they were left in the oven. According to (Andrade et al. 1999), the samples can be considered completely dry once the weight loss in 24 hours is less than 0.5 g.

3.2.3 Forced dried specimens

It was considered that in order to assess the influence of the moisture content in the resistivity of concrete samples, tests with relative humidities of 75% and 50% would be adequate. Accordingly, two rows of specimens, 6 and 7, were placed into the oven to accelerate the drying process and reach those humidities respectively.

As mentioned before, each cube required a different mass loss depending on its volume and after calculating each of them, they were dried superficially and placed inside the oven, to oven-dry at 50°C. All the parameters related to weights, times in the oven and estimations can be found in Appendix D. In previous studies by others, the cube samples were sealed on all its sides except for two in order to only ensure 1-dimensional evaporation, see e.g. (Solgaard et al. 2013), (Andrade et al. 1999) but, as the fibre orientation was a parameter investigated in this study, the samples were directly placed in the oven allowing 3-dimensional evaporation.

When monitoring the drying process for specimens in row 4, it was noticed that the samples with higher fibre volumes, dried significantly faster than the ones with less fibres and this difference became even more noticeable when compared to the specimens of plain concrete. This behaviour could be due to two effects. The first one is related to the porosity, as the addition of fibres, especially in higher contents, will increase the addition of entrained or entrapped air increasing the porosity of the samples. Another possible explanation lies on the higher thermal conductivity of steel with respect to concrete, which means that steel fibres could have conducted the heat towards the inner zones of the concrete more efficiently, accelerating thus the drying process.

Once the estimated mass loss was reached, there was a need to redistribute the moisture as it was assumed that, due to the position in the oven and the contact with the trays, the moisture gradients were not equal in the three directions. The samples were then sealed on all its six sides to prevent further moisture loss before placing the specimens back in the oven to accelerate the redistribution. According to (Andrade et al. 1999), this phase can last up to 27 days with a

minimum duration of 14 days. In the present experiment, the redistribution phase lasted 14 days,

3.2.4 Natural dried specimens

At the same time that some samples were force-dried to different relative humidities, it was thought that some samples should be left drying naturally to study if whether this would have any influence on the resistivity. In order to ease the comparison if results, and according to the symmetry of the slabs, row 1 was left to dry in an environment with 50% relative humidity (as row 7) and row 2 was placed in an environment with 75% relative humidity (as row 6).

The procedure followed before placing the specimens in the different environments was the same for all the cases: superficial drying with dry paper and weighing. Once this was made, the samples in row 1 were placed in a climate room at a constant temperature of 20°C and 50% relative humidity and they were left there until equilibrium was reached. For row 2, set to reach a relative humidity of 75%, a sealed box was required. According to (Andrade et al. 1999), placing the samples over a saturated solution of sodium chloride (NaCl) containing excess solid salt in a sealed box with sufficient air circulation and placed it in a controlled temperature environment would be enough to reach 75% relative humidity. They were placed in a sealed glove box as described inside the same climate room as row 1 and left there until they reached equilibrium. In both cases, and according to (Andrade et al. 1999), the equilibrium was assumed when the weight loss in between two consecutive measurements after 24 h was less than 0.1 g. In the experiment, the samples were measured after 56 days in their respective environments.

3.2.5 Effects of steel fibres on the resistivity of concrete under DC

For this part of the project, one single series of specimens was used for the experimental investigation concerning the effects of steel fibre reinforcement on the resistivity of specimens when subjected to a DC field. The samples used were the ones in row 5, which were submerged in tap water from the day after they were cut and the measurements were made after submerged for 56 days. Three specimens per fibre content were studied in the x-direction of the cubes.

The idea of the experiment was to measure the current that flowed through the concrete samples while applying them a varying voltage to assess the threshold value at which the passive layer of the fibres, which insulate them, broke down. To achieve this, the test arrangement, illustrated in Figure 19, was similar to the one used in the resistivity measurements: the concrete sample was placed between two conductive plates that acted as electrodes. Between the plates and the specimen, wet sponges were placed to ensure the good electrical contact as the nature of the test requires. The difference from the resistivity test is that the steel plates are now connected in parallel to a voltmeter and in series to an ammeter. A data logger was used for the data acquisition storing measurements at a frequency of 1 Hz.

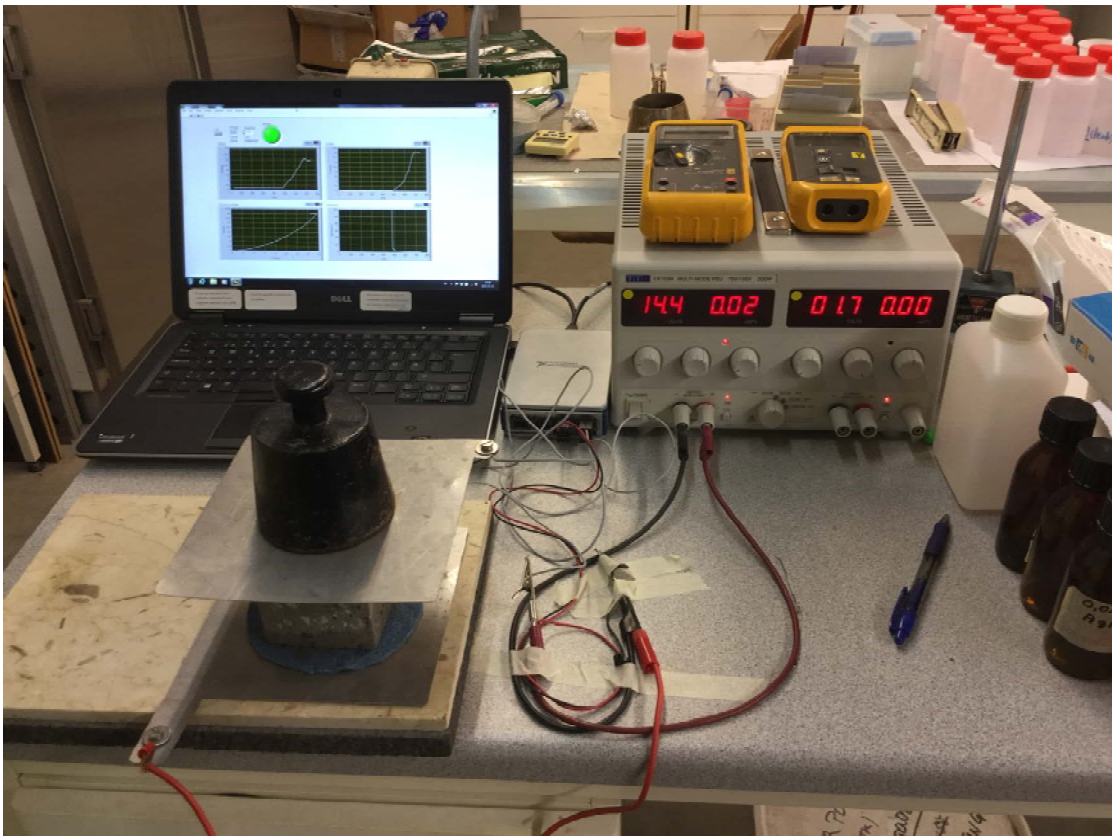

Figure 19 Test arrangement to study the effects of steel fibres on the resistivity of concrete under DC

First, the specimens were taken out of the tap water and with the help of dry paper, they were superficially dried. Then the specimens were placed in between the conductive plates and a constant DC field of 1 V was applied to the specimen with the help of a power supply. Once the current through the specimen was stabilized, with a difference between two consecutive readings of less than 0.5%, the voltage was manually increased until the current reached an upper limit of 20 mA. At that moment, the voltage was kept constant again until the current stabilized to the same criterion. Once this state was reached, the process was reversed by decreasing the voltage until it reached 1 V again.

Based on the assumption that the curves for plain concrete should be linear see e.g. (Wen & Chung 1999) or (Hixson et al. 2003) and after comparing the ascending and the descending curves in the specimens made of plain concrete, it was decided that the values that should be considered for the study were the ones of the descending curve, considering the ascending process as a preconditioning process.

4 Experimental programme to study corrosion rate

Four mixes were also used for this part of the investigation. Three of them had fibre dosages of 1%, 0.75% and 0.5% and the fourth one was made of plain concrete to work as a reference for the influence of fibres. In this experiment, the influence of the orientation was not investigated and consequently the concrete was poured in the moulds without any special considerations.

4.1 Test specimens

A special formwork with a compartment for each mix was made with plywood. The dimensions of each compartment, and thus, each specimen were 270x120x180 mm (l x w x h). Each specimen had embedded three ø12mm reinforcement bars that acted as a working electrode connected to three embedded ø12mm stainless steel bars acting as counter electrodes (Figure 20).

The materials for casting the different mixes were the same as the ones used for the resistivity studies: cold drawn steel wire fibres with hooked ends, d=0.55 mm and l=35 mm, aggregates with a maximum size of 8 mm and tap water for the mixing. In this case, NaCl was included in the mix as a source of chlorides to ensure an earlier corrosion initiation on the specimens: by adding chlorides to the concrete mix, the steel may never be passivated and thus, the initiation period, could be considered zero (Domone & Illston 2010). The mixture proportions are described in Table 6.

Table 6 Mixture proportions, kg/m3

Component	Mix 1	Mix 2	Mix 3	Mix 4
Cement (CEM I 42.5 N SR3 MH/LA)	385	385	385	385
Limestone filler (Limus 40)	180	180	180	180
Fine aggregate (Sand 0/4)	478	474,2	472	470
Fine aggregate (Sand 0/4)	482	477,8	476	474
Coarse aggregate (5/8)	635	629,9	627	625
Effective water	181	181	181	181
Superplasticizer-Glenium 51/58	7.7	7,7	7.7	7.7
NaCl (Volume, %)	2	2	2	2
Fibre-Steel Dramix® 65/35-BN (Volume, %)	0	0.5	0.75	1

In this case, the dry-mix was skipped and all the elements, except for the NaCl, were directly added at the same time together with the tap water. The chlorides were dissolved in 0.5 litres of the required water and poured at the very end of the mix to minimize the accelerating effects of chlorides on the setting of concrete.

From each fibre volume, a specimen with three reinforcement bars and three steel bars, with a diameter of 12 mm each, was cast together with two cubes with side length 100 mm to test the compressive strength of concrete (Appendix A) and two standard cylinders with a 100 mm diameter and 200 mm length for resistivity measurements. Finally, the moulded concrete was covered with a plastic sheet to

avoid evaporation from the surface and then, after curing for 24 hours at laboratory conditions, the samples were de-moulded. The specimens with the reinforcements were partially submerged in a solution with a 10% volume of chlorides while the cubes and the cylinders were submerged in tap water.

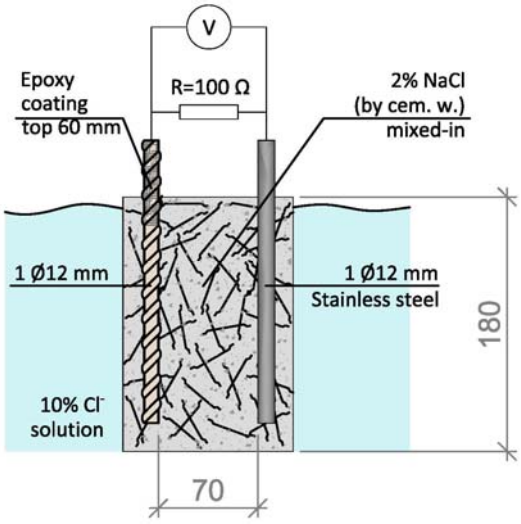

Figure 20 Test specimen for corrosion rate experiments

This part of the study is based on the principle described in the *Standard Test Method for determining effects of chemical admixtures on corrosion of embedded steel reinforcement in concrete exposed to chloride environments* (ASTM G109 2013) and thus, the test specimens were prepared in a similar way, following some of the instructions that can be found on it

First of all, the bars were manually wire brushed in order to remove the excess of initial rust which varied in quantities from 0.02 g to 0.05 g (Figure 21). Then two paint coatings of epoxy resin were applied along 6 cm in one of the ends of the bars, letting them dry for 24 h between the coatings.

Figure 21 Reinforcement bars before and after being manually brushed

4.2 Methodology

The main aim of these tests was to quantify the influence of the addition of steel fibres on the corrosion rate of traditional reinforcement bars embedded in

concrete. For that, four concrete specimens with embedded reinforcement, containing each different fibre contents, were studied by continuously measuring the galvanic current that flowed through them. Within each bar, three reinforcement bars are embedded and connected to a stainless steel bar with a 100 Ω resistance. The bars were placed 70 mm apart so that fibres could flow between them ensuring homogeneity within the sample. With this arrangement, the minimum cover thickness was 13 mm.

To expose the specimens to an accelerating corrosion environment, they were partially submerged in a 10% NaCl solution, inside a plastic tank (Figure 22) that was covered by a plastic sheet to avoid evaporation and ensure the chloride concentration in the solution remained constant during the time the experiments last. With this, the conductivity of the electrolyte was increased while the resistivity of the reinforced concrete was lowered. Additionally, as explained before, 2% NaCl per weight of cement was added directly to the mix to shorten the initiation period explained in the service life model described by (Tuutti 1982). Under this corrosion favourable environment, pitting corrosion was expected to start directly from day one so that, after three months, the results should be significant enough to show differences.

Figure 22 Beam partially subjected in a 10% NaCl solution

The beams also had embedded a reference electrode ERE20 from FORCE Technologies placed closed to the reinforcement bar in the middle of the specimen (blue wire in Figure 22) to monitor the half-cell potential. The stainless steel bars were connected to the reinforcement bars using a known resistance of 100 Ω and each couple electrode-reinforcement bar was connected to a port in a data logger. As soon as the specimens were submerged in the chloride solution, the measurements started recording data each 25 min so that there is a continuous control of the corrosion rate of the reinforcement bars.

After three months partially submerged in the chloride solution, the accumulated weight loss of the reinforcement bars associated to the reduction of their cross section was estimated according to Faraday´s law and compared between the

specimens to try to assess whether the addition of fibres is beneficial or detrimental with respect of the corrosion of the reinforcement bars.

5 Resistivity test results

As previously explained in section 3.2, rows A to C were numbered from 1 to 7 and each row was subjected to different conditions in order to investigate several parameters.

The results of this project are presented in several plots that summarize all the test results gathered during the three months the experimental programme lasted. All the resistivity measurements where made under controlled laboratory conditions using a known mass (2 kg), wet sponges, two stainless steel plate-shaped electrodes and an *Agilent U1733C handheld LCR Meter* as shown in Figure 23.

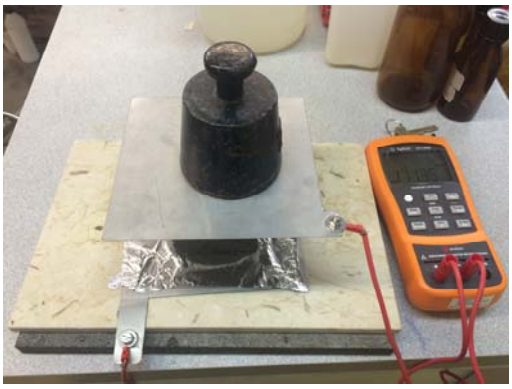

Figure 23 Resistivity test arrangement

In addition to the time evolution of the concrete resistivity, the influence of other parameters such as the fibre content, the fibre orientation, the AC frequency and the moisture content, on the electrical resistivity of concrete were also investigated.

5.1 Saturated specimens in tap water

The specimens in row 5, were placed in water as soon as they were cut from the slab which was done the day after cutting them. Thereafter, they were stored in a small tank, submerged in tap water, which was periodically re-filled to compensate the loss of water due to evaporation. The first measurements were made after one week of immersion and the following measurements were performed weekly during the first two months and every second week the last month. In total, 10 measurements were performed over a period of twelve weeks of study.

5.1.1 Effects of degree of hydration and frequency

For the study of how the degree of hydration affects the concrete resistivity at increasing fibre dosages, the resistivity test was performed using AC current. Assuming total homogeneity in the samples (Lataste et al. 2008), the position in the slab, i.e. A, B or C and the axis in which resistivity is measured, is not taken into account in this section. These means that what is represented in the graphs

are the average resistivity values measured, each single point is an average of nine measurements.

At the same time, the influence of the frequency was studied. For this, all the measurements were made at three different frequencies: 100 Hz, 120 Hz and 1000 Hz and all the information is presented in Figure 24Figure 26:

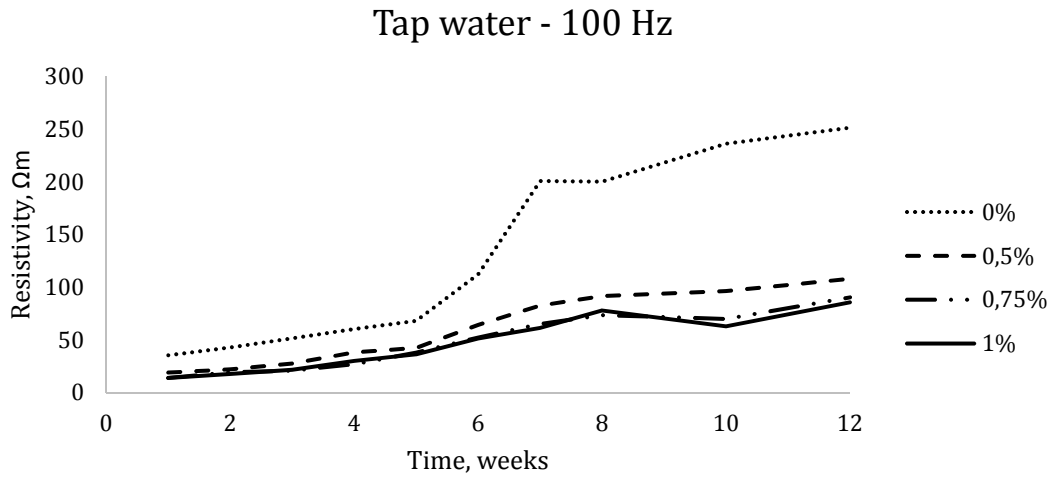

Figure 24 Grade of hydration, tap water, 100 Hz. Average values of position and direction of measurement

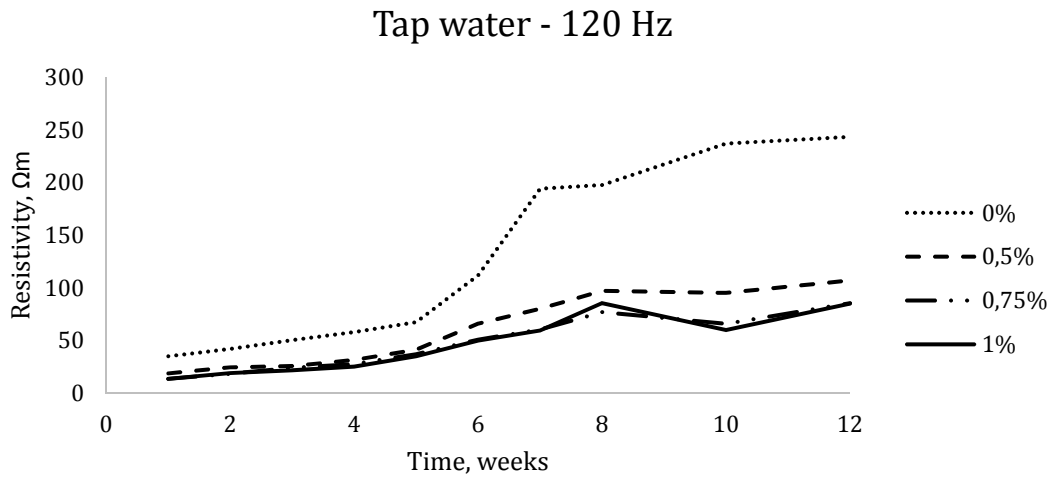

Figure 25 Grade of hydration, tap water, 120 Hz. Average values of position and direction of measurement

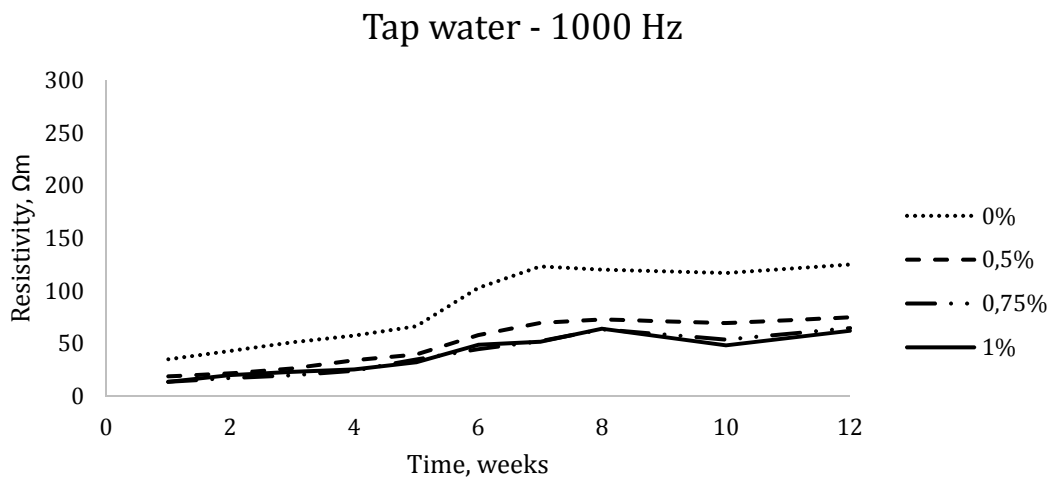

Figure 26 Grade of hydration, tap water, 1000 Hz. Average values of position and direction of measurement

5.1.2 Effects of fibre orientation and frequency

The resistivity measurements in each specimen were made in three directions (x-, y- and z-axis) to validate the assumption that the conductivity of the fibres depends on if they are parallel or perpendicular to the current flowing through the specimen.

In this case, the influence of the position in the slab was not studied and thus, each value represents the averaged measurements for each of the three specimens A, B and C.

There is a chart for each fibre dosage and two set of charts are presented in this section, ones being measured at 100 Hz and others at 1000 Hz to show the influence of the frequency on the electrical resistivity. In this section, it was decided to omit the data of the measurements at 120 Hz since they resembled the results at 100 Hz.

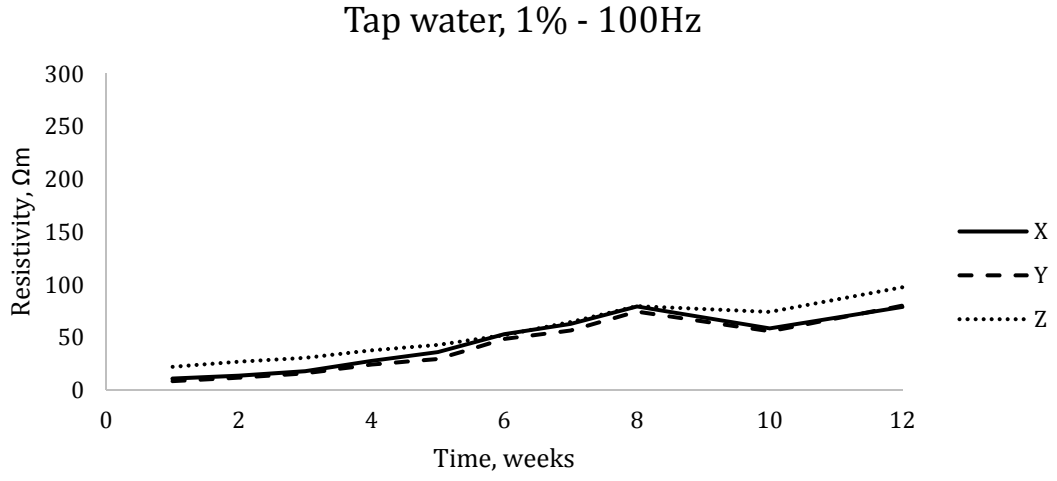

Figure 27 Fibre orientation, tap water, 1% fibre volume – 100 Hz. Average value of position in the slab

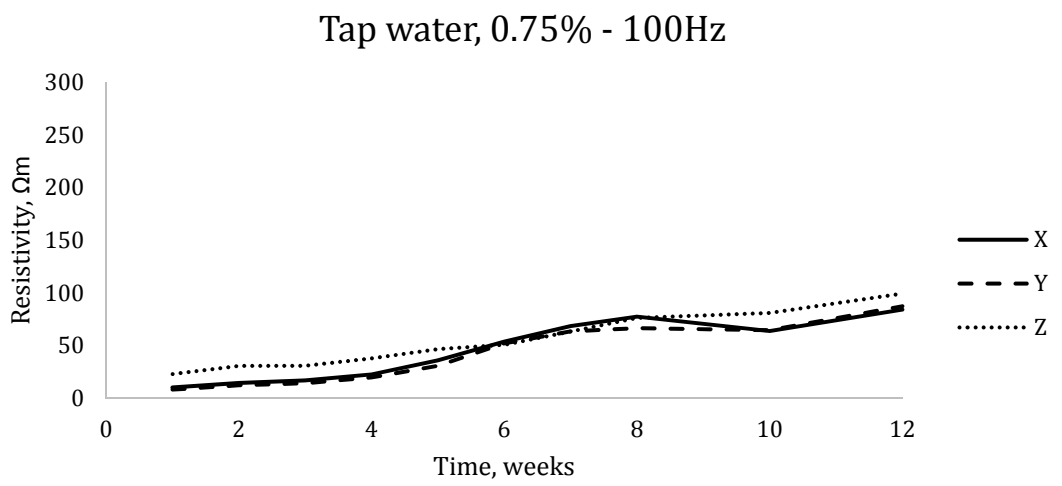

Figure 28 Fibre orientation, tap water, 0.75% fibre volume – 100 Hz. Average value of position in the slab

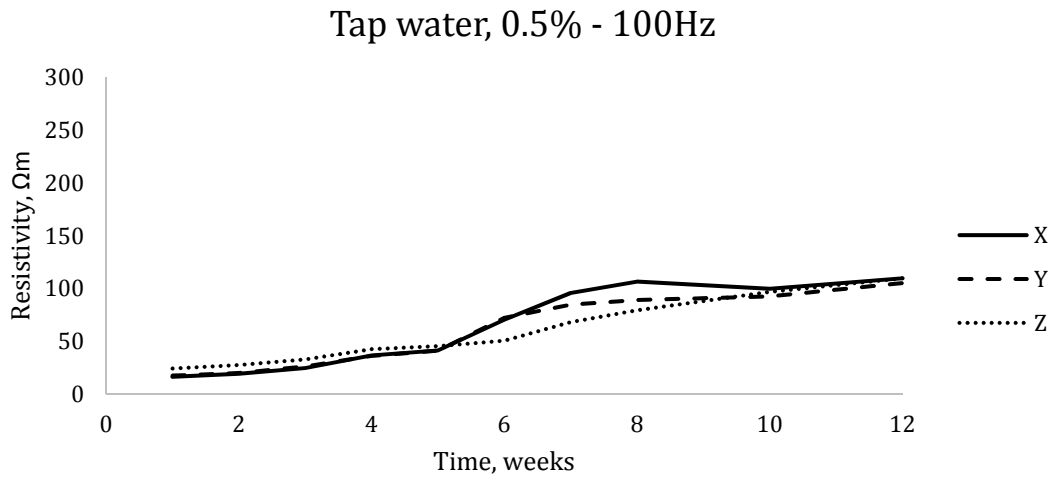

Figure 29 Fibre orientation, tap water, 0.5% fibre volume – 100 Hz. Average value of position in the slab

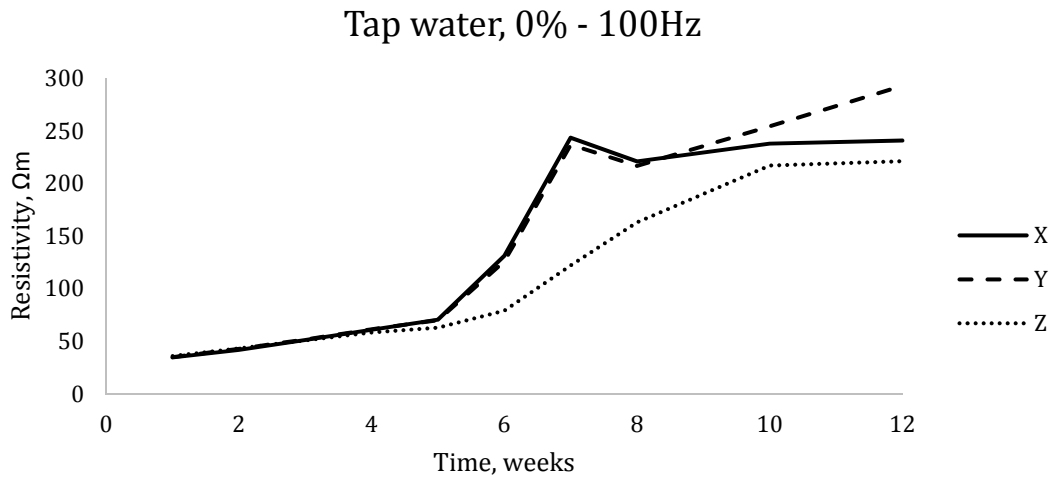

Figure 30 Fibre orientation, tap water, 0% fibre volume – 100 Hz. Average value of position in the slab

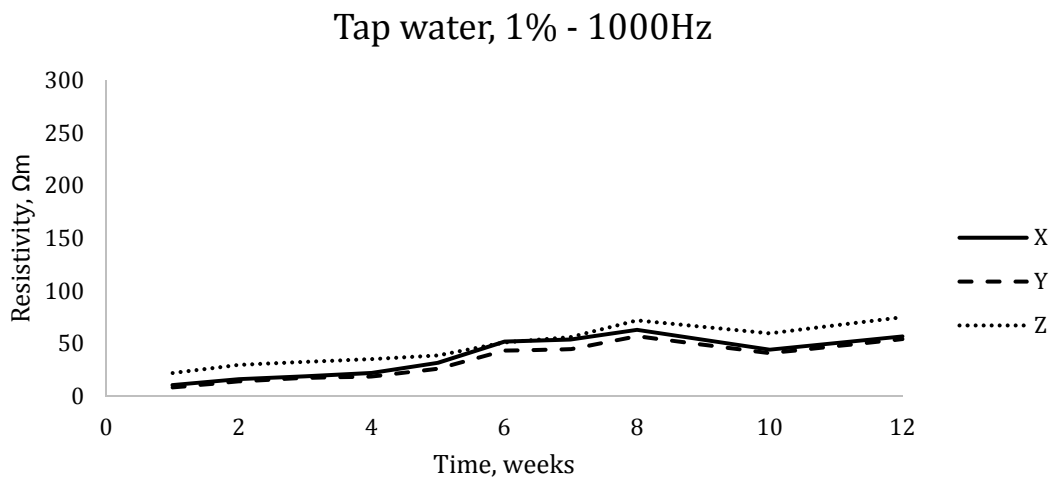

Figure 31 Fibre orientation, tap water, 1% fibre volume – 1000 Hz. Average value of position in the slab

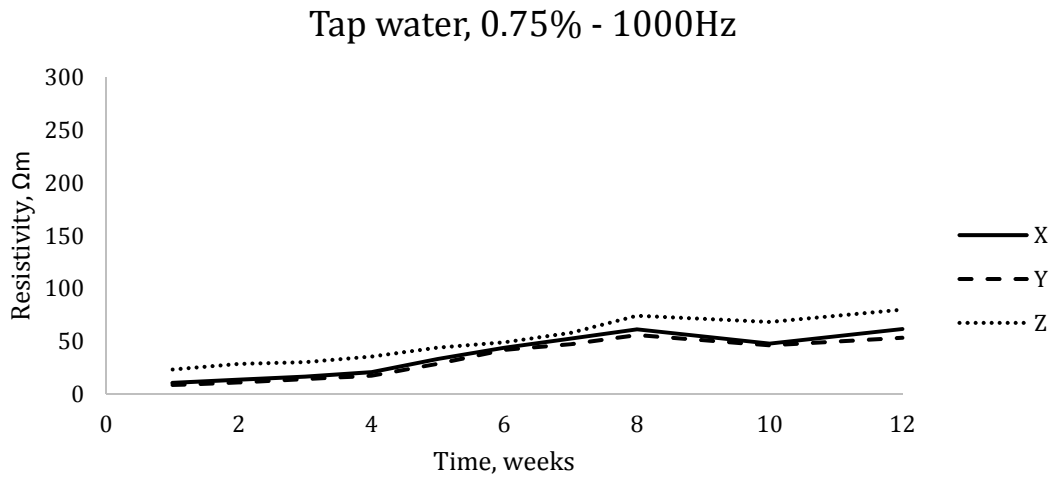

Figure 32 Fibre orientation, tap water, 0.75% fibre volume – 1000 Hz. Average value of position in the slab

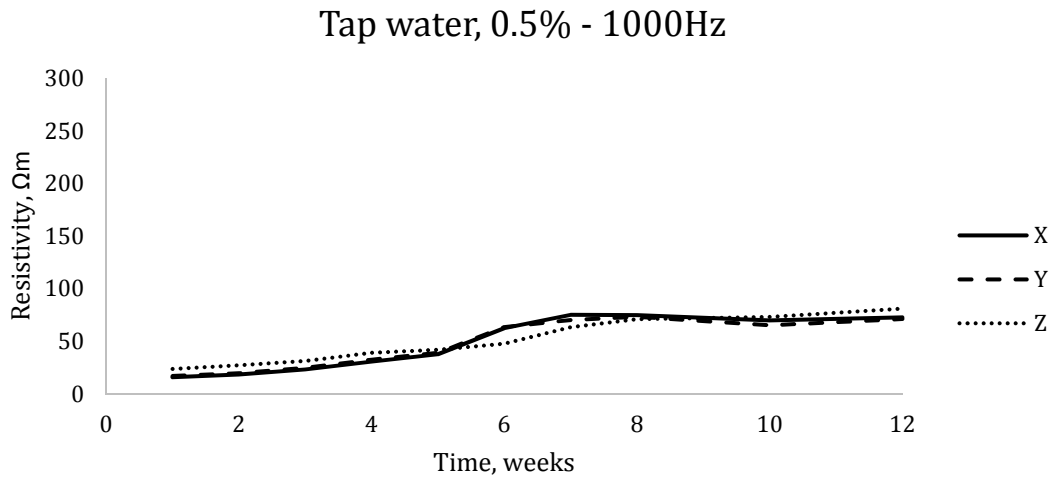

Figure 33 Fibre orientation, tap water, 0.5% fibre volume – 1000 Hz. Average value of position in the slab

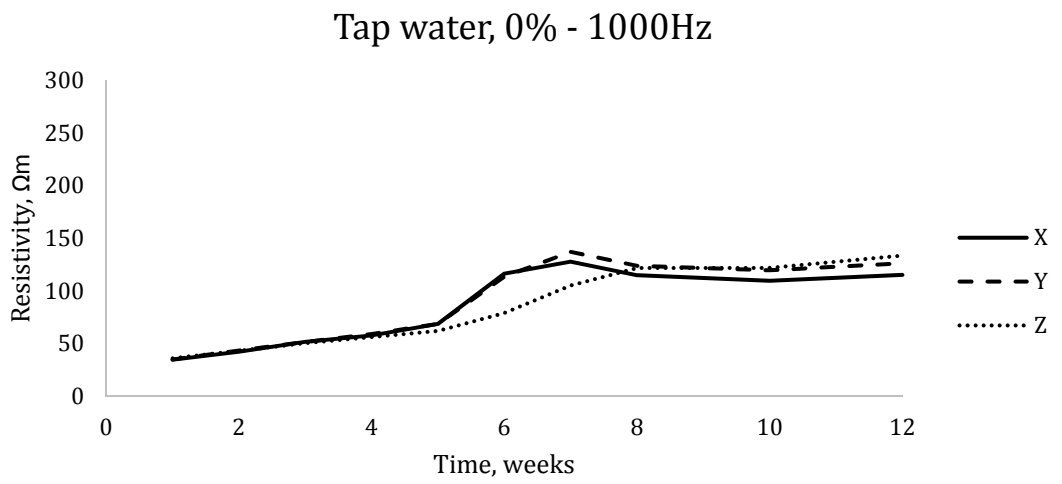

Figure 34 Fibre orientation, tap water, 0% fibre volume – 1000 Hz. Average value of position in the slab

5.1.3 Position in the slab

In this section, the direction in which the measurements were made (x-, y- and z-axis) was again studied but including the influence of the position of the specimen in the slab (either A, B or C). The aim here was to check if the way of casting had a real effect on the electrical resistivity and thus, the fibre orientation. All the measurements correspond to AC at a frequency of 1000 Hz.

The data are presented in four charts, one per fibre content, having each nine groups of data, divided in x-, y- and z- directions and in the position in the slab (A, B or C). Also for each group, the initial resistivity and then, the monthly evolution are presented.

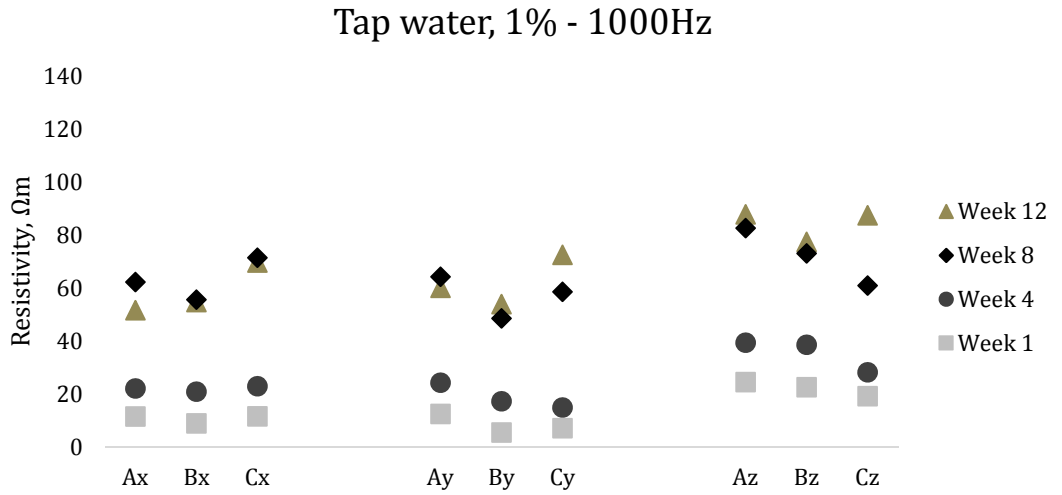

Figure 35 Position in the slab and fibre orientation, tap water, 1% fibre content, 1000 Hz

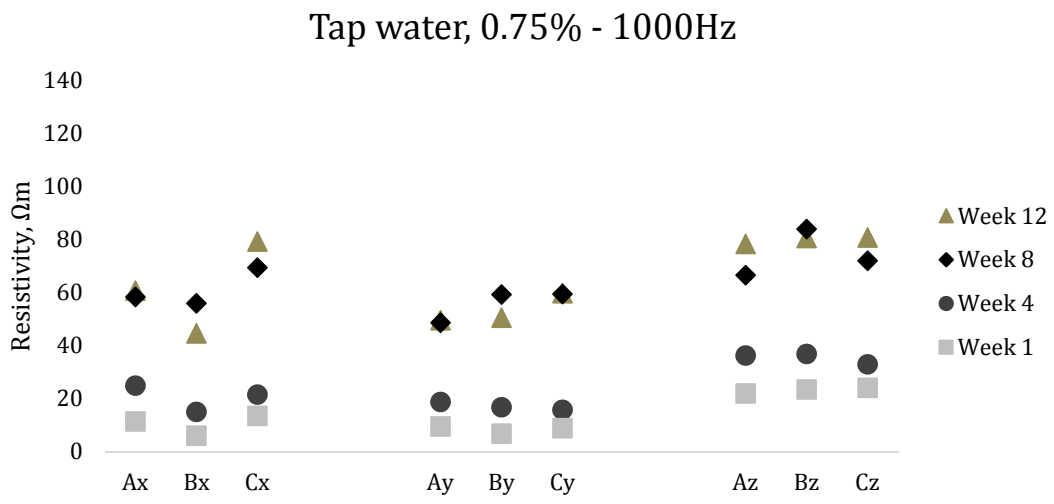

Figure 36 Position in the slab and fibre orientation, tap water, 0.75% fibre content, 1000 Hz

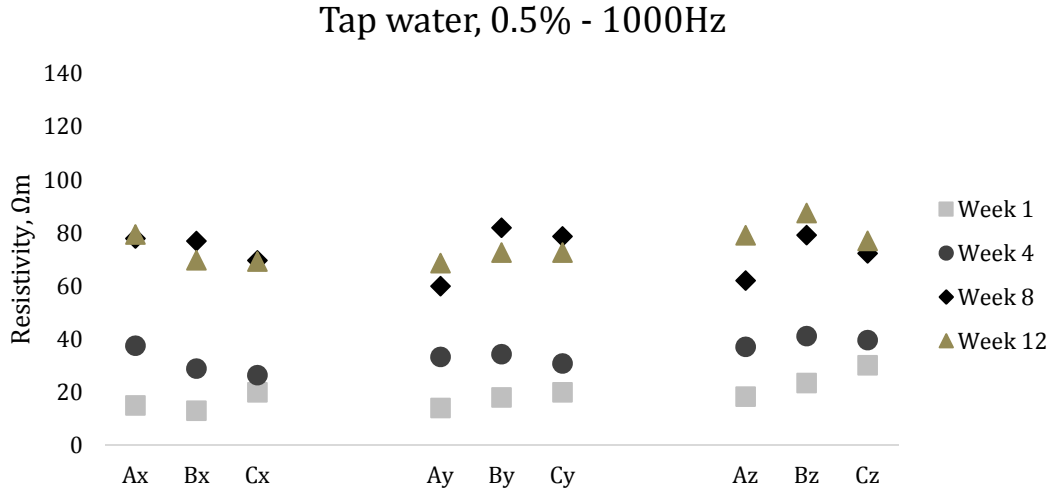

Figure 37 Position in the slab and fibre orientation, tap water, 0.5% fibre content, 1000 Hz

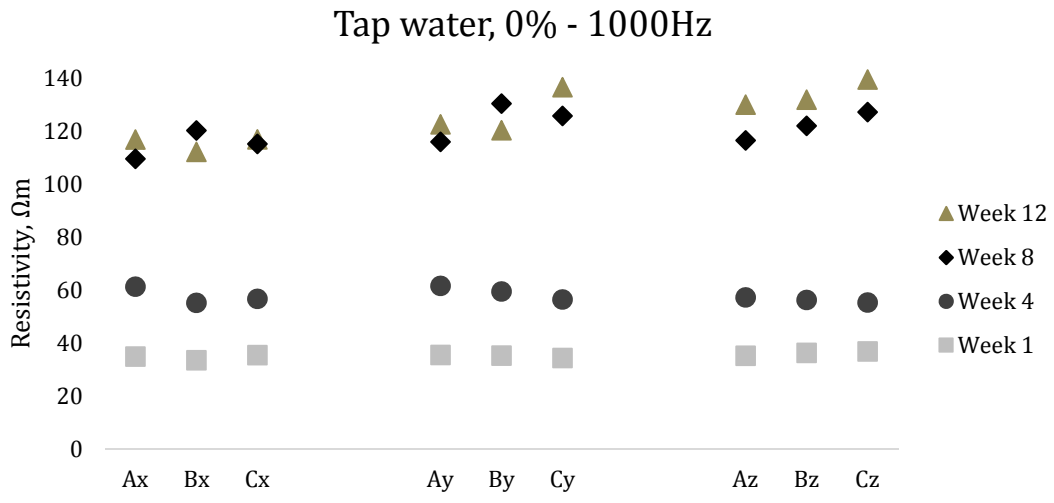

Figure 38 Position in the slab and fibre orientation, tap water, 0% fibre content, 1000 Hz

5.2 Saturated specimens in chlorides

The specimens in row 3, were placed in a solution with a 3.5% NaCl content when they were cut from the slab. Following the exact same procedure the specimens in row 5 underwent, they were submerged in the solution while the experiment was on-going. In this case, the container was covered by a plastic sheet to avoid water evaporation which could have altered the percentage of chlorides in the solution. The initial resistivity value was considered the one measured after one week of immersion. After that, the resistivity was measured weekly during the first month, every second week until week eight and the last measurement was made in week twelve, one month after the previous one. The reason why the measurements were not performed as often as for the ones in row 5 was due to a slower variation of the measured resistivity.

5.2.1 Effects of degree of hydration and frequency

For the study of how the degree of hydration affects the concrete resistivity for increasing fibre dosages, the resistivity test was performed using AC current. The position in the slab, which means being A, B or C or the axis in which resistivity is measured, is not taken into account in this section. The average values of the resistivity per row and in the three directions are represented in the graphs.

The influence of the frequency was also studied. For this, all the measurements were made at three different frequencies: 100 Hz, 120 Hz and 1000 Hz and all the information is represented in the three charts below:

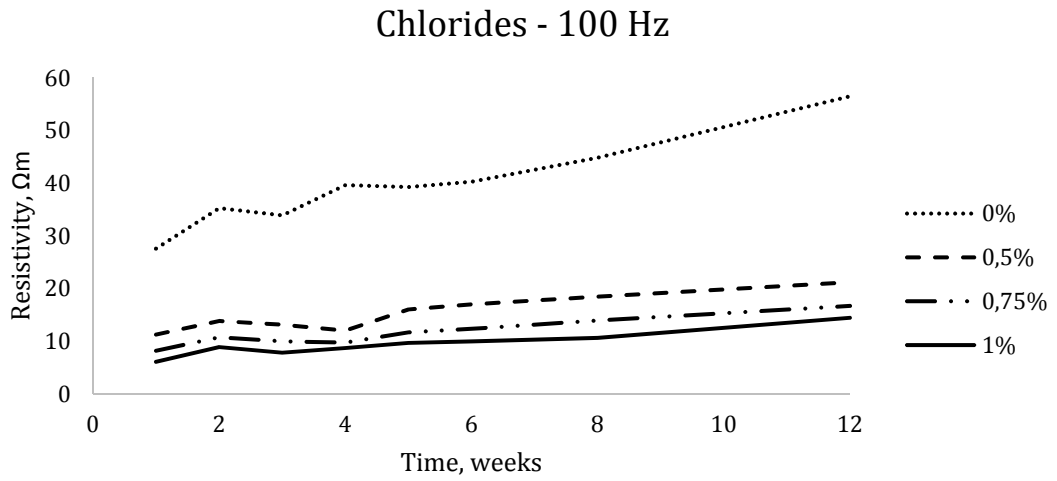

Figure 39 Grade of hydration, chloride solution, 100 Hz. Average values of position and direction of measurement

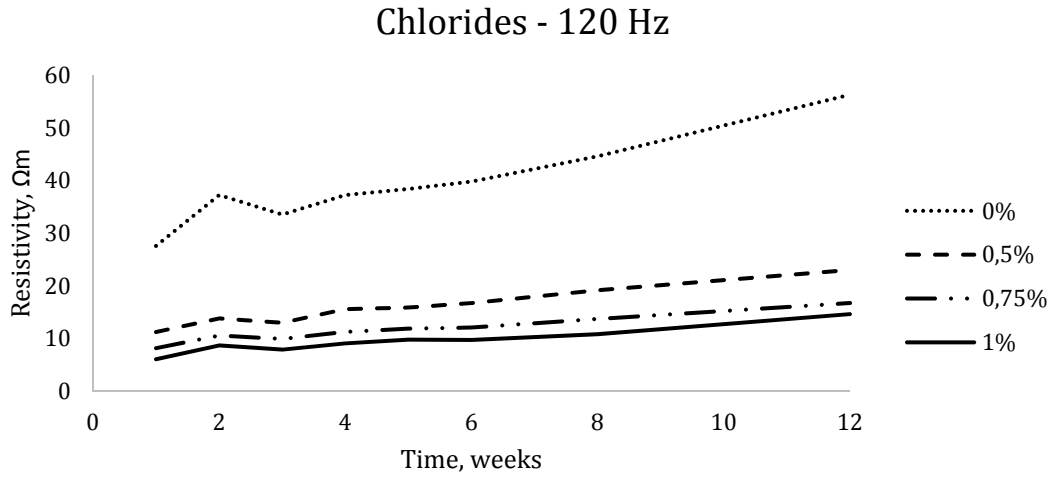

Figure 40 Grade of hydration, chloride solution, 120 Hz. Average values of position and direction of measurement

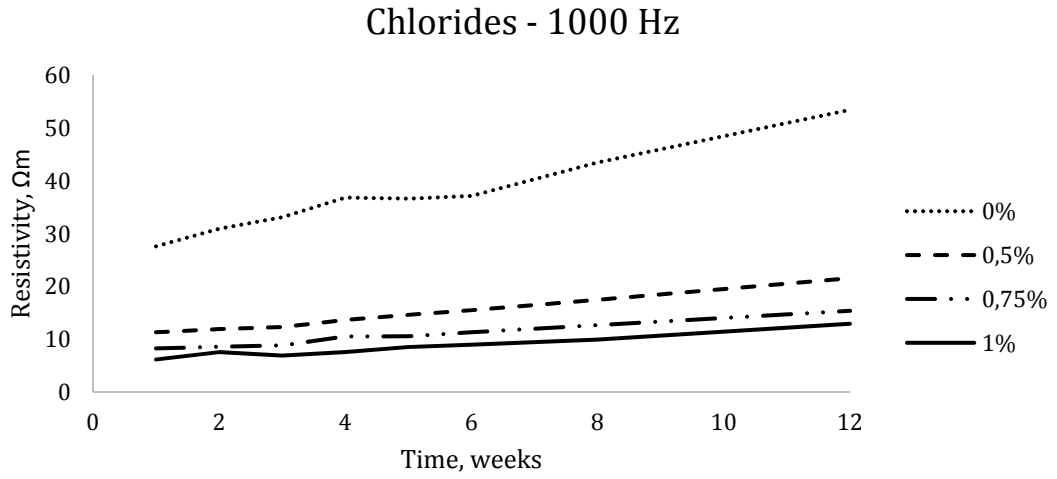

Figure 41 Grade of hydration, chloride solution, 1000 Hz Average values of position and direction of measurement

5.2.2 Effects of fibre orientation and frequency

The resistivity measurements for each specimen were made in three directions (x-, y- and z-axis) to investigate whether the orientation of fibres has a direct effect on the measured resistivity of the specimens.

In this case, the influence of the position in the slab is not study and thus, each value represented is the average value of the measurements in each three specimens A, B and C for each dosage.

Two charts per fibre volume, one measured at 100 Hz and the other at 1000 Hz are found in this section so both, direction an frequency effects are compared. The data measured at 120 Hz was similar to the one at 100 Hz and is thus, not included here.

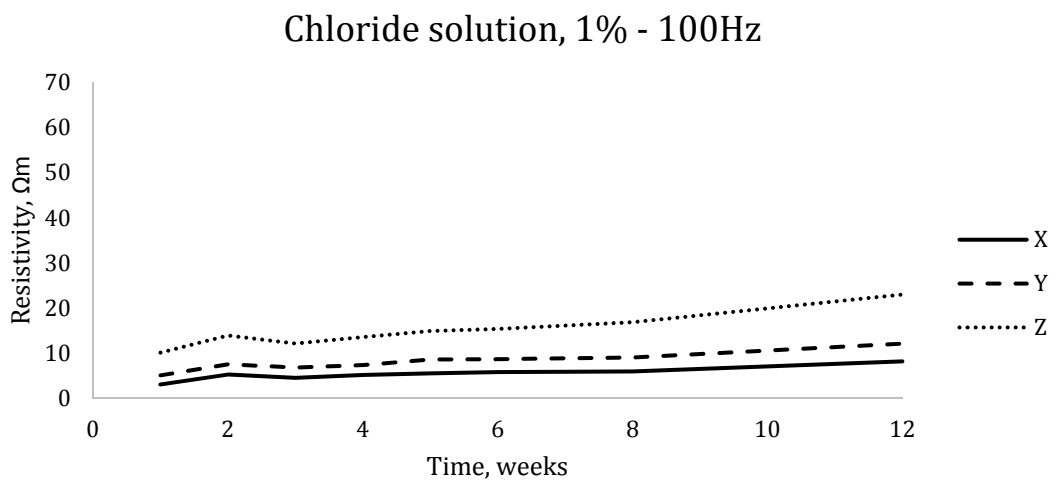

Figure 42 Fibre orientation, chloride solution, 1% fibre volume – 100 Hz. Average value of position in the slab

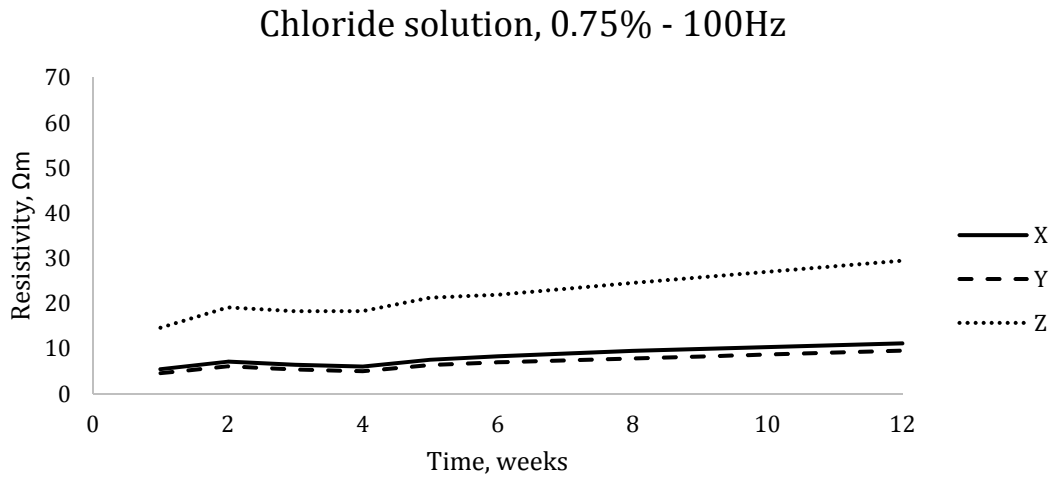

Figure 43 Fibre orientation, chloride solution, 0.75% fibre volume – 100 Hz. Average value of position in the slab

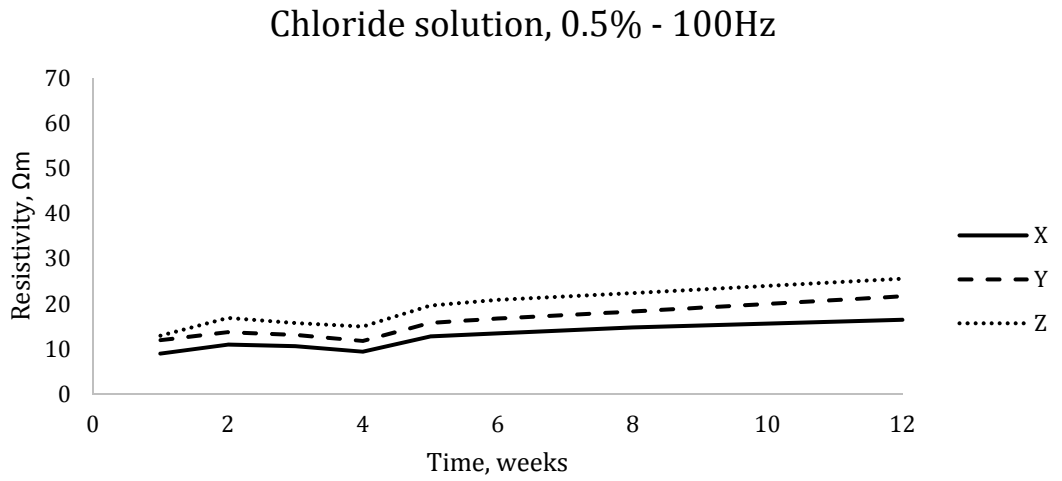

Figure 44 Fibre orientation, chloride solution, 0.5% fibre volume – 100 Hz. Average value of position in the slab

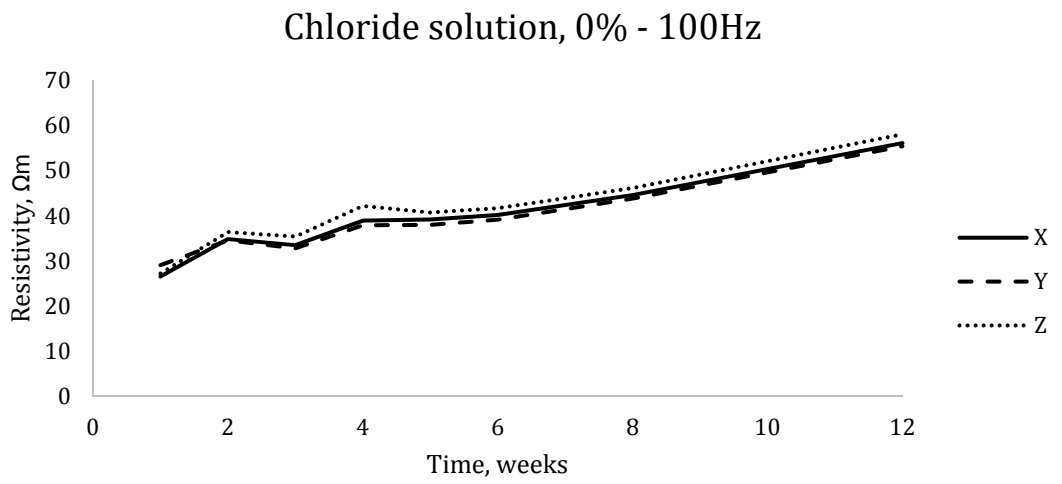

Figure 45 Fibre orientation, chloride solution, 0% fibre volume – 100 Hz. Average value of position in the slab

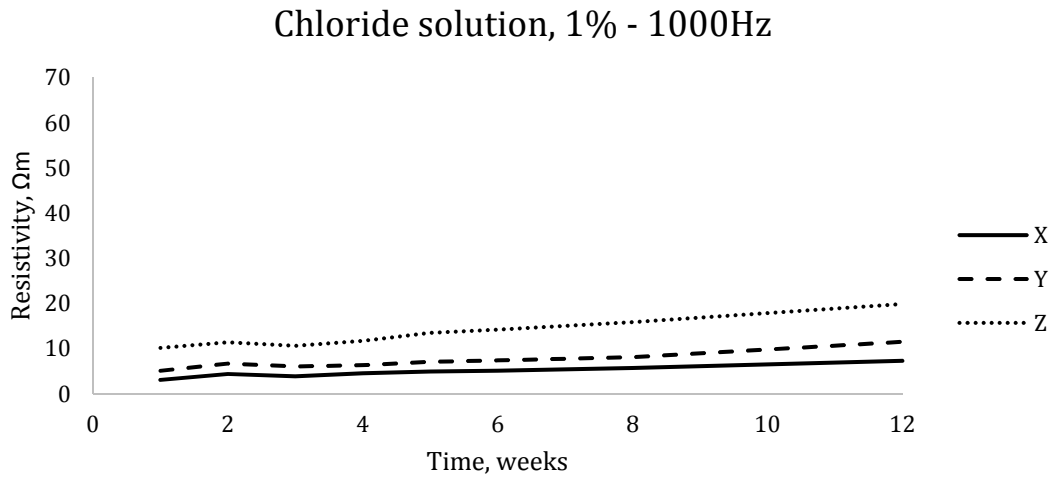

Figure 46 Fibre orientation, chloride solution, 1% fibre volume – 1000 Hz. Average value of position in the slab

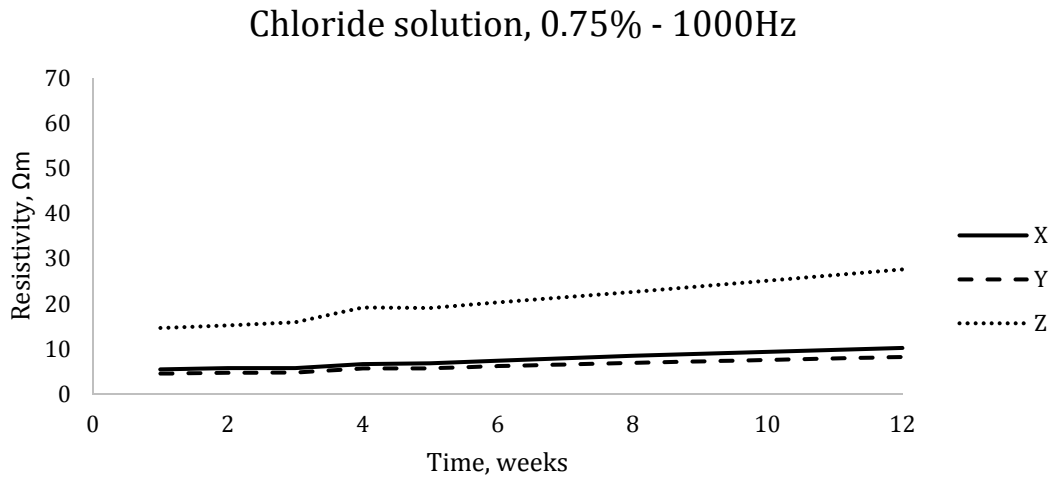

Figure 47 Fibre orientation, chloride solution, 0.75%fibre volume – 1000 Hz. Average value of position in the slab

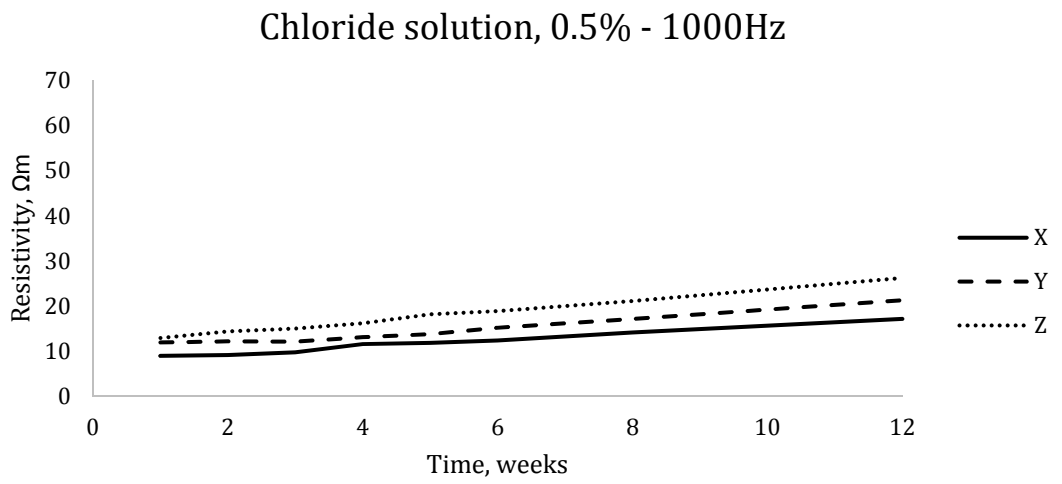

Figure 48 Fibre orientation, chloride solution, 0.5% fibre volume – 1000 Hz. Average value of position in the slab

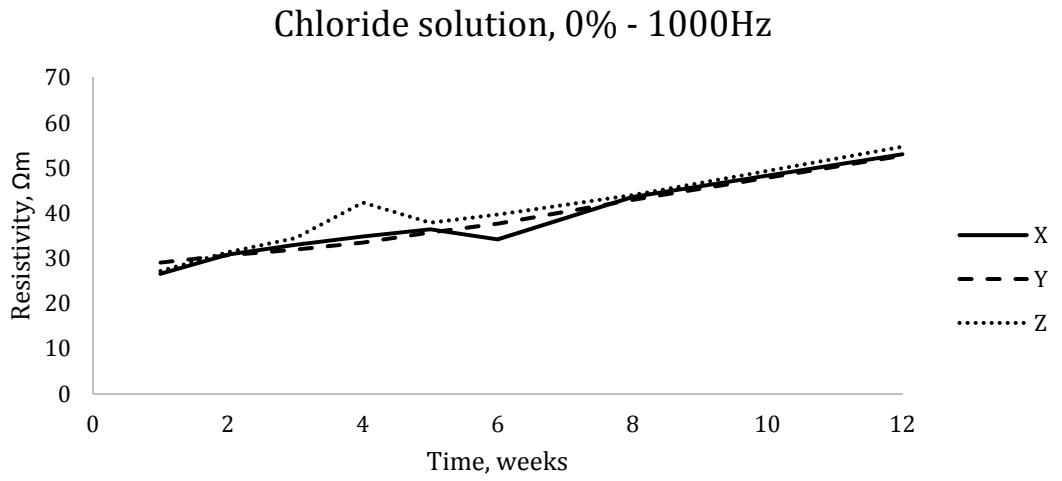

Figure 49 Fibre orientation, chloride solution, 0% fibre volume – 1000 Hz. Average value of position in the slab

5.2.3 Position in the slab

In this section, the direction in which the measurements were made (x-, y- and z-axis) is compared for different positions in the slab (A, B or C) to check if any tendencies in the values measured can be found. If this tendency is real, that would mean that the way of casting had an effect on the fibre distribution and orientation. The data analysed here was conducted by measuring with AC at 1000 Hz.

The data are presented in four charts, one per fibre content, having each nine groups of data, one per position (A, B or C) and direction of measurement (x-, y- and z-axis). For each group, the initial resistivity and the monthly evolution are shown.

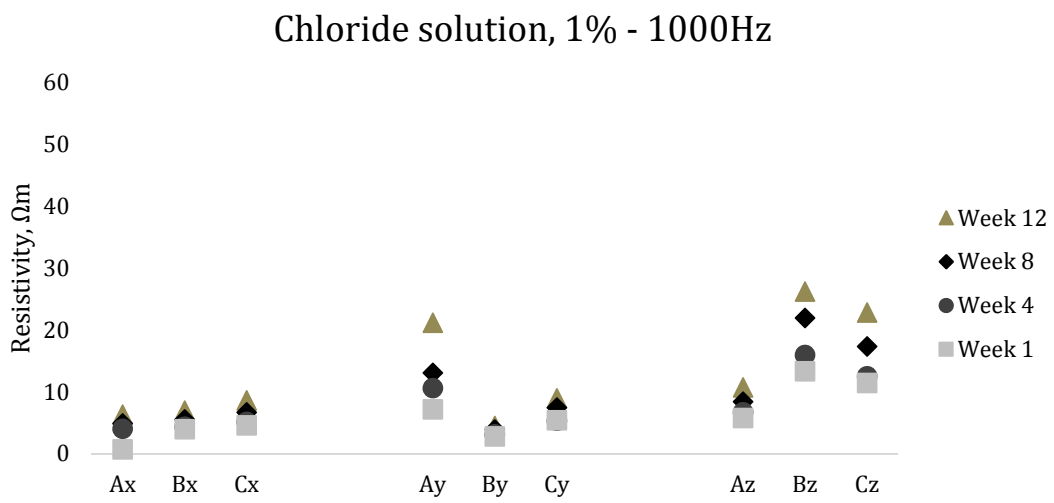

Figure 50 Disposition in the slab and fibre orientation, chloride solution, 1% fibre content, 1000 Hz

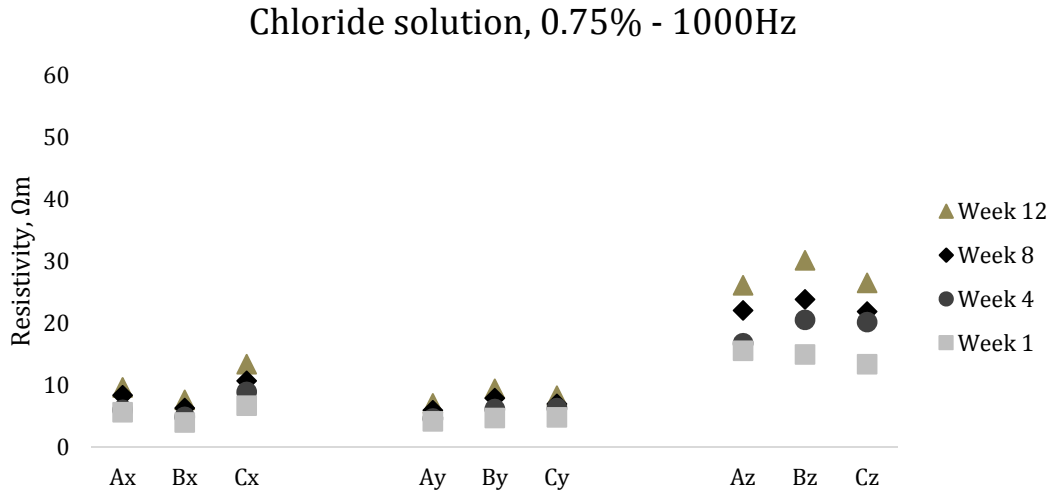

Figure 51 Disposition in the slab and fibre orientation, chloride solution, 0.75% fibre content, 1000 Hz

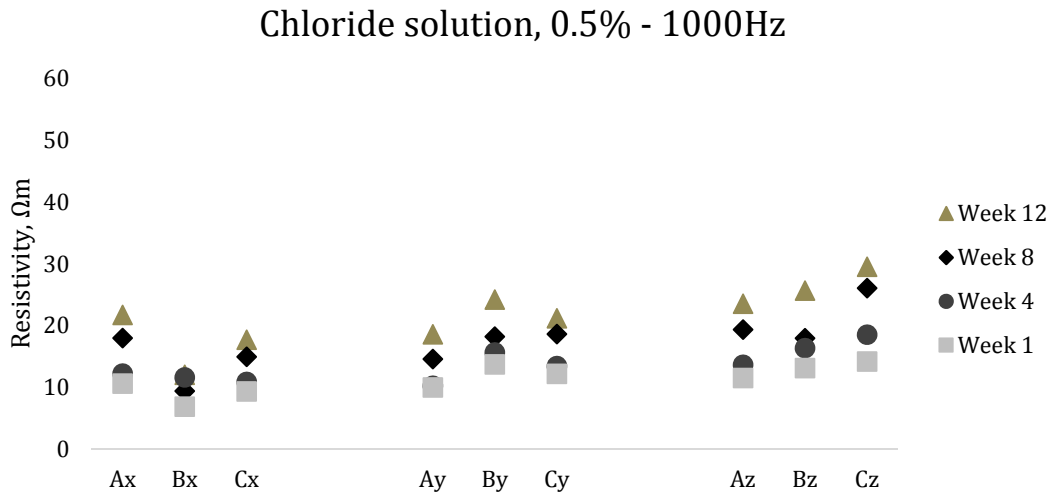

Figure 52 Disposition in the slab and fibre orientation, chloride solution, 0.5% fibre content, 1000 Hz

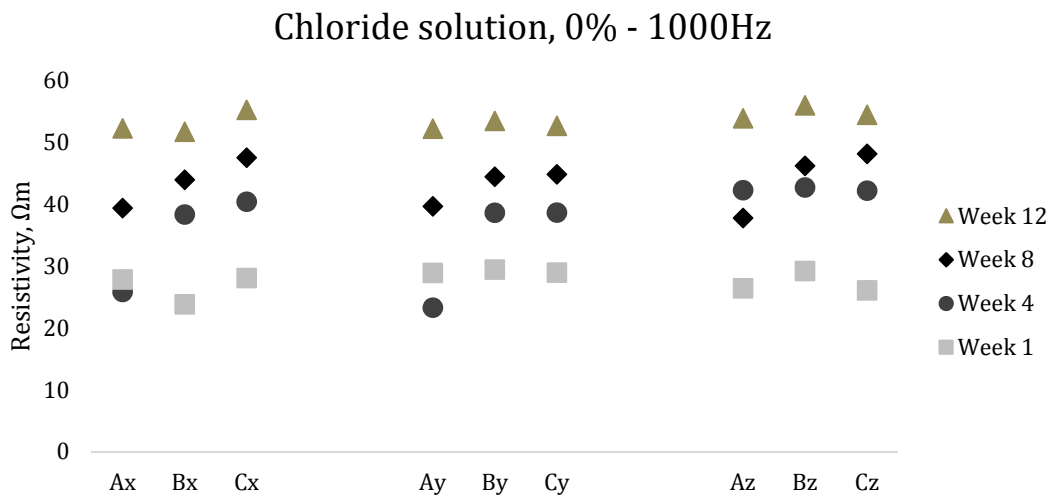

Figure 53 Disposition in the slab and fibre orientation, chloride solution, 0% fibre content, 1000 Hz

5.3 Effect if moisture content

After three months in their respective environmental exposures, the resistivity values of the specimens: that was left to completely dry in the oven; the ones that were naturally dried in the climate chamber; and the ones that were forced dried in the oven were measured. In this case, only the frequency of 1000 Hz was used to compare these values to the ones of the saturated specimens. Four charts, one per fibre dosage were made comparing the seven rows of each slab. The exact final weights of the specimens and thus, their estimated moisture contents can be found in the Appendix D together with the errors with respect to the modelled final weights. It has to be noted, that the forced dried results, will not be compared to the other results as their actual moisture content differed significantly from the one considered in the plan.

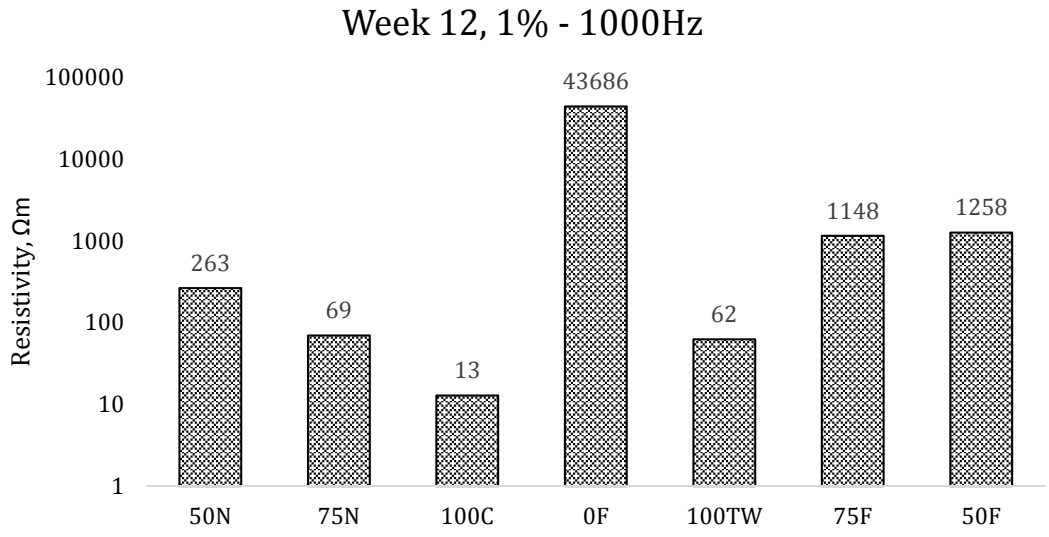

Figure 54 Comparison of rows with 1% fibre content. Average value of all the specimens in the three directions

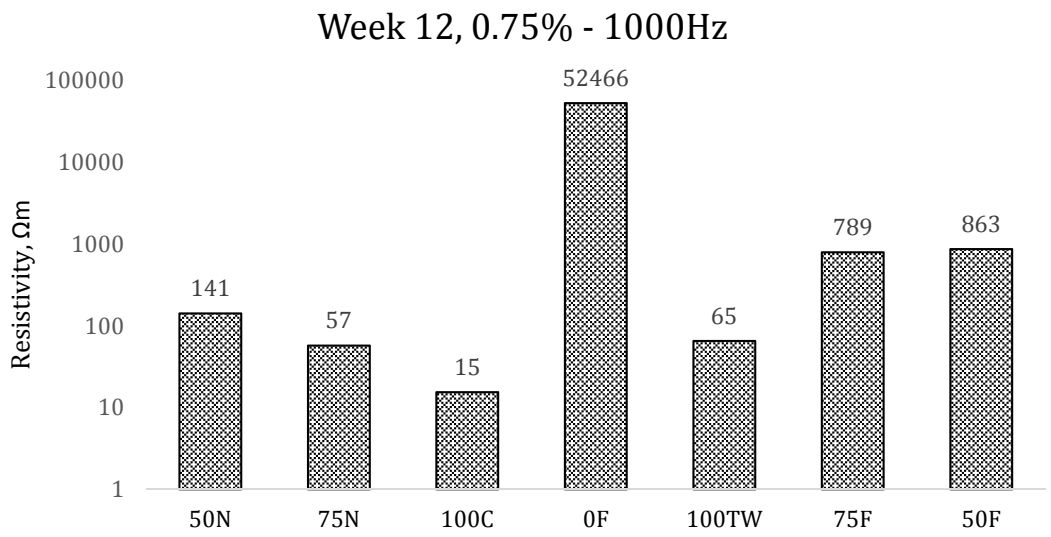

Figure 55 Comparison of rows with 0.75% fibre content Average value of all the specimens in the three directions

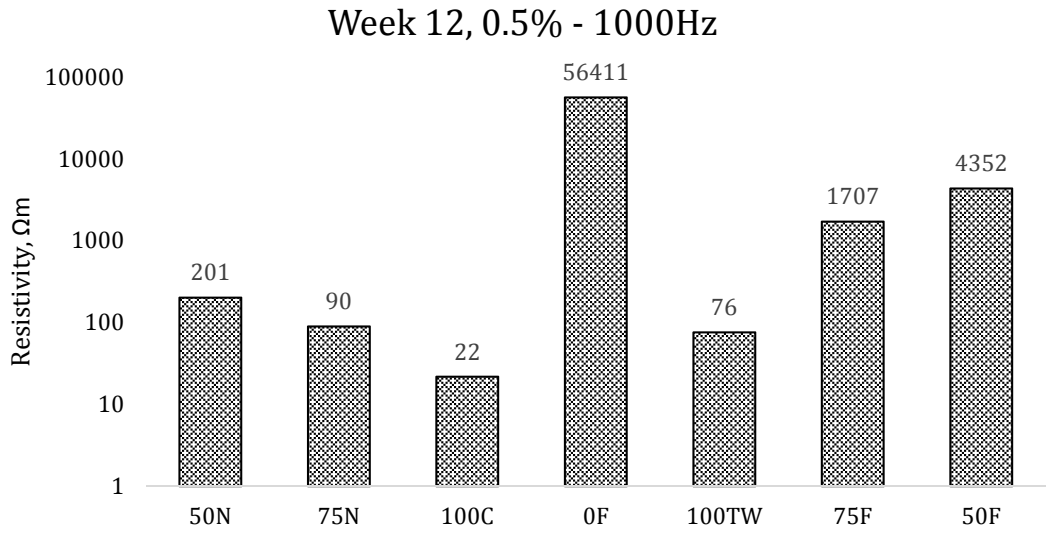

Figure 56 Comparison of rows with 0.5% fibre content. Average value of all the specimens in the three directions

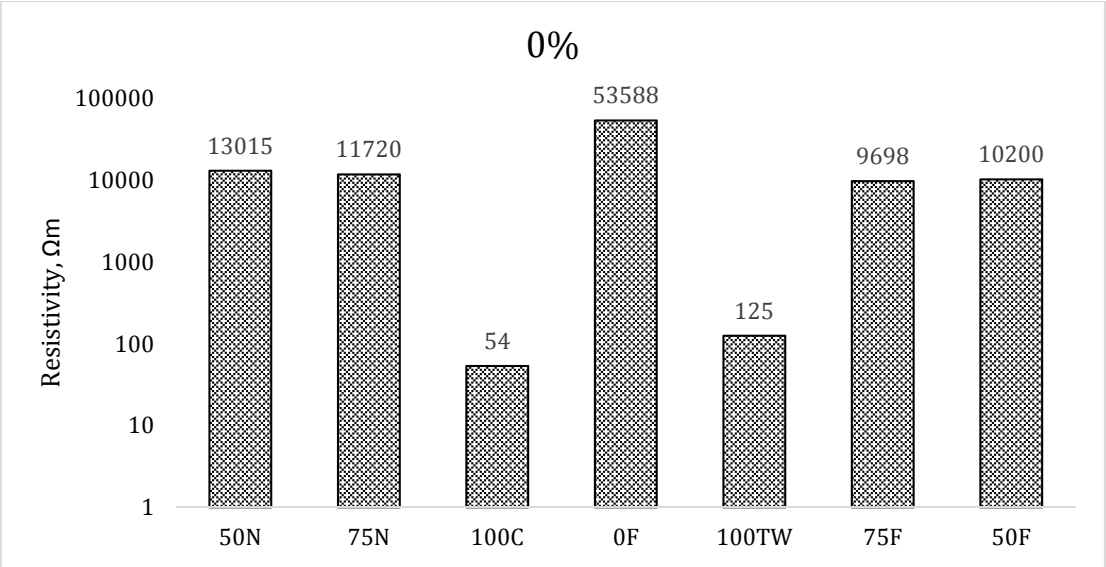

Figure 57 Comparison of rows with 0% fibre content. Average value of all the specimens in the three directions

5.4 DC Measurements

To present the results of the experiments for the effects of DC on the resistivity of concrete containing steel fibres, resistivity was measured in the x-direction and the data are grouped under three graphs in which the different fibre contents are compared with each other for each position in the slab, that is cubes A, B and C. By doing this, the behaviour when applying them to a decreasing voltage can be compared between different fibre contents and with those made of plain concrete which acts as a reference. Data for the increasing voltage were also taken and studied but in the following, only the evolution of current with decreasing voltage is presented.

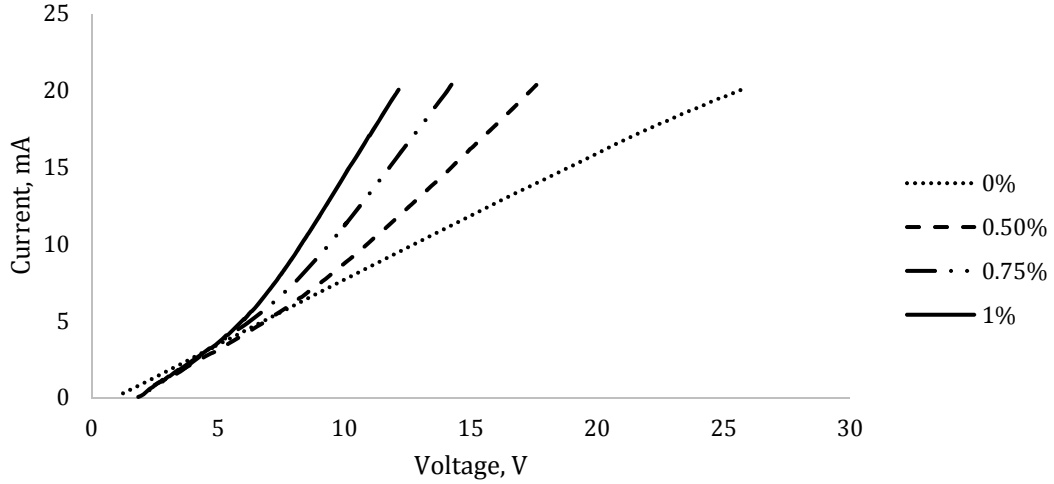

Figure 58 Current vs. voltage in cubes A

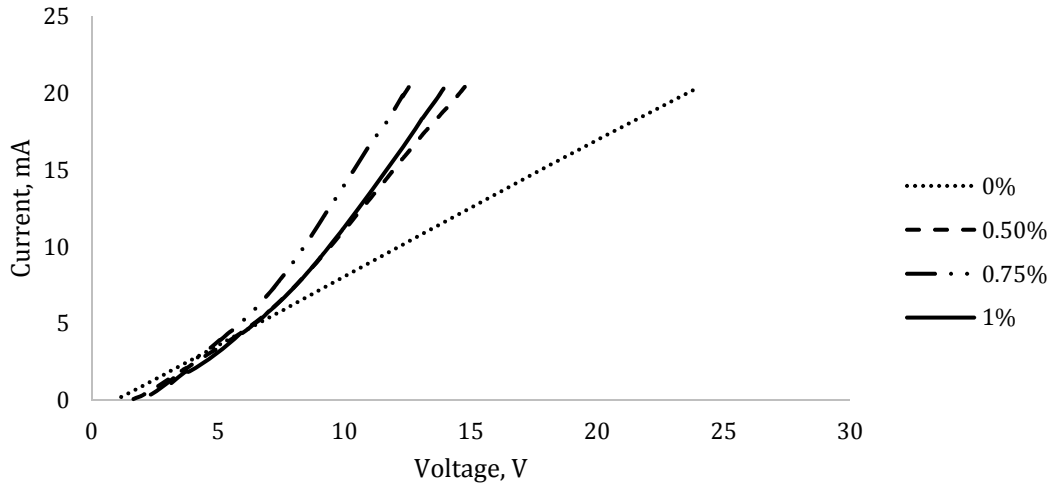

Figure 59 Current vs. voltage in cubes B

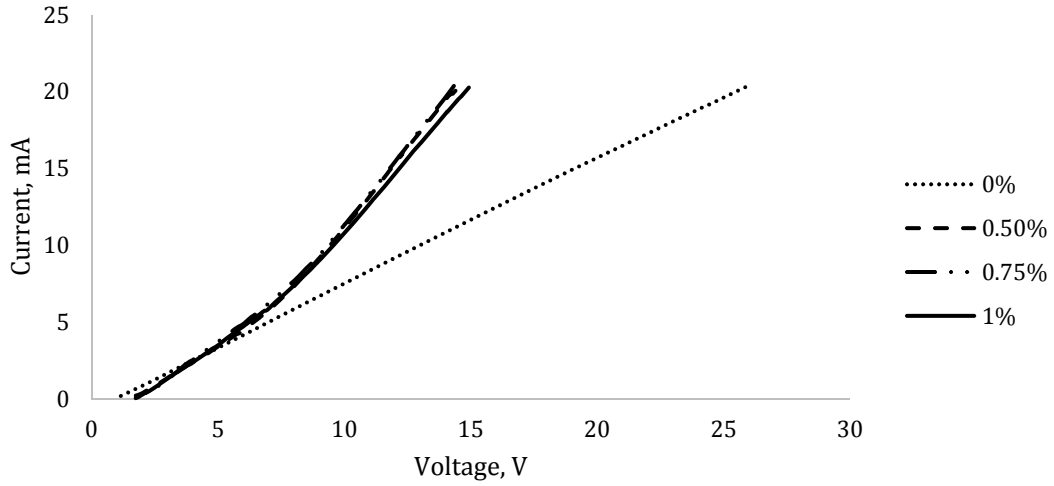

Figure 60 Current vs. voltage in cubes C

As can be seen in Figure 58 to Figure 60, a non-linear "two-slope" behaviour is found for the samples containing fibres. From these graphs the resistivity was calculated both for the high voltage and low voltage regions. In addition, the results are presented for both the increasing and the decreasing voltage measurements as both the results are significant for the study.

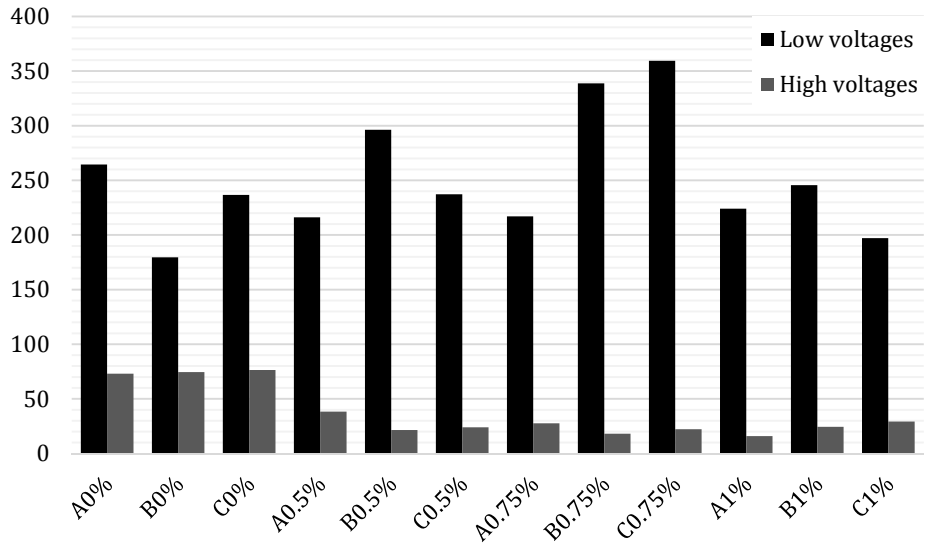

Figure 61 Resistivity values calculated with an increasing voltage at low and high voltages

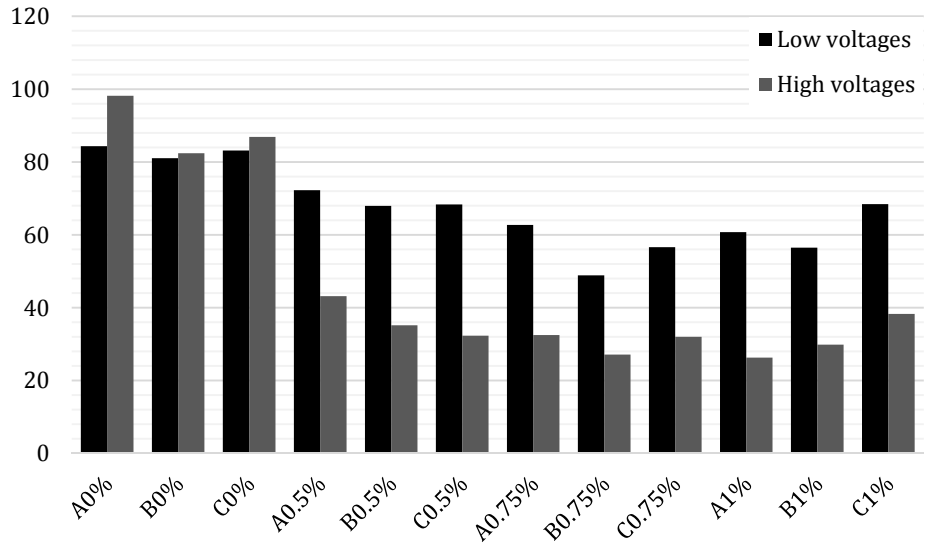

Figure 62 Resistivity values calculated with a decreasing voltage at low and high voltages

6 Corrosion rate results

During the three months the study took place and as previously described in section 4.2, the galvanic current through the bars was recorded every 25 minutes. With these data, it was possible to calculate the theoretical weight loss of each bar caused by the reduction of their cross section due to corrosion using Faraday´s Law.

For each specimen and reinforcement bar a comparison is made between the four mixes (0%, 0.5%, 0.75% and 1.0%), in this way the influence of fibres can be compared easily. The couples were called a, b and c where b is the reinforcement bar placed in the middle, with less surface in direct contact with chlorides.

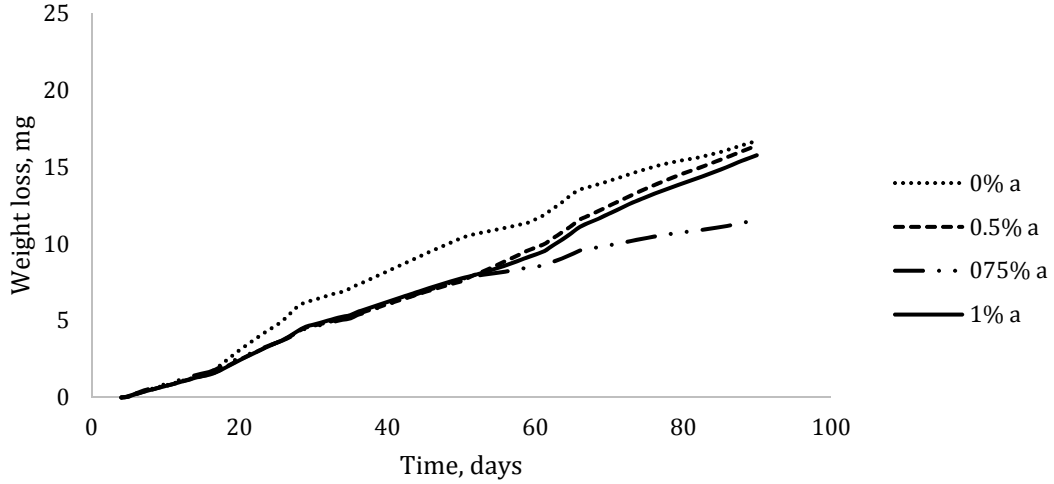

Figure 63 Estimated reinforcement bar weight loss in position a

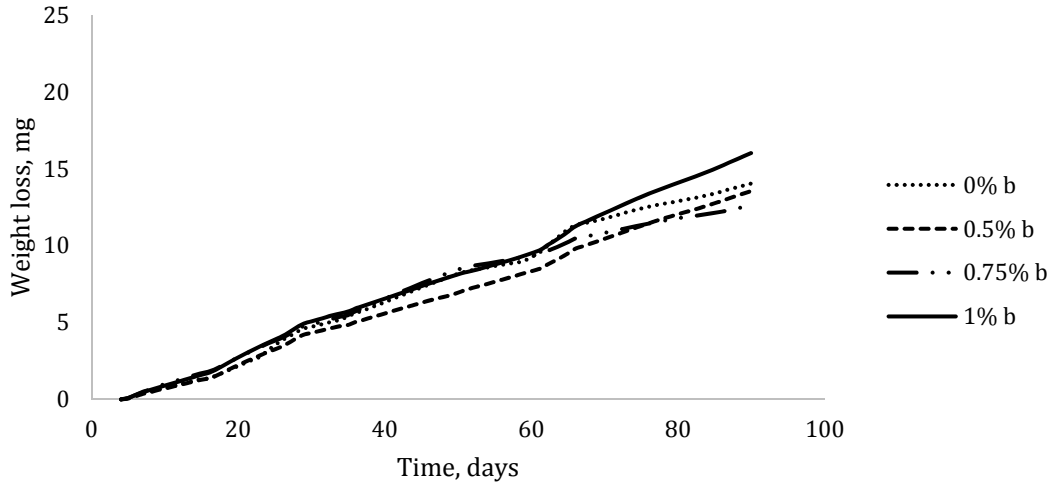

Figure 64 Estimated reinforcement bar weight loss in position b

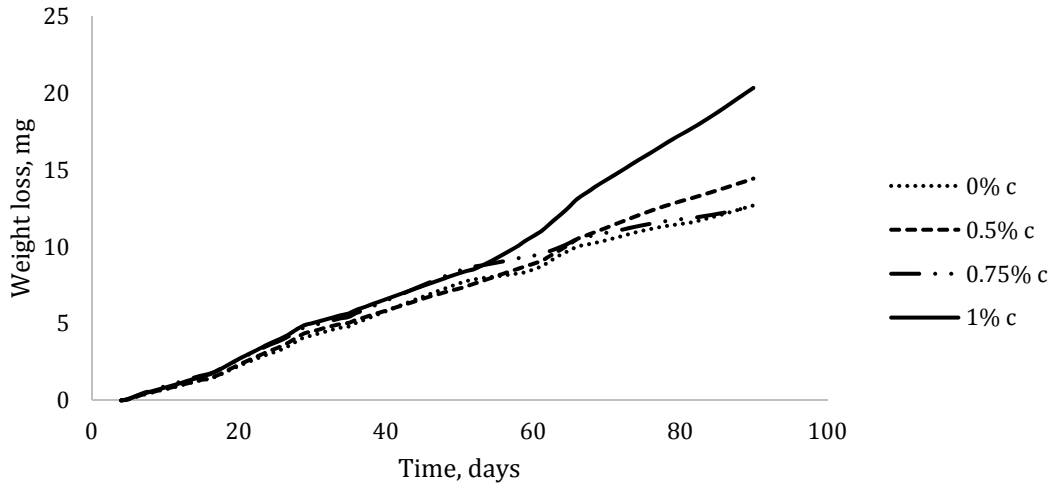

Figure 65 Estimated reinforcement bar weight loss in position c

As explained before, corrosion is classified from negligible to very high depending on its penetration rate (μm/year). In Figure 66Figure 68 the penetration rates are shown. There is a graph per position in which the penetration rates with respect to the fibre content are plotted against each other to analyse the effect of fibres in the corrosion rate of the specimens studied.

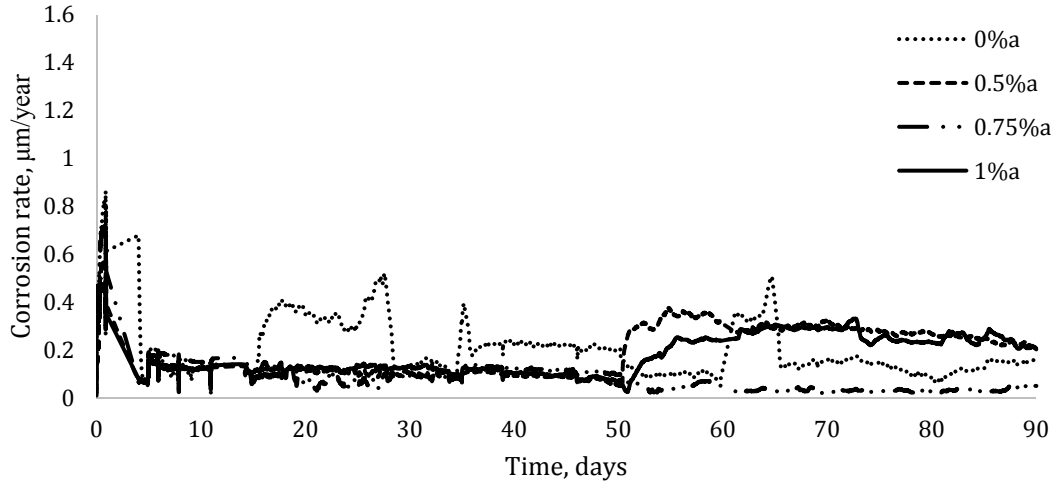

Figure 66 Estimated penetration rate in position a

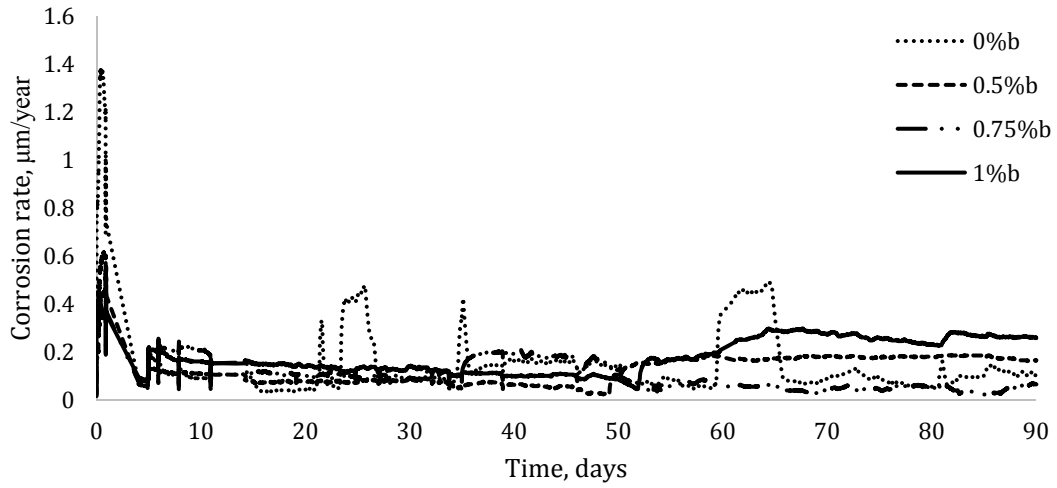

Figure 67 Estimated penetration rate in position b

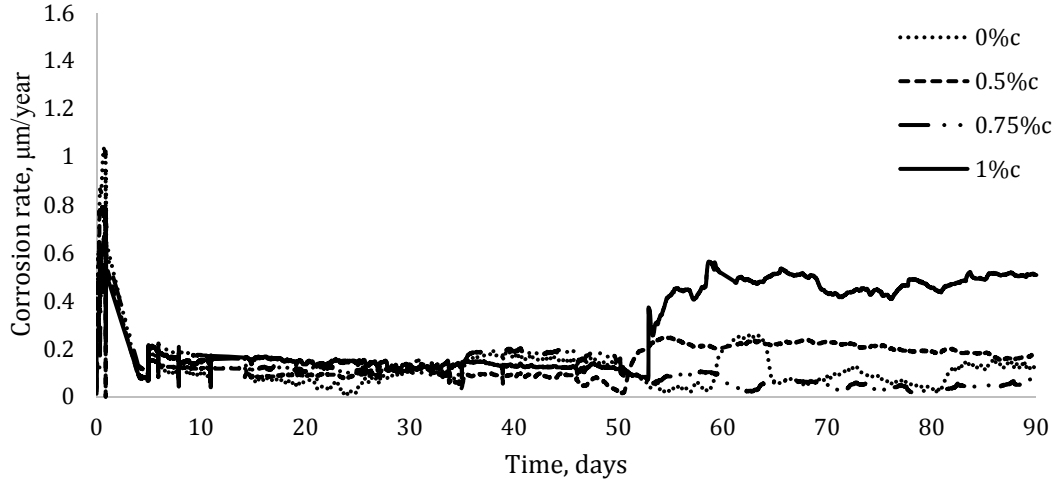

Figure 68 Estimated penetration rate in position c

7 Discussion of the electrical resistivity results

In this chapter, the results presented in Chapter 5 will be discussed and comparisons of the results from the different mixes, exposure and measurement conditions will be compared to each other in order to draw conclusions. This chapter is divided into four sections in which the discussed results correspond to: (1) specimens submerged in tap water, (2) specimens submerged in chlorides (a comparison between both types of saturated specimens will be included also in this section), (3) influence of the moisture content in the electrical resistivity and (4) DC resistivity measurements.

7.1 Saturated specimens in tap water

In this section, the previously selected parameters that influence the electrical resistivity of reinforced concrete will be examined individually with respect to the experiments carried out in the laboratory. The figures presented in Chapter 5 will be first commented highlighting the main observations and then developed in relation to previous studies.

7.1.1 Effects of degree of hydration and frequency

Three main conclusions can be drawn from the results presented in Figure 24 to Figure 26:

- Resistivity increases with time
- Resistivity decreases with increasing fibre volume content
- Resistivity decreases with increasing frequency

As expected, electrical resistivity increased with time, this tendency is attributed to the degree of hydration which increases with time. This is in agreement with what (Monfore 1968) and (Mc Carter et al. 1981) found.

Compared with the initial resistivity, the samples containing fibres almost doubled their value for frequencies of 100 and 120 Hz after three months while the ones of plain concrete multiplied by five in the same time. However, this increase of resistivity is less notable when measured at 1000 Hz, even for plain concrete.

Differing from the results of (Mc Carter et al. 1981) and (Hope et al. 1985), the greater raise in the resistivity did not occur during the first month. However, the evolution of resistivity showed an irregular growth, a behaviour that is clearly shown in Figures 24 to 26 and that may be explained by the formation of a surface calcite ($CaCO_3$) layer on the surface of the specimens, caused by the reaction of calcium with water. This compound, present in the samples in the form of a white compound on their surface, is formed at the concrete surface due to the reaction of the calcium in the cement paste with water, increasing its electrical resistance as the pores are clogged.

During the experimental procedure, the samples were submerged in tap water inside a container and during the first six weeks, they were placed directly at the

bottom of the container, potentially preventing the development of the calcite layer in one of the surfaces (in the z-direction). The greatest growth in the resistivity was reached during week seven and at that moment, the samples were placed over a metallic structure so the bottom surface was not in direct contact with the bottom of the tank and the calcite layer was able to develop in all the six surfaces. At that point also, the water was refilled to completely immerse the samples and the growth became less steep.

Also according to previous studies, the resistivity of the samples decreased with increasing fibre volume content. Steel fibres act as an electrical conductor in the concrete matrix increasing its conductivity. The fibre volume content used in the experiments was not so high (from 0.5 to 1%) and the differences between the two dosages, although they exist, are minor. Also the relatively small size of the specimens used compared to the length of the fibres, might have led to a possible size effect. The main change in the resistivity appears when fibres are added in the mix in the first place. Comparing plain concrete with fibre reinforced concrete, the differences can already be observed in week one, when the resistivity of plain concrete is higher than the resistivity of specimens containing fibres while the ones of the samples with fibres seem to be almost independent on the dosage.

Obtaining the same results as in (Solgaard et al. 2010), the influence of fibres becomes more determinant with an increasing moisture content. In this case, as the degree of hydration of the samples increases with time, the differences in resistivity values also grow.

Studies such as those included in (Torrents et al. 2000), (Peled & Shah 2001) or (Mason et al. 2002) showed that frequency affects resistivity and that this effect is, at the same time, affected by the moisture content or degree of hydration. However, the effect of frequency in the range 100 to 1000 Hz should be fairly small (Larsen et al. 2007). As it can be seen in FiguresFigure 24, Figure 25 and Figure 26, the values measured at 1000 Hz are lower than the ones measured at 100 and 120 Hz, which are quite similar, but the differences observed are higher than expected, reaching factors of two in some cases, i.e plain concrete.

7.1.2 Effects of fibre orientation and frequency

Based on the previous results, it was decided that measurements with 100 and 120 Hz are quite similar and then only the results of 100 Hz and 1000 Hz were compared. Apart from the effects of fibre content and time, two trends can be found from the results presented in Figures 27 to 34:

- Resistivity measurements in x- and y-direction have similar behaviour, while it is different from that of the z-direction.
- Resistivity decreases with increasing frequency

The behaviour of resistivity in relationship with time and frequency coincides with the one in the previous section: resistivity increased with hydration grade and thus, through time and the measurements made with 1000 Hz showed lower resistivity values so no further explanations are needed.

By the way the concrete was poured (from the centre) and assuming that (Lataste et al. 2008) statements about the influence of fibre orientation in electrical resistivity of concrete are valid, the resistivity measured in the z-direction should be higher than the one measured in x- and y-directions as theoretically, it is the one in which the fibres are placed perpendicularly. When examining the results measured at 100 Hz (Figures 27 to 30), resistivity values measured in z-direction are higher during the first weeks and although the difference is small, it is more noticeable with higher fibre volumes. During weeks six to eight, the difference is reduced to finally show a higher value measured in z-direction in the last weeks of the experiments. In samples with 0.5% fibre content however, the results from fibre orientation are so small that could be considered negligible.

For the samples with no fibres, it is in the z-direction in which resistivity is lowest. This could be possibly related by the effects of the mould in the formation of the calcite layer as explained in section 7.1.1 and also by the aggregate distribution.

For the measurements made with 1000 Hz, the behaviour of the samples is similar although in a reduced scale due to the smaller values measured due to the higher frequency used. In this case, the resistivity in z-direction is lower again from weeks six-seven. But in this case, the later formation of the calcite layer in the bottom surface was enough to reverse the effects of the lack of it in the samples with 0.5% and after the three months, resistivity measured in z-direction was higher, as expected.

7.1.3 Position in the slab

The main purpose of this part of the study was to investigate whether the casting procedure had an effect on the distribution of fibres within the slab. Theoretically, the fibre distribution should follow a pattern of concentric circles. With regards to the electrical resistivity, this would mean a higher measured resistivity value in z-direction as the fibres would be oriented perpendicularly to the direction of the measurement and also, due to symmetrical reasons, a similar behaviour in the samples placed in columns A and C. At first sight, the conclusions that can be drawn from of the results presented in Figures 35 to 38 are:

- Higher resistivity in z-direction
- Similar resistivity in columns A and C

Whether more or less fibres remain in the centre or go to the sides is not clear. It would be logical to think that the steel fibres would follow the flow of the concrete towards the ends of the slab, which would lead to a higher fibre content in samples in columns A and C when comparing them to the ones in the B column. This would mean a higher conductivity in those columns and thus, a lower resistivity. However, with the results extracted from the experiments, it seems that there is not a trend that could be extracted although it also seems that a symmetry effect between A and C is found. The main conclusion out of this, is that the homogeneity assumption used before seems to be right.

7.2 Saturated specimens in chloride solution

Following the same structure as in Chapter 5 and as in the specimens submerged in water, the results obtained when studying the parameters that affect electrical resistivity of concrete when this is submerged in chlorides are commented in this section. After that, also a comparative study between samples submerged in water and samples submerged in chlorides is made.

7.2.1 Effects of degree of hydration and frequency

Directly from the results showed in Figure 39 to Figure 41, some conclusions can be extracted in the same direction as those observed in the samples submerged in tap water:

- Resistivity increases with time
- Resistivity decreases with increasing fibre volume content
- Resistivity decreases with increasing frequency

For all the samples studied, an upward trend of electrical resistivity with time is clearly shown in the graphs. These results agree with those of (Monfore 1968) and (Mc Carter et al. 1981) which determined that, under a moist environment such as the submersion in chloride solution, the electrical resistivity of concrete increases with the hydration grade.

Also in agreement with (Monfore 1968), resistivity doubled its value from 7 to 90 days in both cases, fibre reinforced concrete and plain concrete. But the expected higher growth during the first month described by (Mc Carter et al. 1981) could not be seen in these experiments.

Another thing that can be noted from Figure 39Figure 41 is that the frequency used to measure the resistivity of samples submerged in chlorides have an influence: i.e. samples of fibre reinforced concrete had maximum values of 21.3 Ωm when measuring at 100 Hz and 15.4 Ωm when measuring at 1000 Hz (for samples with 0.5% fibre content at week twelve). For plain concrete, the maximum value, also obtained in week twelve is 52.5 Ωm when measured at 100 Hz and 21.6 Ωm when measuring at 1000 Hz. This means that, as expected, resistivity values measured decrease with increasing frequency but also that this decrease is higher with lower fibre content.

The results clearly show that the addition of steel fibres decreases the electrical resistivity of concrete when measured with AC. The greatest difference is found when comparing plain concrete with fibre reinforced concrete: by analysing the results measured at 100 Hz it can be noted that in week one, plain concrete had an initial resistivity of 27.6 Ωm while the resistivity at a fibre content of 0.5% was 11.3 Ωm. This results, around 40% of the value for plain concrete seems to maintain a certain proportion after three months when this proportion was around 37% (56.5 Ωm for plain concrete and 21.2 Ωm for 0.5% fibre content). The differences in resistivity within samples with steel fibres are smaller as the differences in fibre contents used are relatively small, the differences between the lower and the higher fibre content is only 5.2 Ωm for the initial electrical resistivity and 6.8 Ωm after three months. These results corroborates that steel fibres are metallic incisions that increase the conductivity of concrete when added and that

an increasing fibre content decreases resistivity, as long as they are in a conductive state.

These results are in agreement with (Solgaard 2013) who concluded that the influence of fibres is more determinant with increasing hydration grade.

7.2.2 Effects of fibre orientation and frequency

As done for the samples submerged in tap water, in this section the results of the measurements conducted at 100 and 1000 Hz are compared. The following principal conclusions can be made:

- The values of the resistivity measured in z-direction are higher than the values measured in x- and y-direction.

As the degree of hydration increases with time, resistivity also increases in a very regular way and also the values measured at 100 Hz are slightly higher than the same ones measured at 1000 Hz. Both results were already explained in section 7.2.1 so no further explanation is deemed necessary. Also explained before, the resistivity of plain concrete is higher as it has no metallic fibres that increase its conductivity.

When it comes to the orientation of fibres, it is noticeable that the resistivity measured in the z-direction differs from that of the x- and y-direction. In order to draw conclusions about the influence of fibre orientation, the concrete was poured from the centre. In that way, the fibres where expected to be perpendicular to the z-direction and thus, the resistivity measured in this direction should be higher. As it can be seen, the results obtained through the three months of experimental investigation fulfilled the expectations and agreed with (Lataste et al. 2008).

It should also be noted that although this difference between z- and x-, y-directions is noticeable for samples with 1% fibre content, it is maximum with 0.75% fibre content. Something that draws the attention as the expected result was that the highest difference was found in the highest fibre content, although this behaviour may be explained by the higher measured slump flow on it.

The behaviour of plain concrete is showing a linear upward trend with time without almost any difference between directions. These results seem to agree with the theoretical behaviour of how the resistivity of plain concrete develops.

7.2.3 Position in the slab

In this section, both, the position in the slab and direction of the measurements have been compared. The main aim for doing this was to determine whether the fibre orientation associated to the casting could have an impact on the electrical resistivity. The main observation from the results was the following:

- Resistivity measured in z-direction is higher than when measured in x- and y-directions.

The expected results for this part of the study were the same as the ones expected in the samples submerged in tap water. Regarding the position in the slab, being

the fibres distributed in concentric circles from the centre, the expected situation is that columns A and C in the slab had a higher fibre content as concrete pushes fibres to the corners, increasing the conductivity there. As the fibres are expected to be mostly oriented parallel to the xy-plane, the resistivity measured in the z-direction should be higher in order to verify this assumption.

With respect to the position in the slab, there are no clear conclusions that can be extracted from the results. As an example, measuring the resistivity in the x-direction, the higher values can be found in C samples with 1 and 0.75% fibre volume content but in A when having 0.5% fibre content. There is not a clear trend for minimum values either: they are measured in A for 1% but in B for 0.75% and 0.5%.

7.2.4 Chlorides compared with tap water

As previously mentioned, the samples were exposed to two different moist environments: one consisting in tap water and the second one consisting in a chloride solution (3.5% NaCl). The conductivity of the chloride solution is considerably higher than the conductivity of tap water and the resistivity of the samples will be affected by this behaviour (McNeill 1980).

The results obtained clearly agree with the assumptions made and the resistivity for the samples submerged in NaCl are noticeably lower than the resistivity of the ones submerged in water, with proportions that range from 80% in the beginning of the investigation to 15% after three months of the tap water value as it can be seen in Table 7.

Table 7 Resistivity [Ωm] of samples submerged in a chloride solution compared to resistivity [Ωm] of samples submerged in tap water

Fibre content	Environment	Week 1	Week 4	Week 8	Week 12
1%	Tap water	13.8	25.5	64.2	68.4
	Chloride solution	6.1	7.5	9.9	12.9
	Ratio	44.2%	29.5%	15.4%	18.9%
0.75%	Tap water	13.9	24.3	63.7	64.9
	Chloride solution	8.2	10.5	12.7	15.4
	Ratio	59.0%	43.2%	19.9%	23.7%
0.5%	Tap water	19.1	34.3	73.2	75.1
	Chloride solution	11.3	13.6	17.5	21.6
	Ratio	59.2%	39.8%	23.9%	28.7%
0%	Tap water	35.4	57.8	120.3	125.2
	Chloride solution	27.6	36.9	43.5	53.5
	Ratio	78.1%	63.8%	36.2%	42.8%

Two observations can be extracted from the results presented above. The first one is that for the samples submerged in 3.5% NaCl, with increasing fibre contents the proportion of their resistivity values compared to those of samples submerged in water, decreases.

The second observation is that the reduction of resistivity seems to get higher until it reaches a maximum in week eight, something that should not be taken as a

significant results as it may be explained by the anomalous behaviour showed by samples submerged in tap water caused, probably, by the formation of a calcite layer in their surface as it was previously mentioned.

7.3 Effect of moisture content

The moisture content is one of the parameter with the highest influence on concrete resistivity and to study how this parameter influences resistivity, the samples were exposed to different environments. The results to be commented in this section are those measured in week twelve for the samples in each group.

Before the analysis, it should be noted that the results showed for environments *75F* and *50F* (which stand for "forced to dry to 75 and 50% relative humidity" respectively) are uncertain as the samples were accidentally dried to a lower moisture content due to a bad sealing during the process of moisture redistribution. As it can be seen in Appendix D, the samples reached values of nearly 30% relative humidity and thus, when comparing between different environments, these ones will not be taken into account as the conclusions extracted from them would not be valid.

From the literature review, an increasing resistivity with decreasing fibre volume content is expected (Solgaard 2013). However, when analysing the results, it can be noted that this trend is only followed for the saturated specimens, the results of which were already commented.

In the case of the specimens that were left to dry in the sealed box to 75% relative humidity, it seems that specimens with 1% fibre content had the second highest resistivity while for the cubes that were left to dry in the climate chamber to 50%, specimens with 1% fibre content had the third highest resistivity. At first, it was thought that this discrepancy could be related to the irregular water losses that the specimens suffered but after checking their final relative humidity, this option was dismissed (see appendix D for more information). A possible explanation for this would be the fibre contents used: having a maximum fibre content of 1% and being the differences between the other fibre contents so small, there is no clear tendency on how the fibres are connected to each other, so the values depend on how the conductive paths made of steel fibres are created inside concrete. In case of the specimens that were completely dried in the oven, the trend within the samples made of fibre reinforced concrete corresponds to a higher resistivity with lower fibre content, but when it comes to plain concrete, of which resistivity should be higher, the results show that the resistivity is in the same range of the samples with lower fibre contents.

The second analysis that was performed with these results was the comparison between the different exposures. One thing that is obvious from the results shown in Figure 54 to Figure 57 and that in agreement with the results found by (Gjørv et al. 1977) and (Büyüköztürk & Taşdemir 2013) is that the oven dried samples have the highest resistivity, as they do not have conductive water in their interior (Hunkeler 1996).

Following this theory, an increasing moisture content should decrease the resistivity of concrete, reaching a minimum value when the specimens are saturated, as there is more pore water to conduct current. When analysing the samples made of fibre reinforced concrete, this trend is followed in all cases except for the samples with 0.75% fibre content. In that slab, it seems that the resistivity of the samples submerged in tap water is higher than the one with a 75% relative humidity, although the difference between them is minimal. A possible explanation for this observation is that the gel pores are still filled with conductive water at that relative humidity and thus, values range around similar values. For the other fibre contents, 1% and 0.5%, even the results named after samples *75F* and *50F*, in which moisture content is actually around 30%, followed this trend agreeing with results from previous studies.

With samples made of plain concrete, the oven dried samples, 0F, increased the resistivity by almost 5 MΩ·cm with respect to the saturated samples and in between this two limit values, the progression followed by the electrical resistivity is the one expected: resistivity decreased with increasing moisture content.

7.4 DC Measurements

As stated before, DC is important to understand how steel fibres can influence the corrosion process of conventional reinforcement in concrete. The main question is whether steel fibres might conduct DC, thus influencing the corrosion rate of reinforcement bars. According to previous studies, steel fibres do not conduce stray current until a threshold voltage is reached (Bertolini et al. 1993).

Trying to find this value, the specimens were subjected to an increasing voltage first until the current through them was 20 mA and once they reached equilibrium, the voltage was decreased manually. The evolution of current with a decreasing voltage was shown in Figure 58 to Figure 60.

The evolution of current in samples made of plain concrete is almost linear, showing a single-slope behaviour while the intensity-voltage curve of all the samples containing steel fibres exhibited a two-slope behaviour. These results are in agreement with the results from (Wen & Chung 1999) and (Hixson et al. 2003).

In fibre reinforced concrete at low voltages, the slope was flatter, following the slope of plain concrete but, when the voltage reached a value of around 6 V, in these experiments, the curves diverged. The assumption is that at that point, the passive layer formed on the surface of the fibres in the concrete environment breaks down (Torrents et al. 2000) and thus, fibres become conductive. As it can be seen from the graphs, the behaviour of the curves differ depending on where in the slab they were cut off.

Samples in columns B and C (Figures 59 and 60) have behaviours that are difficult to summarize as it seems that there is no tendency between them. While the samples in column C have no difference with respect to the fibre content, samples in cubes B show difference but with no specific order: cubes with 1 and 0.5% fibre

content behaved in a similar way while the cube with 0.75% show a lower resistivity.

When it comes to samples in column A (Figure 58) though, two conclusions can be drawn: first, the slope gets steeper with a higher volume content and thus, resistivity decreases, a result that satisfies the expectations. Secondly, fibres become conductive at lower voltage values with a higher fibre content. This is explained by the higher possibility of forming a metallic path through concrete with a higher fibre content, although a complete path is unlikely to happen.

For each sample, resistivity was calculated at both, low and high voltages trying to confirm that at low voltages, the resistivity should be higher following the only trend shaped by the fibre content and that, at higher voltages, this resistivity should decrease specially in the samples containing fibres as these become conductive lowering the resistance of steel reinforced concrete. This behaviour is shown in Figure 62 in which the resistivity of plain concrete is higher than the resistivity of reinforced concrete and that all resistivity values measured at high voltages lowered their value. However the values found at low voltages, around 90 Ω·m for plain concrete and below 40 Ω·m for samples with 1% fibres are significantly lower compared with the same values measured with AC (approximately 220 Ωm and 80 Ωm respectively). When the same values are calculated with the results shown in Figure 61, while the calculated resistivity of plain concrete matches the values measured with AC, the results for fibre reinforced concrete are quite higher, in values that range from 200 to 350 Ωm while the AC values ranged 80-110 Ωm.

8 Discussion of the corrosion rate experiment

In this section, the results shown in Chapter 6 will be commented and discussed to try to determine whether an impact of the steel fibres on the corrosion rate of traditional reinforcement bars exist or not. The results are presented in two groups of three graphs each, one with the accumulated steel loss in the reinforcement bars (mg) and another with the instantaneous penetration rate (μm/year).

In Figure 63 to Figure 65, the calculated theoretical steel loss during the ninety days the study took place is plotted. As it can be seen, the maximum loss (~20 mg) corresponds to one of the reinforcement bars with three surfaces exposed to chlorides in the beam with 1% fibre content. A shared fact is that all reinforcement bars show a low weight loss, which could have two explanations: either the exposure environment was not enough corrosive to achieve a significant amount of corrosion in three months or that micro-cell corrosion is taking place rather than macro-cell and therefore, as cathode and anode are both in the reinforcing bars, the current flowing could not be measured. There is however a small tendency that, after 8 weeks of exposure, the weight loss of the bars with fibres seems increasing, probably due to the ingress of chlorides from the external 10% NaCl solution. Longer exposure experiment is, however, needed to confirm this tendency.

The theoretical penetration rate is shown in Figure 66 to Figure 68 and as it can be seen in all the three graphs and each bar, the higher values are found during the first week of measurement, probably due to the reduced oxygen availability caused by the continuous hydration of cement. When analysing the penetration rate there is again, no pattern followed. When looking at the bars in position a and position b, all the values are relatively low although there are some peaks in the penetration rate of rebars embedded in the beam made of plain concrete. However this phenomenon does not occur in the bar in position c, which is supposed to have the same behaviour as the one in position and thus, the results from this experiment with 3 months exposure are still uncertain.

If the results are analysed without considering the first week, none of the reinforcement bars exceeds a penetration rate of 1 μm/year which according to (Bertolini et al. 2004) can be categorized as a negligible corrosion rate. Therefore the main problem in this part is that it seems that the exposure environment to which the beams were exposed, 2%NaCl per weight of cement added directly to the mix and a partial submersion in a 10%NaCl solution, is not corrosive enough to draw conclusions in three months. Further experiment for severed and longer exposure is needed to confirm the results

Regardless of the low values obtained, there is no evidence that steel fibres increased the corrosion rate of conventional steel bars embedded in concrete exposed to a chloride environment.

9 Conclusions

This Master thesis had two main objectives: first, to study the influence of steel fibres on the electrical resistivity of concrete under different exposure conditions, including both, moist-curing and air-curing environment (all the specimens were moist-cured for 28 days before exposing them to their respective environments). The second objective was to try to determine whether the use of steel fibres in conventionally reinforced concrete structures could be beneficial or detrimental with respect to the service life. To try to answer these two questions, the project was divided into two parts: resistivity studies and a corrosion rate experiment. For each of them, a literature review was firs carried out and then, based on it, an experimental programme was designed and performed.

Following this structure, this chapter is divided in two subsections, one per part of the project. In both of them, the conclusions are drawn out of both, the literature review and the laboratory experiments.

9.1 Conclusions of the resistivity part

During the literature review, the main parameters affecting electrical resistivity of concrete were determined. How these parameters affect was analysed by comparing previous studies and the main conclusions that can be drawn of this phase are:

- The most important parameter affecting the electrical resistivity is the moisture content, not only by its direct influence over it but also by its indirect influence on the effects of other parameters
- Increasing moisture content decreases the electrical resistivity
- Increasing temperature reduces the viscosity of the electrolyte and increases the mobility of ions and thus, decreases the electrical resistivity
- Resistivity increases with time
- Chlorides increase the conductivity of the electrolyte and thus decrease the electrical resistivity of concrete
- An increasing fibre content decreases electrical resistivity, this effect is higher at lower moisture content
- The electrical resistivity is higher when it is measured in a direction in which fibres are oriented perpendicularly to it
- Frequency effects depend on temperature and moisture content
- When applying them a voltage, fibres become conductive when surpassing a threshold value, this has been found to be 1.2 V.

For the experimental process, it was decided that neither the composition of concrete, except from the fibres, nor temperature were parameters to study during the performance of this Master thesis. After three months of study, the main conclusions drawn are:

- Electrical resistivity increases with time
- Electrical resistivity decreases with increasing fibre volume content, the effect is higher at lower frequencies
- Electrical resistivity decreases with increasing frequency

- For the concrete placed in water a calcite layer is thought to have been formed on its surface which caused an increase of the resistivity
- From the results of the experiments, it can be concluded that resistivity is higher when the fibres are oriented perpendicularly to the direction of measurement in specimens immersed in chlorides. This behaviour is also observed in the samples submerged in chlorides although the results are not conclusive due to some contradictions.
- A submersion in a chloride solution decreases electrical resistivity, the effect is more noticeable with higher fibre contents
- Electrical resistivity decreases with an increasing moisture content
- When looking at its current-voltage curve, plain concrete has a single-slope behaviour curve while steel fibre reinforced concrete has a two-slope behaviour curve.
- There is a voltage threshold value above which fibres become conductive. This value was found to be around 6 V in this experiment, corresponding to 86 V/m, higher than that in the literature and being potentially lower for increasing fibre contents. This existence of this threshold value would explain the two-slope behaviour.

9.2 Conclusions of the corrosion rate part

The question that was being investigated in this section was whether the addition of fibres in low dosages (0.5-1%) would influence the corrosion rate of conventional reinforced bars embedded in concrete. In order to achieve this objective, first a literature review was made and then, an experimental programme was developed. The main conclusions from the literature review are:

- There is no agreement between different studies and thus, it is not yet clear if the addition of fibres have any effect in the corrosion or traditional reinforcement bars and in case of existing, whether this effect is beneficial or not.

The experimental part of this section of the project also took three months in which the reinforcement bars were continuously controlled in terms of galvanic current to calculate their theoretical weight loss and their penetration rate both based on Faraday´s law. As previously mentioned during the discussion chapter, the values obtained showed a very low corrosion for all the specimens, meaning that probably corrosion is not developing as expected. In any case, the conclusions from the experiments carried out in the laboratory are:

- The position in the beam, which determines the amount of surface area directly exposed to the chloride solution is not relevant
- From the results of the experiment, there is no evidence that the steel fibres have any effect on the corrosion rate of reinforcement bar.
- The setup used for the experiment might not be the adequate as micro-cell corrosion might be more critical.

10 References

ACI Committee 544.5R-10, 2010. *Report on the Physical Properties and Durability of Fiber-Reinforced Concrete*,

Alonso, C., Castellote, M. & Andrade, C., 2002. Chloride threshold dependence of pitting potential of reinforcements. *Electrochimica Acta*, 47(21), pp.3469–3481.

Andrade, C., 2003. Determination of chloride threshold in concrete. *Corrosion of Steel in Reinforced Concrete Structures*, pp.100–108.

Andrade, C. et al., 1999. Rilem TC 116-PCD : Preconditioning of Concrete Test Specimens for the Measurement. *October*, 32(April), pp.174–176.

Andrade, C. & Andrea, R., 2010. Electrical resistivity as microstructural parameter for modelling of service life of reinforced concrete structures. *2nd International Symposium on Service Life Design for Infrastructure, Delft, Netherlands*, (October), pp.379–388.

Andrade, C.. & Alonso, C., 1996. Corrosion rate monitoring and on-site. , 10(5), pp.315–328.

ASTM G109, 2013. Standard Test Method for Determining Effects of Chemical Admixtures on Corrosion of Embedded Steel Reinforcement in Concrete Exposed to Chloride Environments. , 07(Reapproved 2013), pp.1–6.

Barnett, S.J. et al., 2010. Assessment of fibre orientation in ultra high performance fibre reinforced concrete and its effect on flexural strength. *Materials and Structures*, 43, pp.1009–1023.

Bertolini, L. et al., 2004. *Corrosion of Steel in Concrete*,

Bertolini, L. et al., 1993. Stray current induced corrosion in reinforced concrete structures. *Proceedings of the Tenth European Corrosion Congress, Barcelona, The Institute of materials*, pp.658–664.

Broomfield, J. et al., 1993. Corrosion Rate Measurement and Life Prediction for Reinforced Concrete Structures. *Proceedings of Structural Faults and Repair*, 2, pp.155–164.

Broomfield, J. & Millard, S.G., 2002. Measuring concrete resistivity to assess corrosion rates. *Concrete*, (128), pp.37–39.

Büyüköztürk, O. & Taşdemir, M.A., 2013. Nondestructive Testing of Materials and Structures. *Nondestructive Testing of Materials and Structures*, pp.703–709. Available at: http://link.springer.com/10.1007/978-94-007-0723-8.

Cavalier, P. & Vassie, P., 1981. Investigation and repair of reinforcement corrosion in a bridge deck. *ICE Proceedings*, 70(3), pp.461–480.

Dauberschmidt, C. & Raupach, M., 2005. Passivity and Depassivation of Steel Fibres and Cold-Drawn Steel Wires in Artificial Pore Solution and Concrete Containing Chlorides. , pp.1–11.

Domone, P.L.J. & Illston, J.., 2010. *Construction materials: Their nature and behaviour.pdf* 4th ed., New York: Spon Press.

Elkey, W. & Sellevold, E.J., 1995. Electrical resistivity of Concrete. *Norwegian Road Research Laboratory*, (80).

Gjørv, O.E., Vennesland, Ø. & El-Busaidy, 1977. Electrical resistivity of concrete in the oceans. *Offshore Technology Conference*, pp.581–589.

González, J. a., Miranda, J.M. & Feliu, S., 2004. Considerations on reproducibility of potential and corrosion rate measurements in reinforced concrete. *Corrosion Science*, 46(10), pp.2467–2485.

Granju, J.-L. & Ullah Balouch, S., 2005. Corrosion of steel fibre reinforced concrete from the cracks. *Cement and Concrete Research*, 35(3), pp.572–577.

Hammond, E. & Robson, T.D., 1955. Comparison of Electrical Properties of Various Cements and Concretes. *The Engineer*, 199(5156; 5166), pp.78–80; 114–115.

Hansson, C.M., Poursaee, a. & Laurent, a., 2006. Macrocell and microcell corrosion of steel in ordinary Portland cement and high performance concretes. *Cement and Concrete Research*, 36(11), pp.2098–2102.

Hedenblad, G., 1996. *Materialdata för fukttransportberäkningar*, Stockholm: Byggforskningsrådet.

Heiyantuduwa, R., Alexander, M. & Mackechnie, J., 2006. Performance of a Penetrating Corrosion Inhibitor in Concrete Affected by Carbonation-Induced Corrosion. *Materials in Civil Engineering*, 18(6), pp.842–850.

Henry, R.L., 1964. *Water vapor transmission and electrical resistivity of concrete*, Port Hueneme, California.

Hixson, a. D. et al., 2003. The origin of nonlinear current-voltage behavior in fiber-reinforced cement composites. *Cement and Concrete Research*, 33, pp.835–840.

Hope, B.B., Ip, A.K. & Manning, D.G., 1985. Corrosion and electrical impedance in concrete. *Cement and Concrete Research*, 15(c), pp.525–534.

Hornbostel, K., Larsen, C.K. & Geiker, M.R., 2013. Relationship between concrete resistivity and corrosion rate - A literature review. *Cement and Concrete Composites*, 39, pp.60–72.

Hughes, B.P., Soleit, A.K. & Brierley, R.W., 1985. New technique for determining the electrical resistivity of concrete. *Magazine of Concrete Research*, 37, pp.243–248. Available at: http://www.icevirtuallibrary.com/content/article/10.1680/macr.1985.37.133.243.

Hunkeler, F., 1996. The resistivity of pore water solution - A decisive parameter of rebar corrosion and repair methods. *Construction and Building Materials*, 10(5), pp.381–389.

Langford, P. & Broomfield, J., 1987. Monitoring the corrosion of reinforcing steel. *Construction Repair*, 1(2), pp.32–36.

Larsen, C.K., Østvik, J.M. & Bjøntegaard, Ø., 2007. *Compilation of 5 papers on Electrical resistivity as a durability indicator and Cracking tendency in hardening concrete*, Oslo.

Lataste, J.F., Behloul, M. & Breysse, D., 2008. Characterisation of fibres distribution in a steel fibre reinforced concrete with electrical resistivity measurements. *NDT & E International*, 41, pp.638–647.

López, W. & González, J. a., 1993. Influence of the degree of pore saturation on the resistivity of concrete and the corrosion rate of steel reinforcement. *Cement and Concrete Research*, 23(2), pp.368–376.

Mangat, P.S. & Gurusamy, K., 1987. Permissible crack widths in steel fibre reinforced marine concrete. *Materials and Structures*, 20(5), pp.338–347.

Mason, T.O. et al., 2002. Impedance spectroscopy of fiber-reinforced cement composites. *Cement and Concrete Composites*, 24, pp.457–465.

Mc Carter, W., Forde, M. & Whittington, H., 1981. Resistivity Characteristics of Concrete. *Proceedings - Institution of Civil Engineers. Part 2. Research and theory.*, 71(MAR), pp.107–117.

McNeill, J.D., 1980. Electrical conductivity of soil and rocks. , (TN--6), p.20. Available at: C:\TIN\e-books\00-Articles\Geonics\TN 5 - Electrical conductivity of soils and rocks.pdf.

Monfore, G.E., 1968. The electrical resistivity of Concrete. *PCA Research and development laboratories*, 10, pp.35–48.

Morris, W. et al., 2002. Corrosion of reinforcing steel evaluated by means of concrete resistivity measurements. *Corrosion Science*, 44(1), pp.81–99.

Nesic, S., Xiao, Y. & Technology, M., 2004. Corrosion 2004. *Corrosion*, (04326), pp.1–16.

Newlands, M. et al., 2007. Sensitivity of electrode contact solutions and contact pressure in assessing electrical resistivity of concrete. , pp.621–632. Available at: http://dx.doi.org/10.1617/s11527-007-9257-6.

Peled, a & Shah, S.P., 2001. Analysis of the impedance spectra of short conductive fiber- by Analysis of the impedance spectra of short conductive fiber-reinforced composites. , 36, pp.4003–4012.

Polder, R. et al., 2001. RILEM TC 154-EMC : Electirical techniques for measuring-Test methods for on site measurement of resistivity of concrete. *Materials and Structures*, 33, pp.603–611.

Polder, R.B., 2001. Test methods for on site measurement of resistivity of concrete - a RILEM TC-154 technical recommendation. *Construction and Building Materials*, 15, pp.125–131.

Powers, T., 1958. Structure and Physical Properties of Hardened Portland Cement Paste. *Methods*, 41.

Rasch, von E. & Hinrichsen, F.W., 1908. Uber eine beziehung zwischen elektrischer leitfahigkeit und temperatur. *ZEITSCHRIFT FÜR ELEKTROCHEMIE*, 5, pp.41–48.

Raupach, M. & Dauberschmidt, C., 2002. Corrosion behaviour of steel fibres in artificial pore solutions. In *15th International corrosion congress, Frontiers in Corrosion Science and Technology.*

Sergi, G., 1986. *Corrosion of Steel in Concrete: Cement Matrix Variables* U. of Aston, ed.,

Smith, K., Schokker, A. & Tikalsky, P., 2004. Performance of Supplementary Cementitious Materials in Concrete Resistivity and Corrosion Monitoring Evaluations. *ACI Mater*, 101(5), pp.385–390.

Solgaard, A., Carsana, M., et al., 2013. Experimental observations of stray current effects on steel fibres embedded in mortar. *Corrosion Science*, 74, pp.1–12. Available at: http://dx.doi.org/10.1016/j.corsci.2013.03.014.

Solgaard, A. et al., 2010. Modelling the influence of steel fibres on the electrical resistivity of cementitious composites. *3rd International RILEM PhD Student workshop on Modelling the Durability of Reinforced Concrete - University of Minho*, (1962), pp.20–27.

Solgaard, A., Geiker, M., et al., 2013. Observations on the electrical resistivity of steel fibre reinforced concrete. *Materials and Structures*, 47, pp.335–350.

Spencer, R.W., 1937. Measurement Of The Moisture Content of Concrete. *Journal Proceedings*, 34(9), pp.45–64.

Spragg, R. et al., 2013. Electrical Testing of Cement-Based Materials: Role of Testing Techniques, Sample Conditioning, and Accelerated Curing. , p.23. Available at: http://dx.doi.org/10.5703/1288284315230.

Torrents, J.M., Mason, T.O. & Garboczi, E.J., 2000. Impedance spectra of fiber-reinforced cement-based composites: A modeling approach. *Cement and Concrete Research*, 30, pp.585–592.

Tuutti, K., 1982. Corrosion of steel in concrete. *CBI Report 4:82, The Swedish Cement and Cocnrete Institute.*, p.468.

Vassie, P., 1984. Reinforcement corrosion and the durability of concrete bridges. *Proceedings of the Institution of Civil Engineers*, 76(1), pp.713–723.

Wen, S. & Chung, D.D.L., 1999. Carbon fiber-reinforced cement as a thermistor. *Cement and Concrete Research*, 29(6), pp.961–965.

Whiting, D. a & Nagi, M. a, 2003. Electrical Resistivity of Concrete - A Literature Review. *Development*.

Woelfl, G. & Lauer, K., 1979. The Electrical Resistivity of Concrete with Emphasis on the Use of Electrical Resistance for Measuring Moisture Content. *Cement, Concrete and Aggregates*, 1(2), p.64.

Yoon, I.S., Çopuroğlu, O. & Park, K.B., 2007. Effect of global climatic change on carbonation progress of concrete. *Atmospheric Environment*, 41(34), pp.7274–7285.

Appendix A: Concrete properties

Porosity

Degree of hydration

$t_{days} := 28$

$t := t_{days} \cdot 24 = 672$ [h]

Water content:

$wc := 0.47$

Maximum degree of hydration:

$$\alpha_{max} := \begin{cases} 1 & \text{if } wc \geq 0.39 \\ \frac{wc}{0.39} & \text{if } wc < 0.39 \end{cases}$$

$\alpha_{max} = 1$

Constants A_α and B_α:

- For OPC at an age of 2.5 years

$$\alpha_{h2\_\alpha.max} := \begin{cases} 1 & \text{if } wc \geq 0.625 \\ 1.265\sqrt{wc} & \text{if } wc < 0.625 \end{cases}$$ (Based on the data from Czermin, 1964)

$\alpha_{h2\_\alpha.max} = 0.867$

- At an early age

$T := 293$

$$E_\alpha := \begin{cases} 36000 & \text{if } T \geq 293 \\ 65000 & \text{if } T < 293 \end{cases}$$

$R := 8.31$

$$\alpha_{h1} := 0.48\sqrt{wc} \cdot \exp\left[\frac{-E_\alpha}{R} \cdot \left(\frac{1}{T} - \frac{1}{293}\right)\right]$$ (Based on the data from Atlassi, 1995)

$\alpha_{h1} = 0.329$

$t_1 := 24$

$t_2 := 2.5 \cdot 365 \cdot 24 = 2.19 \times 10^4$

$$B_\alpha := \frac{\ln\left(\frac{\ln(\alpha_{h2\_\alpha.max})}{\ln\left(\frac{\alpha_{h1}}{\alpha_{max}}\right)}\right)}{\ln\left(\frac{\ln(t_1)}{\ln(t_2)}\right)}$$

$B_\alpha = 1.793$

$$A_\alpha := \frac{-\ln\left(\frac{\alpha_{h1}}{\alpha_{max}}\right)}{\ln(t_1)^{-B_\alpha}}$$

$A_\alpha = 8.838$

$$\alpha_h := \alpha_{max} \cdot \exp\left[-A_\alpha \cdot (\ln(t))^{-B_\alpha}\right] = 0.735$$

$\alpha_h = 0.735$

Non-evaporable water

- Cement content:

  $C := 385$ [kg/m^3]

- Silica fume

  $SF := 0$

  $k_{SF} := 0.0212t^{0.44}$

- Fly ash:

  $FA := 0$

  $k_{FA} := 0.0286t^{0.286}$

- Slag coefficient

  $SL := 0$

  $k_{SL} := \alpha_h$

$$W_n := 0.25\alpha_h \cdot C - 0.34k_{SF} \cdot SF + 0.25k_{FA} \cdot FA + 0.25k_{SL} \cdot SL$$

$W_n = 70.792$ [Kg/m³ concrete]

Gel quantity

$$W_{gel} := \alpha_h \cdot C + k_{SF} \cdot SF + k_{FA} \cdot FA + k_{SL} \cdot SL + W_n$$

$W_{gel} = 353.958$ [Kg/m³ concrete]

Diffusible porosity under the capillary saturated condition

$m_C := 385$

$\rho_C := 3.2 \cdot 10^3$

$m_{Limus} := 180$

$\rho_{Limus} := 2.76 \cdot 10^3$

$m_{Bsand} := 478.2$

$\rho_{Bsand} := 2.63 \cdot 10^3$

$m_{Ssand} := 481.8$

$\rho_{Ssand} := 2.65 \cdot 10^3$

$m_{stone} := 635.1$

$\rho_{stone} := 2.62 \cdot 10^3$

$$Sum_{solids} := \frac{m_C}{\rho_C} + \frac{m_{Limus}}{\rho_{Limus}} + \frac{m_{Bsand}}{\rho_{Bsand}} + \frac{m_{Ssand}}{\rho_{Ssand}} + \frac{m_{stone}}{\rho_{stone}}$$

$Sum_{solids} = 0.792$

$\varepsilon_{air} := 0.02$

$$\varepsilon := 1 - Sum_{solids} - 0.75\frac{W_n}{1000} - \varepsilon_{air}$$

$$\varepsilon = 0.135$$

Compressive strength test

A compressive strength test was made on each of the mixes for both parts of the investigation. For the resistivity part, cubes with side length 150 mm were used while the ones used for the corrosion rate part had 100 mm side length.

The procedure followed for these tests was the standard one: the concrete was poured in the mould and covered by a plastic sheet to avoid evaporation from the surface for 24h after which it was de-moulded and submerged in tap water until it reached the age of 28 days, time when they were tested.

Table 8 Compressive strength test for the concrete used in the resistivity tests

Cube	Weight [g]	*h* [mm]	*l* [mm]	*b* [mm]	Density [kg/m³]	Load (Q1) [kN]	$f_{c,cube}$ [MPa]
1% A	7825	150	150	150	2320	1205,18	53.6
1% B	7870	150	150	152	2300	1176,87	51.6
0,75% A	7937	150	149,5	149,5	2370	1275,07	57.0
0,75% B	7861	149,5	150	149,5	2340	1285,42	57.3
0,5% A	8075	150	150	151	2380	1396,49	61.7
0,5 % B	7880	149,5	150	148	2370	1366,04	61.5
0% A	7983	149,5	150	149	2390	1414,05	63.3
0% B	7988	150	150	148,5	2390	1457,96	65.5

Table 9 Compressive strength test for the concrete used in the corrosion rate tests

Cube	Weight [g]	*h* [mm]	*l* [mm]	*b* [mm]	Density [kg/m³]	Load [kN]	f_{cc} [MPa]
1% A	2460	100	99	100	2480	723,29	73.1
1% B	2497	100	99	100,5	2510	709,08	71.3
0,75% A	2461	100	99,5	100	2470	712,01	71.6
0,75% B	2474	101	99	100,5	2460	685,50	68.9
0,5% A	2471	100	99	100,5	2480	702,02	70.6
0,5 % B	2467	100	99	101,5	2460	717,66	71.4
0% A	2418	101	100	100	2390	686,61	68.7
0% B	2418	100	101	99,5	2410	691,18	68.8

Appendix B: Sorption curves

In his investigation, Hedenblad defined the sorption isotherms for different types of materials. When it comes to concrete, the parameters that were used were the *w/c* ratio and the cement content. All the four mixes used for the studies in this project had a *w/c* ratio of 0.47 and also a cement content of 385kg/m^3. There are existing curves for w/c ratios of 0.4 and 0.5 but not for 0.47 so it had to be calculated. First of all, the correction factors 385/450 and 385/360 defined by Hedenblad were used in order to correct the curves for 0.4 and 0.5 respectively. Once this was done, linear behaviour of concrete in terms of its *w/c* ratio was assumed and thus, linear interpolation was used for getting the desorption curve related to the mix.
All the calculated values for the different water-cement ratios are listed in Table 10 and the curves, graphed together with the originals from Hedenblad can be seen in Figure 69 for water-cement ratios 0.4 and 0.5 respectively. In Figure 70, the sorption curve for the mix in the project can be seen.

Table 10 Calculated absorption and desorption values

	***w/c*=0.4**		***w/c*=0.5**		***w/c*=0.47**	
RH	W_{des}	W_{abs}	W_{des}	W_{abs}	W_{des}	W_{abs}
0	0.00	0.00	0.00	0.00	0.00	0.00
0.05	14.80	5.15	15.45	9.12	15.26	7.93
0.1	20.79	8.20	22.16	15.44	21.75	13.27
0.15	25.51	11.81	28.58	20.47	27.66	17.87
0.2	28.29	14.16	32.01	23.72	30.89	20.85
0.25	30.64	16.30	36.29	26.22	34.59	23.25
0.3	32.00	17.88	39.26	28.27	37.08	25.15
0.35	33.52	19.53	41.86	30.12	39.36	26.94
0.4	35.59	20.62	45.01	31.85	42.19	28.48
0.45	37.39	21.71	47.99	33.45	44.81	29.93
0.5	40.02	22.24	52.07	34.65	48.45	30.93
0.55	42.78	23.48	57.28	36.23	52.93	32.41
0.6	46.39	24.84	62.31	37.33	57.53	33.59
0.65	50.56	26.78	68.82	39.00	63.34	35.34
0.7	54.59	29.97	76.07	41.98	69.63	38.37
0.75	58.62	33.29	82.96	47.00	75.65	42.89
0.8	63.63	36.90	90.58	51.56	82.50	47.16
0.85	69.48	44.01	97.66	63.00	89.21	57.30
0.9	77.56	55.03	108.08	77.52	98.92	70.78
0.95	90.26	81.59	125.96	107.70	115.25	99.87
1	96.25	96.25	139.03	139.03	126.19	126.19

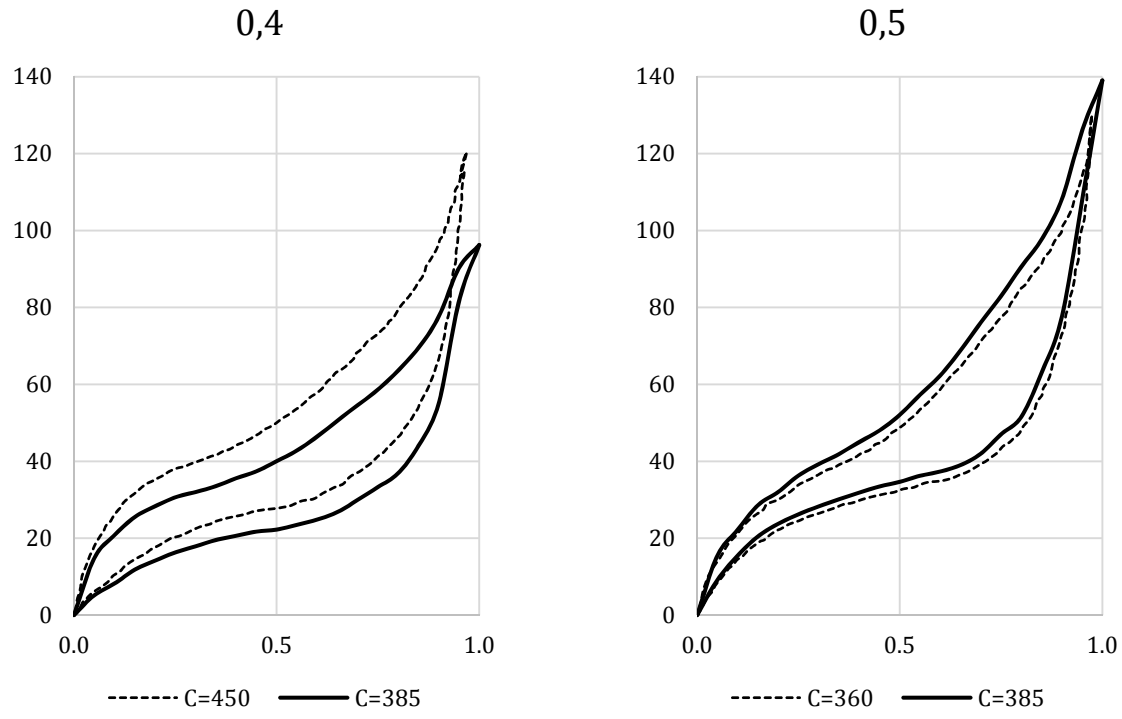

Figure 69 Corrected curves from (Hedenblad 1967)

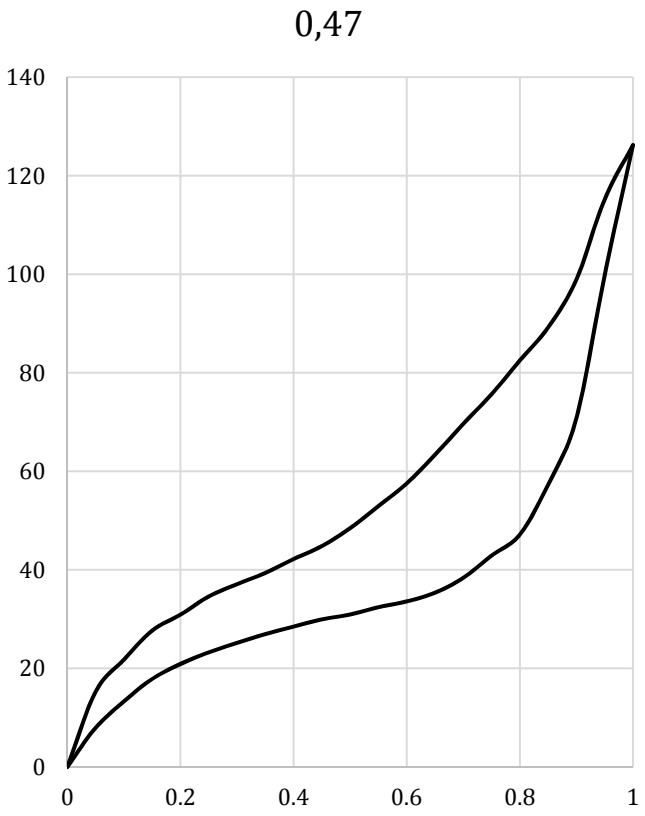

Figure 70 Calculated desorption curve, w/c=0.47 and C=385

Appendix C: Water loss modelling

Once the desorption curves were obtained with the previous procedure, a row of specimens was placed in the oven at 50°C, in this case number 4, to monitor the water loss. This was done by weighing the samples each hour at first, days in which the water loss was really high and then daily until it was more or less stabilized. At that time, the measurements were made periodically but without any fix period. By doing this, it was possible to determine an approximation of the required water losses to reach the two conditions of the study: 50% and 75% RH.

By the end of the study, 62 days after placing the samples in the oven for the first time, the samples could be considered dried as the water loss in between two consecutive measurements was less than 0.5g (Andrade et al. 1999).

The results extracted from the samples in the oven were standardised compared to the assumptions from the desorption curves to see if they were accurate enough. The results are summarized in Table 11

Table 11 Initial and final state of Row 4

	A4 - 1%	**A4 - 0.75%**	**A4 – 0.5%**	**A4 - 0%**
Initial weight [g]	797.43	797.34	827.84	804.58
Final weight [g]	753.39	753.26	783.91	760.56
Initial water content [kg/m³]	44.17	43.32	44.19	43.09
Final water content* [kg/m³]	0.13	-0.76	0.26	-0.93
Error	0.30%	-1.75%	0.59%	-2.17%
	B4 - 1%	**B4 - 0.75%**	**B4 – 0.5%**	**B4 - 0%**
Initial weight [g]	788.32	834	794.72	788.55
Final weight [g]	745.19	787.73	752.85	744.97
Initial water content [kg/m³]	43.51	45.13	42.11	42.04
Final water content* [kg/m³]	0.38	-1.14	0.24	-1.54
Error	0.86%	-2.53%	0.56%	-3.66%
	C4 - 1%	**C4 - 0.75%**	**C4 – 0.5%**	**C4 - 0%**
Initial weight [g]	763.88	828.7	832.19	783.19
Final weight [g]	721.42	782.77	788.4	739.92
Initial water content [kg/m³]	42.58	44.68	44.50	42.13
Final water content* [kg/m³]	0.12	-1.25	0.71	-1.14
Error	0.29%	-2.79%	1.59%	-2.71%

The model built on the desorption curves was accurate enough to use it go estimate the water losses required for the other rows of specimens to get to the determined conditions of the study.

Appendix D: Moisture content

Row 1 was left to dry inside a climate chamber with 50% RH. The values that are found in Table 12 are the ones measured after being inside the climate chamber for 1349h. The final RH and the error were calculated according to the model created with row 4.

According to (Andrade et al. 1999), the weight loss measured during the last 24h placed inside the camber indicates that the samples are in equilibrium with the environment surrounding them, but this assumption is not verified with the model.

Table 12 Initial and final state of Row 1

	A1 - 1%	**A1 - 0.75%**	**A1 – 0.5%**	**A1 - 0%**
Initial weight [g]	824.26	776.38	816.53	834.55
Final weight [g]	799.78	753.94	794.72	812.58
Weight loss during the last 24h [g]	0.06	0.05	0.06	0.06
Equilibrium*	Yes	Yes	Yes	Yes
Initial water content [kg/m³]	45.65	41.88	44.94	45.03
Final water content [kg/m³]	21.17	19.44	23.13	23.06
Final RH (%)	60.39	60.45	67.02	66.68
Error	20.78%	20.91%	34.04%	33.36%
	B1 - 1%	**B1 - 0.75%**	**B1 – 0.5%**	**B1 - 0%**
Initial weight [g]	834.55	827.29	764.03	787.97
Final weight [g]	801.83	741.55	766.95	807.59
Weight loss during the last 24h [g]	0.05	0.06	0.06	0.06
Equilibrium*	Yes	Yes	Yes	Yes
Initial water content [kg/m³]	46.27	41.25	41.73	44.47
Final water content [kg/m³]	20.81	18.77	20.71	22.73
Final RH (%)	58.57	59.25	64.63	66.55
Error	17.14%	18.51%	29.26%	33.11%
	C1 - 1%	**C1 - 0.75%**	**C1 – 0.5%**	**C4 - 0%**
Initial weight [g]	790.91	760.03	798.55	840.87
Final weight [g]	766.9	737.58	777.24	818.51
Weight loss during the last 24h [g]	0.06	0.06	0.06	0.06
Equilibrium*	Yes	Yes	Yes	Yes
Initial water content [kg/m³]	43.75	41.17	42.30	45.13
Final water content [kg/m³]	19.74	18.72	20.99	22.77
Final RH (%)	58.76	59.21	64.61	65.70
Error	17.53%	18.43%	29.23%	31.40%

*According to (Andrade et al. 1999)

Row 2 was left to dry naturally inside a sealed box with a saturated solution of sodium chloride in its base, which simulated an environment with a 75% RH. The values that are found in Table 13 were measured after being exposed to those conditions for 1347h. The final RH and the error were calculated according to the model created with row 4.

According to (Andrade et al. 1999), the weight loss measured during the last 24h placed inside the camber indicates that the samples are in equilibrium with the environment surrounding them, but this assumption is not verified with the model.

Table 13 Initial and final state of Row 2

	A2 - 1%	**A2 - 0.75%**	**A2 – 0.5%**	**A2 - 0%**
Initial weight [g]	793.42	800.19	833.21	803.45
Final weight [g]	774.88	782.51	816.75	787.57
Weight loss during the last 24h [g]	0.02	0.02	0.06	0.09
Equilibrium*	Yes	Yes	Yes	Yes
Initial water content [kg/m³]	44.07	43.47	44.13	43.08
Final water content [kg/m³]	25.53	25.79	27.67	27.20
Final RH (%)	72.47	74.22	78.44	78.99
Error	-3.38%	-1.04%	4.59%	5.32%
	B2 - 1%	**B2 - 0.75%**	**B2 – 0.5%**	**B2 - 0%**
Initial weight [g]	823.18	784.19	834.33	809.33
Final weight [g]	804.69	766.92	817.88	792.54
Weight loss during the last 24h [g]	0.03	0.06	0.04	0.05
Equilibrium*	Yes	Yes	Yes	Yes
Initial water content [kg/m³]	45.37	42.49	44.54	43.44
Final water content [kg/m³]	26.88	25.22	28.09	26.65
Final RH (%)	74.12	74.25	78.90	76.75
Error	-1.18%	-1.00%	5.20%	2.33%
	C2 - 1%	**C2 - 0.75%**	**C2 – 0.5%**	**C2 - 0%**
Initial weight [g]	710.31	838.19	857.31	784.01
Final weight [g]	694.09	820.27	840.84	769.07
Weight loss during the last 24h [g]	0.03	0.08	0.04	0.02
Equilibrium*	Yes	Yes	Yes	Yes
Initial water content [kg/m³]	39.18	45.29	45.58	42.15
Final water content [kg/m³]	22.96	27.37	29.11	27.21
Final RH (%)	73.31	75.60	79.90	80.76
Error	-2.26%	0.80%	6.54%	7.68%

*According to (Andrade et al. 1999)

Row 6 were supposed to be force to dry to 75% RH in the oven at 50°C. Once the samples reached the water loss calculated with the model in row 4 (25 to 44 hours, depending on the sample) they were sealed with plastic foil and placed again in the oven for 14 days in order to achieve a redistribution of the moisture that was left inside them.

As it can be seen in Table 14, the final water content and thus, the final relative humidity of the samples is below the modelled one. This was because the samples were not correctly sealed when they were placed again in the oven to achieve the redistribution. This caused the samples to reach an average value of 30.54% relative humidity.

Table 14 Initial and final state of Row 6

	A6 - 1%	**A6 - 0.75%**	**A6 – 0.5%**	**A6 - 0%**
Initial weight [g]	827.74	804.26	830.59	822.54
Final weight [g]	792.98	770.8	795.83	789.68
Weight loss during the last 24h [g]	0.03	0.1	0.11	0.09
Equilibrium*	Yes	Yes	No	Yes
Initial water content [kg/m³]	45.72	43.41	44.05	44.24
Final water content [kg/m³]	10.96	9.95	9.29	9.95
Final RH (%)	30.00	28.67	26.39	28.14
Error (%)	-60.01%	-61.77%	-64.81%	-62.49%
	B6 - 1%	**B6 - 0.75%**	**B6 – 0.5%**	**B6 - 0%**
Initial weight [g]	823.28	808.84	787.2	796.62
Final weight [g]	789.94	776.55	755.52	765.5
Weight loss during the last 24h [g]	0.11	0.11	0.11	0.11
Equilibrium?	No	No	No	No
Initial water content [kg/m³]	45.70	43.70	41.88	42.57
Final water content [kg/m³]	12.36	11.41	10.20	11.45
Final RH (%)	33.83	32.67	30.48	33.66
Error (%)	-54.89%	-56.44%	-59.36%	-55.12%
	C6 - 1%	**C6 - 0.75%**	**C6 – 0.5%**	**C6 - 0%**
Initial weight [g]	824.79	821.51	821.19	802.28
Final weight [g]	787.91	789.9	787.43	771.06
Weight loss during the last 24h [g]	0.08	0.12	0.1	0.08
Equilibrium?	Yes	No	Yes	Yes
Initial water content [kg/m³]	45.60	44.23	43.75	43.10
Final water content [kg/m³]	8.72	12.62	9.99	11.88
Final RH (%)	23.93	35.69	28.56	34.47
Error (%)	-68.09%	-52.41%	-61.92%	-54.04%

*According to (Andrade et al. 1999)

Row 7 were supposed to be force to dry to 50% RH in the oven at 50°C. Once the samples reached the water loss calculated with the model in row 4 (74 to 122 hours, depending on the sample) they were sealed with plastic foil and placed again in the oven for 14 days in order to achieve a redistribution of the moisture that was left inside them.

As it can be seen in Table 15, and as it happened with row 6, the final water content and thus, the final relative humidity of the samples is below the modelled one. These samples were not correctly sealed either when they were placed again in the oven, causing them to reach an average value of 29.48% relative humidity.

Table 15 Initial and final state of Row 7

	A7 - 1%	**A7 - 0.75%**	**A7 – 0.5%**	**A7 - 0%**
Initial weight [g]	791.23	791.82	832.55	815.98
Final weight [g]	756.76	758.62	798.6	785.72
Weight loss during the last 24h [g]	0.1	0.11	0.09	0.11
Equilibrium*	Yes	No	Yes	No
Initial water content [kg/m³]	43.85	42.96	44.13	43.77
Final water content [kg/m³]	9.38	9.76	10.18	13.51
Final RH (%)	27.85	29.58	30.05	40.19
Error (%)	-44.30%	-40.84%	-39.90%	-19.62%
	B7 - 1%	**B7 - 0.75%**	**B7 – 0.5%**	**B7 - 0%**
Initial weight [g]	799.27	800.88	811.76	818.24
Final weight [g]	763.5	766.38	777.83	785.52
Weight loss during the last 24h [g]	0.07	0.11	0.1	0.09
Equilibrium*	Yes	No	Yes	Yes
Initial water content [kg/m³]	44.44	43.57	42.93	43.88
Final water content [kg/m³]	8.67	9.07	9.00	11.16
Final RH (%)	25.40	27.10	27.30	33.11
Error (%)	-49.20%	-45.80%	-45.40%	-33.78%
	C7 - 1%	**C7 - 0.75%**	**C7 – 0.5%**	**C7 - 0%**
Initial weight [g]	764.61	818.8	802.3	807.71
Final weight [g]	730.85	783.48	767.66	776.52
Weight loss during the last 24h [g]	0.08	0.1	0.08	0.1
Equilibrium*	Yes	Yes	Yes	Yes
Initial water content [kg/m³]	42.27	44.31	42.57	43.26
Final water content [kg/m³]	8.51	8.99	7.93	12.07
Final RH (%)	26.23	26.42	24.26	36.34
Error (%)	-47.54%	-47.17%	-51.49%	-27.32%

*According to (Andrade et al. 1999)